Dietary unsaturated fat improves high density lipoprotein function: opposing roles of apoE and apoCIII

Citation

Morton, Allyson Michelle. 2018. Dietary unsaturated fat improves high density lipoprotein function: opposing roles of apoE and apoCIII. Doctoral dissertation, Harvard University, Graduate School of Arts & Sciences.

Permanent link

http://nrs.harvard.edu/urn-3:HUL.InstRepos:41128478

Terms of Use

Share Your Story

Dietary unsaturated fat improves high density lipoprotein function:

opposing roles of apoE and apoCIII

A dissertation presented

by

Allyson Michelle Morton

to

The Committee on Higher Degrees in Biological Sciences in Public Health

in partial fulfillment of the requirements

for the degree of

Doctor of Philosophy

in the subject of

Biological Sciences in Public Health

Harvard University

Cambridge, Massachusetts

March 2018

Dissertation Advisor: Professor Frank M. Sacks, MD   Allyson Michelle Morton

Dietary unsaturated fat improves high density lipoprotein function: opposing roles of apoE and apoCIII

Abstract

Cardiovascular disease is the leading cause of death worldwide. Atherosclerosis, the buildup of cholesterol-rich plaques in the arteries, is the pathophysiological process behind cardiovascular disease mortality. High density lipoproteins (HDL) are the body's only vehicle for removal and excretion of cholesterol from atherosclerotic plaques, a process called reverse cholesterol transport. Presumably as a result of this important function, plasma concentrations of HDL-cholesterol (-C) are one of the strongest inverse predictors of cardiovascular disease risk. However, therapeutics that increase HDL-C do not protect against cardiovascular disease mortality. This paradox has compelled a shift to improving HDL function rather than necessarily increasing plasma HDL-C. Emerging evidence suggests that the protein content of HDL, which largely has been underutilized in HDL research, could be leveraged to improve HDL function. Apolipoproteins (apo) E and CIII are two HDL proteins that have established roles in lipid metabolism. ApoE is essential for the clearance of triglyceride rich lipoproteins (TRL) from plasma, and it presumably serves a similar function on HDL. ApoCIII impedes the clearance of TRL and promotes the development of hypertriglyceridemia. HDL containing apoCIII no longer has a protective association with cardiovascular disease risk, suggesting that apoCIII makes HDL dysfunctional. ApoE and apoCIII form subpopulations, or subspecies, on HDL, and have opposing functions in vitro, in vivo,

and in human metabolic studies of apoB-containing lipoproteins. Thus, my first aim was to verify that HDL subspecies have metabolic implications in humans, with the goal of finding a subspecies that was especially active in reverse cholesterol transport. Using a metabolic tracer study in humans, I tested if HDL subspecies defined by presence or absence of apoE/apoCIII had metabolic features typical of reverse cholesterol transport: increased synthesis into plasma, size expansion representing cholesterol uptake, and increased clearance from circulation. I found all of these features in a subspecies of HDL containing apoE but not apoCIII. Finally, unsaturated fat has demonstrated cardioprotective effects, but its role in HDL metabolism is unclear. Thus, my second aim was to determine the impact of dietary unsaturated fat on HDL metabolism, assessing its ability to promote reverse cholesterol transport in humans. Using a dietary intervention tracer study, I also tested if these HDL subspecies would respond metabolically to dietary intervention. I showed that dietary unsaturated fat primarily works through HDL containing apoE to make HDL more proficient in reverse cholesterol transport.

TABLE OF CONTENTS

Dedicated to Jesse Lee Morton,

who I promised to make proud

4/13/84 – 8/31/07

Acknowledgments

There is a saying, "it takes a village to raise [a Ph.D. student]," and I am certainly no exception. I will start by acknowledging the people who raised me in the most literal sense: my parents. You have been a source of comfort and inspiration to me for as long as I can remember; I could not have done this without you. To my brother James, you were the first "smart person" I ever knew. I admired you then and I admire you now. To my cousins, who appreciate me not for my intelligence but because I could get them into Duke Basketball games. To Aunt Cindy who has sent me a steady stream of care packages these past six years.

Friends make life better, and additionally are valuable resources in completing a doctorate degree. Thank you to Vanessa, Julia, and Christin, with whom I have talked daily about both science and life. Thank you to Amanda for always reminding me where I'm from. Thank you to all the friends I made on Student Government, with a special shout-out to the Executive Board team of 2015-2016: Christin, Christine, Mohit, Erika, and Abhi. You guys made everything exciting. Public health has some amazing people coming its way.

I also want to thank some non-science mentors I've had over the years – while they did not teach me how to run experiments or analyze data, their contributions to my career development have been invaluable. Deirdre – I have loved all of our adventures. Thank you for all your help and for tirelessly advocating for graduate students. Nancy – thank you for always hearing me and for reminding students that our voices matter. To all my

CHAPTER 1

Introduction

1.1 Introduction

Cardiovascular disease is the leading cause of death, accounting for approximately one-third of all deaths in the United States and worldwide (1, 2). Atherosclerosis is the pathological process that underlies cardiovascular mortality. It results from the progressive accumulation of cholesterol, as well as lipids (in both native and oxidized forms), extracellular matrix, inflammatory cells such as macrophages, and cell debris in the arterial intima and media (3). Atherosclerosis is associated with several co-morbidities including obesity, diabetes, and systemic inflammation (4).

Although cholesterol is an essential component of cell membranes and steroid hormones, it is toxic at large quantities (5). The human body can synthesize unlimited amounts of cholesterol, but is unable to catabolize it and thus must tightly regulate cholesterol concentration in each tissue (6, 7). Lipoproteins are the body's exclusive transport mechanism for cholesterol and are directly related to atherosclerosis pathogenesis. Low density lipoproteins (LDL), of which apolipoprotein (apo) B is the major structural and functional protein (8), are the major vehicle for transport of cholesterol from the liver to peripheral tissues including the artery wall (3). LDL, as well its larger precursors intermediate density lipoprotein (IDL) and very low density lipoprotein (VLDL), can be oxidized and internalized by macrophages, contributing to atherosclerotic lesions (9). On the other hand, high density lipoproteins (HDL) remove excess cholesterol from peripheral tissues, including atherosclerotic plaques, and deliver it to the liver, where it is converted into bile acids and excreted. This process is known as reverse cholesterol transport. Reverse cholesterol transport is a critical

method of maintaining bodily cholesterol homeostasis and has been postulated as a main mechanism of cardiovascular disease protection (10).

1.2   Reverse cholesterol transport

HDL was first discovered by the French physician-scientist Michel Macheboeuf, who described in his 1929 doctoral thesis (11) the isolation of an "alpha-globulin" from horse serum. Twenty years later, this alpha-globulin would be officially designated as HDL upon the development of ultracentrifuge methods to isolate lipoproteins (12, 13). In 1968, John Glomset elucidated the plasma lecithin:cholesterol acyltransferase (LCAT) reaction, discovering that free cholesterol from HDL was the preferred substrate in the formation of cholesterol esters (14, 15). Although the broader meaning of the reaction was then mysterious, Glomset auspiciously hypothesized that the reaction could have a "broader, extracellular function," and that "one possibility is that it plays a role in the transport of cholesterol from peripheral tissues to the liver" (14). This process, the minutiae of which remains a focus of research even fifty years later, came to be known as reverse cholesterol transport, the hallmark of HDL function.

The accepted dogma of reverse cholesterol transport (**Figure 1.1**) (16) begins with the liver secreting into the plasma a nascent discoidal HDL particle consisting of phospholipids, a small amount of unesterified cholesterol, and two molecules of apoA-I, the primary structural and functional protein of HDL. ApoA-I, which is synthesized primarily in the liver and to a much lesser extent in the small intestine (17), accounts
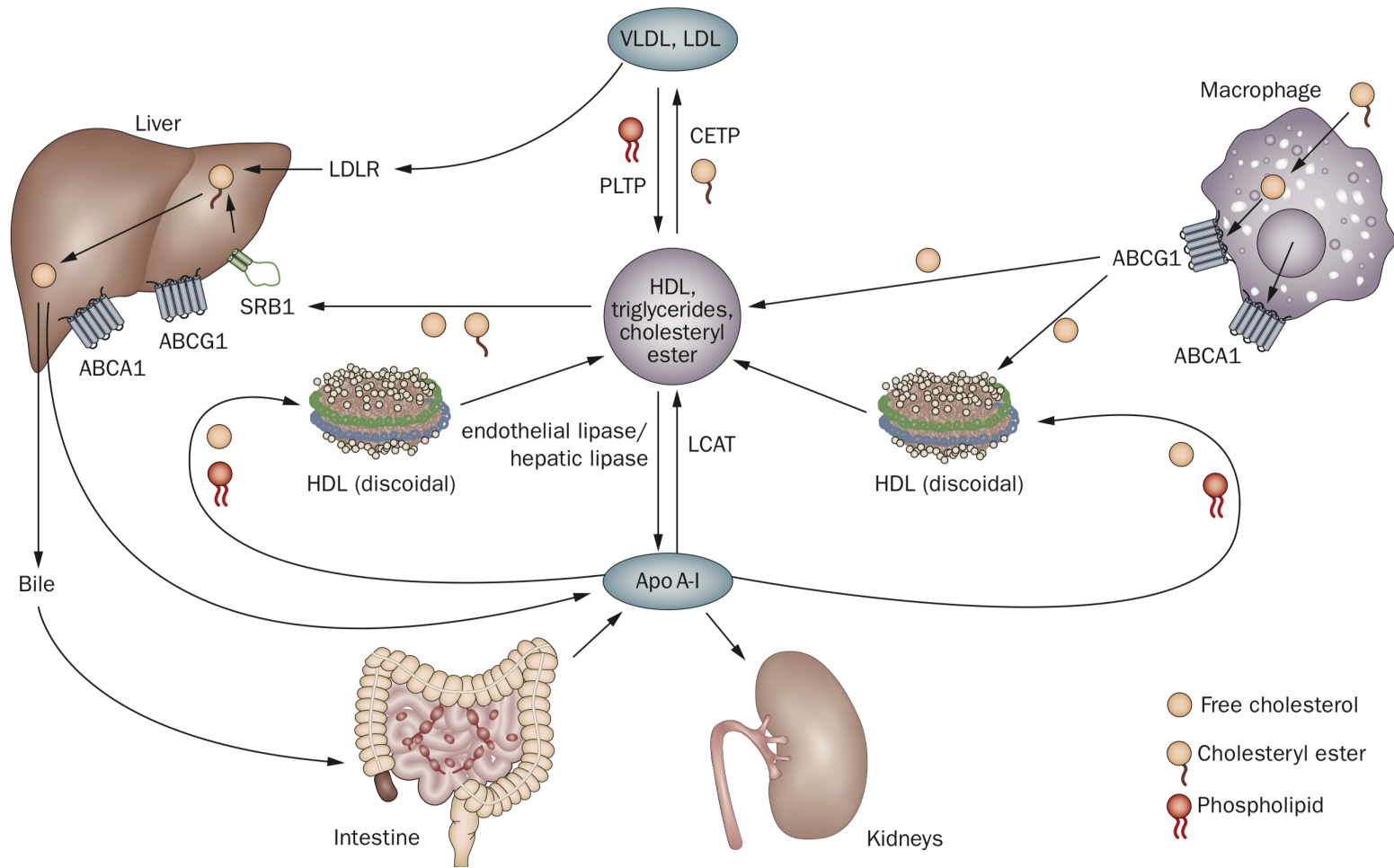
Figure 1.1: HDL has a central role in the reverse cholesterol transport pathway.

Figure 1.1 (continued): HDL has a central role in the reverse cholesterol transport pathway. Lipid-poor apoA-I is secreted by the liver and rapidly acquires cholesterol via the hepatocyte ABCA1 transporter and promotes cholesterol efflux from macrophages. Free cholesterol is esterified to cholesterol esters by LCAT to form mature HDL, which transfers its cholesterol to apo B-containing lipoproteins, such as VLDL and LDL, via CETP-mediated transfer. This cholesterol is subsequently taken up by the liver via the LDL receptor. PLTP transfers phospholipids from triglyceride- rich lipoproteins to HDL, which promotes HDL remodeling. Hepatic cholesterol can be excreted into the bile after conversion to bile acid or expelled directly into the bile as cholesterol. Bile and its components are either reabsorbed by the intestine or ultimately excreted in feces. HDL can be remodeled by lipases, such as endothelial lipase and hepatic lipase, which hydrolyze HDL phospholipids and HDL triglycerides, respectively. The kidneys are an important site of apo A-I catabolism. Abbreviations: ABC, ATP-binding cassette; apo A-I, apolipoprotein A-I; CETP, cholesteryl ester transport protein; LCAT, lecithin–cholesterol acyltransferase; LDLR, LDL receptor; PLTP, phospholipid transfer protein; SRB1, scavenger receptor class B member 1.

for up to 70% of HDL protein mass (18). Although the complete crystal structure of apoA-I has not been elucidated, consensus models have been developed based on decades of data using partial crystal structures, electron microscopy, and small angle X-ray scattering. These models suggest that two apoA-I molecules adopt a "double belt" arrangement around discoidal HDL (19). Discoidal HDL circulates and is transcytosed over the vascular endothelium (20), where it acquires free cholesterol from peripheral cells and tissues, including macrophages, by activating ATP-binding cassette transporter, sub family A, member 1 (ABCA1) (21). Mutations in ABCA1 lead to Tangier's disease (22-24), which is characterized by the near-complete absence of plasma HDL with concomitant cholesterol accumulation in vessel walls (25, 26). Free cholesterol (2-5% of weight, increasing with HDL size (27)), once obtained by HDL, embeds into the phospholipid monolayer along with other resident proteins. Eventually, free cholesterol is converted to cholesterol ester by the LCAT enzyme, which resides on the HDL particle (28). This reaction converts discoidal HDL to a spherical particle as the highly hydrophobic cholesterol ester (12-25% of weight, increasing with HDL size) and a small amount of triglycerides (TG) (5% by weight, regardless of HDL size) sequester into the core of the particle (27). Spherical HDL can then accept more cholesterol by activating ATP-binding cassette transporter, sub family G, members 1 & 4 (ABCG1/4), becoming progressively larger as it circulates (29). Models of established structures for synthetic HDL adapted to authentic human plasma HDL suggest that anywhere from 3-7 apoA-I can be present on spherical HDL depending on its size (27). Scavenger receptor class B type 1 (SR-B1) is also present on the macrophage cell surface and is involved in the bi-directional flux of cholesterol between mature HDL and plasma

membranes (30). Eventually, HDL can be cleared as an intact particle in the liver (holoparticle uptake) (31, 32) via an unknown receptor, or in the kidney by cubilin (33, 34). The lipid cargo can also be selectively transported into hepatocytes by uptake mechanisms including SR-B1, which recycles apoA-I in plasma for further use (30). The cholesterol content of HDL is excreted in feces as a component of bile acids (35). Another important mechanism of cholesterol removal is via the action of cholesterol ester transfer protein (CETP), which catalyzes the exchanging of cholesterol for triglycerides with apoB-containing lipoproteins in plasma (36). These lipoproteins are also eventually cleared by the liver. Phospholipid transfer protein (PLTP) is involved in HDL remodeling via the transfer of phospholipids from triglyceride-rich lipoproteins to HDL (37).

Elucidating the intricacies of reverse cholesterol allowed researchers the opportunity to fully investigate hypotheses that were previously only observational in rare human mutants, with the assumption and goal of leveraging the relevant components as therapeutic targets.

1.3   HDL epidemiology and genetic variants

Plasma lipoprotein concentrations have a profound effect on cardiovascular disease risk. Lipoproteins are typically quantified by their plasma cholesterol content (for example, LDL-cholesterol and HDL-cholesterol). Consistent with the role of LDL in atherosclerosis pathogenesis, concentrations of LDL-C and its resident protein apoB are positively associated with risk of cardiovascular disease (38).

In 1951, it was first shown that a minor constituent of plasma lipoproteins was reduced in individuals with coronary heart disease, in contrast to the remaining lipoproteins in plasma which were significantly increased (39). In 1975, the first large prospective study showed that individuals with ischemic heart disease had lower HDL-C than healthy controls (40). It was hypothesized that the reduction in HDL-C would accelerate the development of atherosclerosis. Since then, it has been shown repeatedly and in diverse cohorts that HDL-C has an independent, inverse association with cardiovascular disease risk, even when LDL-C is low (38, 41-49). Low HDL (<40 mg/dL for males and <50 mg/dL for women) (50) is a strong independent risk factor for premature coronary heart disease in both diabetics and nondiabetics (51-53). The concentration of apoA-I is also inversely associated with CHD risk (54). For every 1 mg/dL increase in HDL-C, cardiovascular disease mortality is reduced by 3-4% (44). The inverse association between HDL and cardiovascular disease risk, and the notion that HDL is protective, are so ubiquitously recognized that it is usually stated without citation.

However, genome-wide association studies (GWAS) have cast some doubt on the causal relationship between HDL and cardiovascular disease. Single nucleotide polymorphisms (SNPs) in *LIPG* (which encodes for hepatic lipase) that increase HDL-C paradoxically are not associated with reduced risk of myocardial infarction (55). Similarly, individuals with heterozygous loss of function mutations in *APOA1*, which lead to marked reductions in HDL-C, do not have increased risk of ischemic heart disease (56). In a large meta-analysis, SNPs located near *ABCA1* were associated with small

8

changes in the levels of HDL-C, but not with the risk of CHD (57). More contemporary

approaches, which take into account genetic pleiotropy, have also shown a null

association between genetic variants affecting HDL-C and risk of CHD (58). In contrast,

genetic loci affecting LDL-C and triglyceride levels reliably predict cardiovascular

disease risk (55, 57-59). Nevertheless, the robust inverse relationship between HDL-C

and cardiovascular disease risk remains valid. This, along with the well-established

basic science relationship of HDL in atherosclerosis **(Section 1.2)**, has made HDL an

attractive therapeutic target.

1.4 HDL therapeutics

Pharmacological interventions to treat cardiovascular disease are mainly focused on

lowering LDL-C and have proven very effective in reducing the risk of cardiovascular

disease (60, 61). These therapies include the first-line therapy statins, which inhibit

HMG-CoA reductase, the rate-limiting enzyme in cholesterol biosynthesis; PCSK9

inhibitors, which prevent the degradation of LDL-R; and cholesterol absorption

inhibitors, which reduce the amount of dietary cholesterol that is taken up in the small

intestine (62). However, about 70% of cardiovascular events are not prevented in statin

trials (63). This residual disease burden has made HDL a popular therapeutic target due

to its well-established basic science relationship with atherosclerosis **(Section 1.2)** and

epidemiological relationship with cardiovascular disease **(Section 1.3)** (64).

Niacin, also known as nicotinic acid or vitamin B3, is the oldest HDL therapeutic. It

increases HDL-C by reducing apoA-I uptake in the liver (65) and was first shown in

1975 to reduce all-cause mortality compared to placebo among men who had history of myocardial infarction (66). It was more recently shown that addition of niacin therapy to patients already receiving a statin did not provide any additional benefit, despite reductions in plasma triglycerides and increases in HDL-C (67). A recent meta-analysis of over 35,000 study participants across thirteen clinical trials reported no benefit of niacin in reducing cardiovascular disease risk or all-cause mortality, despite a mean increase of HDL-C of 21% (68). Additionally, unpleasant side effects occur in up to 70% of patients receiving niacin therapy (69), and a range of safety concerns have been reported, including myopathy and elevation in liver enzymes (70). Given these considerations, niacin therapy likely adds little benefit to cardiovascular disease risk reduction (71).

Fibrates perform several actions on the lipoprotein system, one of which is increasing HDL-C by increasing apoA-I production in the liver (72, 73). Although fibrates are well-tolerated and generally effective at lowering plasma triglycerides and LDL-C, they are usually prescribed secondary to statins for treating increased cardiovascular disease risk caused by increased LDL-C (71). A meta-analysis of eighteen fibrate trials with 45,000 participants reported a mean 15% increase in HDL-C, a 10% reduction in risk of cardiovascular events, but no significant reduction in all-cause mortality or cardiovascular mortality (74). Importantly, the degree to which HDL-C was affected by treatment did not predict the effectiveness of fibrate therapy, such that patients who had large reductions in HDL-C had no difference in risk than HDL-C "non-responders." Recently, it was shown that addition of fenofibrate to diabetic patients already receiving

simvastatin therapy did not reduce the rate of fatal cardiovascular events, myocardial infarction, or stroke (75). There has been, however, some post-hoc evidence of fibrate therapy being more effective in patients with TG > 200 mg/dL or in patients with metabolic syndrome (76).

In the last decade, a set of CETP inhibitors, once thought to be the savior of HDL therapeutics, have proven overall ineffective (77). CETP catalyzes the unidirectional movement of cholesterol from HDL to apoB-containing lipoproteins in exchange for triglycerides (78). Inhibition of CETP halts this pathway, keeping cholesterol in HDL rather than shunting it to VLDL and LDL (79). Almost thirty years ago, it was discovered that Japanese families with genetic *CETP* deficiency had higher HDL-C and lower LDL-C compared to normal humans (80). Expanding on these findings, more recent discoveries have shown that SNPs in *CETP* lead to increased HDL-C and reduced LDL-C and TG, and also are associated with lower risk of CHD (81-83). To date, there are four CETP inhibitors that have completed phase III clinical testing. Torcetrapib, studied in patients with high cardiovascular risk, raised HDL-C by 72% (vs. statin therapy alone), but the trial was halted prematurely due to increased mortality and morbidity (84). Dalcetrapib, which did not have the same off-target effects as its predecessor, increased HDL-C by 30-40% but did not reduce the risk of recurrent cardiovascular events (vs. placebo) in patients with a recent acute coronary syndrome, and it was halted early for futility (85). Evacetrapib similarly increased HDL-C, but it did not reduce the risk of cardiovascular events (vs. placebo) among patients with high-risk vascular disease and was also halted early for futility (86). Anacetrapib, the last of the major

CETP inhibitors, recently saw modest success (87). Among patients with atherosclerotic vascular disease who were receiving statin therapy, addition of anacetrapib increased HDL-C by 100% (vs. placebo) and reduced the risk of major coronary events by about 9%, but did not affect risk of mortality. However, the study participants already had well-controlled, low levels of LDL-C due to intensive statin therapy, and the benefit of anacetrapib appeared to be mostly related to its lowering of non-HDL-C (88). This raised questions about the long-term efficacy of anacetrapib in high-risk patients. Merck, the sponsor of anacetrapib, recently declined to seek regulatory approval for the drug, effectively concluding the narrative on CETP inhibitors (89).

A broad conclusion from these trials and others is that increasing HDL-C does not protect against heart disease (61), despite the overwhelming evidence from population studies that high levels of HDL-C are protective. This is the so-called "HDL paradox." Reconciling these two conflicting lines of evidence has necessitated the placement of greater emphasis on improving HDL function, rather than increasing plasma HDL-C, which is probably just a marker for overall HDL function (90, 91). The ability of HDL to remove excess cholesterol from the body remains its functional hallmark. Emerging evidence suggests that the protein content of HDL could be leveraged to help promote this process.

1.5   The concept of lipoprotein speciation

In 1964, Petar Alaupovic (92) first proposed defining lipoproteins by their protein moiety instead of the standard conventions of hydrated density or major lipid content (93-96).

He argued that the functional capabilities of lipoproteins were carried out by the protein contained therein, not an artifact of their density class or lipid content; he hypothesized that proteins were not randomly scattered across lipoproteins but were sequestered into specific subfractions, forming discrete "subspecies" with functional significance (97). At that time, only some preliminary "apo's" had been classified: apoA-I and apoA-II (originally grouped as a single "apoA"); apoB; apoCI, apoCII, and apoCIII (originally grouped as a single "apoC"), and later, apoE. With the development of mass spectrometry, it became clear that the traditional "apo's" responsible for lipid metabolism were not the only protein cargo carried by HDL. The current list, kept up to date by Sean Davidson's group at the University of Cincinnati (98), stands at almost 100 distinct functional proteins that have been confirmed by at least three independent groups to exist on HDL. These proteins have diverse functions relating not only to lipid metabolism, but also to complement regulation, proteinase inhibition, antithrombosis, and the acute-phase response (99, 100). This evidence, along with the considerations from the failures of HDL therapeutics, has shifted the focus to considering HDL not as a single entity but as a complex, heterogeneous particle system composed of proteins and lipids that work in symphony to direct HDL function. Two of the most-studied HDL proteins are apoE and apoCIII.

ApoE is a 34 kDa 299 amino acid protein (101) that exists across the lipoprotein spectrum (102). It is synthesized primarily by the liver, but is also secreted by macrophages, astrocytes, and other cell types (17). ApoE binds to various liver receptors, including low density lipoprotein (LDL)-receptor (-R) (103), LDL-R related

protein (LRP) (104), and heparin/heparan sulfate proteoglycans (105-108). ApoE is required for the liver clearance of plasma chylomicrons, which cannot bind to LDL-R, and large VLDL (109). In humans, VLDL and IDL that contain apoE are cleared from the circulation much more quickly than those without apoE (110, 111).

Based on evidence *in vitro* and in animal models, apoE is thought to protect against atherosclerosis via several mechanisms: 1) It reduces monocyte proliferation and infiltration into the arterial intima (112), is anti-inflammatory (113, 114) and prevents oxidative stress (101-104); 2) ApoE secreted by macrophages stimulates cholesterol efflux via ABCA1, ABCG1, SR-B1, and aqueous diffusion (115-118), processes that are supported by apoA-I. As a proof of principle, *APOE*-knockout mice have hypercholesterolemia and develop spontaneous atherosclerotic plaques (119, 120), which can be corrected by transplantation with bone marrow from wild-type mice (120).

Much less is known about the role of apoE in HDL metabolism, but evidence from *in vitro* studies and in animal models suggests that apoE also facilitates removal of cholesterol-containing HDL from the system (121-124). *In vitro*, HDL apoE also increases HDL biogenesis (125) and size expansion in the circulation (126-128). The only human metabolic study of HDL containing apoE was performed in participants with abetalipoproteinemia, a condition in which apoB is markedly deficient in plasma and HDL is the main plasma lipoprotein. In this population, Ikewaki et al. (129) associated exogenously labeled apoA-I and apoE with autologous lipoproteins from the study participants and demonstrated that apoA-I on HDL containing apoE had faster

clearance than apoA-I on HDL that did not contain apoE. This finding suggests that apoE may affect *in vivo* HDL metabolism in normal humans.

There are three common apoE polymorphisms in humans that differ in their metabolic functions. ApoE3 (possessing a cysteine (C) at amino acid position 112, and an arginine (R) at position 158) is the most common isoform with an allele frequency of 78%, and is considered to be wild-type (130). The apoE2 allele (R158 → C, a mutation in the receptor-binding region) is present in 7% of the population and is associated with markedly impaired receptor binding (131). Furthermore, homozygosity for apoE2 is an essential factor in type III hyperlipoproteinemia (132), a disorder characterized by delayed clearance of remnant lipoproteins and premature development of atherosclerosis (133). ApoE4 (C112 → R, a mutation in the lipid-binding region) is present in 14% of the population and is impaired in stimulating cholesterol efflux (134, 135) and in preventing inflammation and oxidation (136, 137). A meta-analysis of 48 studies concluded that carriers of the apoE4 allele have a 42% higher risk for CHD compared to apoE3/E3 homozygotes (138).

ApoCIII is an 8.8 kDa 79 amino acid protein (139) also present across the lipoprotein spectrum. It is synthesized in the liver and to a lesser extent the small intestine (17). ApoCIII is directly implicated in triglyceride metabolism, inhibiting the clearance of triglyceride-rich lipoproteins *in vitro* and in humans (140-145). High concentrations of apoCIII also inhibit lipoprotein lipase and hepatic lipase (141, 146-148), which prevent triglyceride clearance. *APOC3*-transgenic mice develop severe hypertriglyceridemia

(149), and *APOC3*-null mice are hypoglycemic and protected from postprandial

hypertriglyceridemia (150). Human heterozygous carriers of a null mutation in the

APOC3 gene have lower postprandial serum triglycerides, higher levels of HDL-C, and

lower levels of LDL cholesterol (LDL-C) and are less likely to have subclinical

atherosclerosis (151). Loss of function mutations in *APOC3* are associated with lower

serum triglycerides and reduced risk of CHD (152) and ischemic cardiovascular disease

(153). Antisense inhibition of *APOC3* robustly lowers serum triglycerides in humans and

is an emerging therapy for treating hypertriglyceridemia (154).

ApoCIII forms discrete subspecies on lipoproteins that have known relations to

cardiovascular disease risk. Some VLDL contain many apoCIII molecules – anywhere

from 60-100 – whereas others have none, even though mathematically the

concentrations of apoCIII and apoB would allow one apoCIII to exist on every VLDL

particle (155). LDL subspecies defined by apoCIII content have divergent relationships

with CHD risk. In two large cohorts, the concentration of LDL (measured by apoB) that

contains apoCIII is associated with increased risk of coronary heart disease, whereas

LDL not containing apoCIII has a null association (156). Less is known about the role of

apoCIII in HDL. About 5-10% of HDL particles contain apoCIII (157, 158). As seen in

LDL, HDL subspecies defined by apoCIII content have opposing relationships with

coronary heart disease risk. Across four separate cohorts, HDL that does not contain

apoCIII (measured by cholesterol content) has a greater inverse association with

incident CHD than undifferentiated HDL-C, whereas HDL that contains apoCIII loses

this protective effect (158). These data suggest that apoCIII makes HDL dysfunctional.

ApoE and apoCIII also have opposing effects on lipoprotein metabolism *in vitro*, *in vivo*, and in human metabolic studies of apoB-containing lipoproteins. In fibroblasts, apoCIII inhibits the ability of apoE to facilitate uptake of VLDL by LDL-R (140, 142). In mice, overexpression of apoCIII reduces VLDL clearance, which is rescued by addition of exogenous apoE or genetic apoE overexpression (143). Similarly, co-expression of the *APOE* transgene in *APOC3* transgenic mice eliminates the hypertriglyceridemia caused by apoCIII (143, 159). In rats, addition of apoCIII to apoE-enriched chylomicrons results in a pronounced inhibition of hepatic chylomicron and triglyceride emulsion clearances (160). Finally, in kinetic studies of human VLDL and IDL, it has been shown repeatedly that apoCIII overrides and attenuates the increased clearance caused by apoE (111, 145, 161). It is unknown if apoE and apoCIII function similarly in HDL.

There is some data in the literature of the effect of therapeutics on HDL subspecies, but most studies are done well after the therapeutic in question has completed phase III testing. Pravastatin treatment decreases the apoCIII content in LDL and VLDL, and decreases the apoE content in VLDL, LDL, and HDL (162). Pre-treatment with either pitavastatin or atorvastatin significantly reduced the ability of apoCIII to promote THP-1 monocyte adhesion to endothelial cells, considered to be one of its most important atherogenic effects (163). It was recently shown that treatment with the CETP inhibitor torcetrapib, which resulted in dramatic increases in HDL-C but suffered from off-target effects that led to increased mortality, also increased the apoCIII content specifically of HDL (164).

Thus, protein subspecies not only exist on HDL, but also have specific functions with relations to disease risk as envisioned by Alaupovic decades ago. Understanding subspecies better might allow therapeutics to be targeted against pathogenic subspecies, or targeted to promote subspecies that promote functions of HDL such as reverse cholesterol transport. Other than the work presented in this thesis, there is minimal data in the literature regarding the effect of therapeutics on HDL subspecies. The ideal subspecies would be linked to both metabolic and disease outcomes, providing both a targetable biological mechanism and a broader clinical significance. One therapeutic that is not pharmacological in nature, which already has demonstrated impacts on HDL, is dietary intervention.

1.6   Diet and HDL metabolism

Early human feeding studies in the 1970's showed that compared to balanced diets, diets very high in carbohydrate (80% of total calories) reduced HDL-C (165). Around the same time, it was shown that diets high in saturated fat and cholesterol increased levels of apoA-I and HDL-C compared to diets high in polyunsaturated fats (166). A later meta-analysis of 60 nutrition trials showed that all types of *cis*-unsaturated and saturated fatty acids, when compared isocalorically to carbohydrates, increase HDL-C to varying degrees, whereas *trans*-unsaturated fats lower HDL-C (167, 168). Dietary unsaturated fat (both polyunsaturated fatty acids, PUFA, and monounsaturated fats, MUFA) intake is associated prospectively with a lower risk of cardiovascular disease and mortality (169, 170), making this nutrient an attractive focus of dietary intervention.

Metabolic, or kinetic, studies in humans are used to elucidate the metabolism of molecules of interest. To study lipoprotein metabolism, a protein or lipid component of the particle is labeled with a tracer, either radioactive or stable isotope, which can be isolated and quantified using a scintillation counter or mass spectrometry, respectively. Information gained from metabolic studies can determine if changing concentrations of the molecule of interest is due to differences in synthesis rates and/or clearance rates. Metabolic studies of HDL typically label apoA-I using L-leucine-5,5,5-D3 (D3-leucine) (171), a stable amino acid isotope tracer, although early studies used radioiodinated (^{125}I-) apoA-I (172). Kinetic modeling is used to mathematically describe the changes in the properties of the system. The outputs of kinetic modeling are 1) pool size (the mass of the molecule of interest in a given body compartment); 2) fractional catabolic rate (FCR, number of pools per time interval, representing the percent of the pool cleared from a body compartment); 3) synthesis rate (mass per time interval, representing the flux of material through each body compartment). Mathematically, synthesis rates are calculated by multiplying pool size by FCR, assuming the concentration of the molecule of interest is in steady state.

The effect of diet on HDL metabolism in humans is poorly understood. Weight loss is often or byproduct (or even a goal) of dietary intervention trials (173), but weight loss increases HDL-C (174) by reducing apoA-I turnover (175, 176). This creates a challenge to isolate the effects of nutrients without confounders. A couple of studies have measured the effect of isocaloric (non-weight change) dietary intervention on HDL

metabolism. One study found in adults with dyslipidemia (high LDL-C concentration) that replacing dietary carbohydrate with monounsaturated fats for four weeks increased the concentration of apoA-I primarily through a reduction of apoA-I FCR (177). Another study found in obese men a heterogeneous response of HDL-C to a Mediterranean diet, and an overall small to no effect on HDL kinetic parameters (178). Neither study utilized a random crossover study design, in which each study participant receives each dietary intervention in random order.

To date, there have been only a couple of isocaloric, random crossover-design dietary intervention trials that measured HDL metabolism in humans. The first was published in 1990 by Eliot Brinton and colleagues (179). Thirteen young adults (mean age 24 years) with normal weight (mean BMI 23 kg/m^2) were recruited and placed on two isocaloric diets for four weeks each: a high fat diet (42% calories from fat, primarily from saturated fatty acids) and a very low-fat diet (9% calories from fat). After each diet, participants were injected with exogenous radioiodinated apoA-I from healthy donors, HDL separated by ultracentrifugation, and protein turnover measured directly from radioactive decay curves. Brinton et al. found that participants had 29% higher HDL-C on the high saturated fat diet due to a 23% higher apoA-I secretion rate.

The second study, published in 2004 by Matthan and colleagues, compared the effects of dietary fat sources on lipoprotein metabolism without altering carbohydrate or protein content (180). Eight post-menopausal hypercholesterolemic women were placed on three diets for five weeks each. The diets were high in either 1) soybean oil (primarily

omega-6 PUFA), 2) margarine (primarily *trans* fats), or 3) butter (primarily saturated fats). Calories from carbohydrate and protein were similar across the three diets. After each diet period, participants received a primed constant infusion of D3-leucine over a 15-hour period with intake of food every hour to maintain fed state. Kinetic parameters were determined by fitting the multicompartmental model to the tracer/tracee ratio data using SAAM-II. Compared to the other two diets, the diet high in *trans*-unsaturated fatty acids reduced the apoA-I plasma concentration and pool size by increasing apoA-I FCR. There were no differences in kinetic parameters between the two diets high in saturated fats vs. high in omega-6 PUFA.

A fixed-sequence crossover study published in 1999 by Vélez-Carrasco and colleagues supported the findings of Brinton et al (181). Researchers placed study participants first on a standard American diet for 6 weeks, then on a low saturated fat diet for 6 or 24 weeks. After the saturated fat restriction, participants had lower 15% HDL-C due to an 8% decrease in apoA-I secretion.

Thus, dietary macronutrients have effects on HDL metabolism. However, there is a lack of information regarding the effects of dietary unsaturated fat versus carbohydrate on HDL metabolism.

1.7   Conclusion

The reverse cholesterol transport pathway as described in **Section 1.2**, which was elucidated after decades of mechanistic *in vivo* and *in vitro* research, has never been

verified in humans. Most *in vivo* studies are performed in rodents, which lack the critical reverse cholesterol transport gene *CETP* and thus have a very different lipoprotein system compared to humans (182). This severely limits their ability to recapitulate the lipoprotein metabolism in humans.

Human metabolic studies are essential for understanding the *in vivo* kinetics of HDL, but most are not designed to quantify reverse cholesterol transport. Like clinical diagnostic tests focusing solely on HDL-C, most human metabolic studies have focused on total HDL particle turnover (typically quantified using apoA-I) (165, 175, 177, 179, 183-189) without size-separating HDL or partitioning into subspecies. Assessing whether the canonical reverse cholesterol transport exists in humans would at minimum require demonstrating size expansion from small to large HDL (representing uptake of cholesterol from peripheral tissues). To date, this has been performed one time, in a study published by our lab (190). We found that, contrary to the dogma, all HDL sizes appear in plasma at the same time, not just small discoidal HDL. We saw minimal evidence of size expansion and all HDL sizes were cleared from circulation, not just the largest cholesterol-rich HDL. Because size expansion was detectable in a small amount, it is possible that a certain subspecies of HDL is responsible for this metabolic effect.

The goals of this dissertation are to address the following outstanding questions in the field of HDL biology:

1. How do HDL proteins work together to drive the metabolism of HDL? Do apoE and apoCIII have opposing effects, and can one protein outcompete the other? Do HDL subspecies defined by apoE and apoCIII content have different abilities in performing reverse cholesterol transport? Importantly, do metabolic differences translate to clinical outcomes, specifically in the reduction of cardiovascular disease risk? **(Chapter 2)**

2. What is the effect of dietary intervention, using unsaturated fat, on HDL metabolism? How does dietary unsaturated fat work through HDL subspecies, specifically HDL containing apoE, to make HDL more proficient in reverse cholesterol transport, its functional hallmark? **(Chapter 3)**

To answer these questions, we performed a dietary intervention trial in overweight and obese humans who had the clinically significant low HDL-C phenotype. After administering a D3-leucine tracer to study participants, HDL was separated into four discrete sizes and into subspecies defined by apoE (the high fat diet had additional separation by apoCIII content). Using mathematical modeling of the tracer enrichment curves, I determined values of kinetic parameters from each individual in the study and developed models of biological significance to determine to what extent HDL subspecies participate in reverse cholesterol transport. I present additional information on kinetic model development methodology **(Chapter 4)** and a side project on the effect of pharmacologic intervention on the concentration of lipoprotein species **(Appendix 1)**.

1.8 References

1. Writing Group Members et al. Heart Disease and Stroke Statistics-2016 Update: A Report From the American Heart Association. *Circulation* 2016;133(4):e38–360.

2. GBD 2015 Mortality and Causes of Death Collaborators. Global, regional, and national life expectancy, all-cause mortality, and cause-specific mortality for 249 causes of death, 1980-2015: a systematic analysis for the Global Burden of Disease Study 2015. *Lancet* 2016;388(10053):1459–1544.

3. Lusis AJ. Atherosclerosis. *Nature* 2000;407(6801):233–241.

4. Rocha VZ, Libby P. Obesity, inflammation, and atherosclerosis. *Nat Rev Cardiol* 2009;6(6):399–409.

5. Hu J, Zhang Z, Shen W-J, Azhar S. Cellular cholesterol delivery, intracellular processing and utilization for biosynthesis of steroid hormones. *Nutr Metab (Lond)* 2010;7(1):47.

6. Nestel PJ. Cholesterol turnover in man. *Adv. Lipid Res.* 1970;8:1–39.

7. Cuchel M, Rader DJ. Macrophage reverse cholesterol transport: key to the regression of atherosclerosis? *Circulation* 2006;113(21):2548–2555.

8. Chan L. Apolipoprotein B, the major protein component of triglyceride-rich and low density lipoproteins. *J. Biol. Chem.* 1992;267(36):25621–25624.

9. Ghosn MG et al. Permeation of human plasma lipoproteins in human carotid endarterectomy tissues: measurement by optical coherence tomography. *J. Lipid Res.* 2011;52(7):1429–1434.

10. Hutchins PM, Heinecke JW. Cholesterol efflux capacity, macrophage reverse cholesterol transport and cardioprotective HDL. *Curr. Opin. Lipidol.* 2015;26(5):388–393.

11. Macheboeuf M. *Recherches sur les phosphoaminolipides et les sterides du serum et du plasma sanguins.* Bulletin de la Société de Chimie Biologique; 1929:

12. Gofman JW, Lindgren FT, Elliott H. Ultracentrifugal studies of lipoproteins of human serum. *J. Biol. Chem.* 1949;179(2):973–979.

13. Delalla OF, Elliott HA, Gofman JW. Ultracentrifugal studies of high density serum lipoproteins in clinically healthy adults. *Am. J. Physiol.* 1954;179(2):333–337.

14. Glomset JA. The plasma lecithins:cholesterol acyltransferase reaction. *J. Lipid Res.* 1968;9(2):155–167.

15. Fielding CJ, Fielding PE. Purification and substrate specificity of lecithin-cholesterol acyl transferase from human plasma. *FEBS Lett.* 1971;15(5):355–358.

16. Navab M, Reddy ST, Van Lenten BJ, Fogelman AM. HDL and cardiovascular disease: atherogenic and atheroprotective mechanisms. *Nat Rev Cardiol* 2011;8(4):222–232.

17. Aguet F et al. Genetic effects on gene expression across human tissues. *Nature* 2017;550(7675):204–213.

18. Davidson WS, Thompson TB. The structure of apolipoprotein A-I in high density lipoproteins. *J. Biol. Chem.* 2007;282(31):22249–22253.

19. Melchior JT et al. A consensus model of human apolipoprotein A-I in its monomeric and lipid-free state. *Nat. Struct. Mol. Biol.* 2017;24(12):1093–1099.

20. Röhrl C, Stangl H. HDL endocytosis and resecretion. *Biochim. Biophys. Acta* 2013;1831(11):1626–1633.

21. Asztalos BF et al. Differential effects of HDL subpopulations on cellular ABCA1- and SR-BI-mediated cholesterol efflux. *J. Lipid Res.* 2005;46(10):2246–2253.

22. Brooks-Wilson A et al. Mutations in ABC1 in Tangier disease and familial high-density lipoprotein deficiency. *Nat. Genet.* 1999;22(4):336–345.

23. Bodzioch M et al. The gene encoding ATP-binding cassette transporter 1 is mutated in Tangier disease. *Nat. Genet.* 1999;22(4):347–351.

24. Rust S et al. Tangier disease is caused by mutations in the gene encoding ATP-binding cassette transporter 1. *Nat. Genet.* 1999;22(4):352–355.

25. Fredrickson DS, Altrocchi PH, Avioli LV, Goodman DWS, Goodman HC. Tangier Disease: Combined Clinical Staff Conference at the National Institutes of Health. *Ann. Intern. Med.* 1961;55(6):1016–1031.

26. Fredrickson DS. The Inheritance of High Density Lipoprotein Deficiency (Tangier Disease). *J. Clin. Invest.* 1964;43(2):228–236.

27. Huang R et al. Apolipoprotein A-I structural organization in high-density lipoproteins isolated from human plasma. *Nat. Struct. Mol. Biol.* 2011;18(4):416–422.

28. Glomset JA, Parker F, Tjaden M, Williams RH. The esterification in vitro of free cholesterol in human and rat plasma. *Biochim. Biophys. Acta* 1962;58:398–406.

29. Wang N, Lan D, Chen W, Matsuura F, Tall AR. ATP-binding cassette transporters G1 and G4 mediate cellular cholesterol efflux to high-density lipoproteins. *Proc. Natl. Acad. Sci. U.S.A.* 2004;101(26):9774–9779.

30. Acton S et al. Identification of scavenger receptor SR-BI as a high density lipoprotein receptor. *Science* 1996;271(5248):518–520.

31. Glass CK, Pittman RC, Keller GA, Steinberg D. Tissue sites of degradation of apoprotein A-I in the rat. *J. Biol. Chem.* 1983;258(11):7161–7167.

32. Glass C, Pittman RC, Civen M, Steinberg D. Uptake of high-density lipoprotein-

associated apoprotein A-I and cholesterol esters by 16 tissues of the rat in vivo and by adrenal cells and hepatocytes in vitro. *J. Biol. Chem.* 1985;260(2):744–750.

33. Kozyraki R et al. The intrinsic factor-vitamin B12 receptor, cubilin, is a high-affinity apolipoprotein A-I receptor facilitating endocytosis of high-density lipoprotein. *Nat. Med.* 1999;5(6):656–661.

34. Moestrup SK, Kozyraki R. Cubilin, a high-density lipoprotein receptor. *Curr. Opin. Lipidol.* 2000;11(2):133–140.

35. Botham KM, Bravo E. The role of lipoprotein cholesterol in biliary steroid secretion. Studies with in vivo experimental models. *Prog. Lipid Res.* 1995;34(1):71–97.

36. Charles MA, Kane JP. New molecular insights into CETP structure and function: a review. *J. Lipid Res.* 2012;53(8):1451–1458.

37. Albers JJ, Vuletic S, Cheung MC. Role of plasma phospholipid transfer protein in lipid and lipoprotein metabolism. *Biochim. Biophys. Acta* 2012;1821(3):345–357.

38. Emerging Risk Factors Collaboration et al. Major lipids, apolipoproteins, and risk of vascular disease. *JAMA* 2009;302(18):1993–2000.

39. Barr DP, Russ EM, Eder HA. Protein-lipid relationships in human plasma. II. In atherosclerosis and related conditions. *Am. J. Med.* 1951;11(4):480–493.

40. Miller GJ, Miller NE. Plasma-high-density-lipoprotein concentration and development of ischaemic heart-disease. *Lancet* 1975;1(7897):16–19.

41. Miller NE, Thelle DS, Forde OH, Mjos OD. The Tromsø heart-study. High-density lipoprotein and coronary heart-disease: a prospective case-control study. *Lancet* 1977;1(8019):965–968.

42. Gordon T, Castelli WP, Hjortland MC, Kannel WB, Dawber TR. High density lipoprotein as a protective factor against coronary heart disease. The Framingham Study. *Am. J. Med.* 1977;62(5):707–714.

43. Castelli WP et al. Incidence of coronary heart disease and lipoprotein cholesterol levels. The Framingham Study. *JAMA* 1986;256(20):2835–2838.

44. Gordon DJ et al. High-density lipoprotein cholesterol and cardiovascular disease. Four prospective American studies. *Circulation* 1989;79(1):8–15.

45. Stampfer MJ, Sacks FM, Salvini S, Willett WC, Hennekens CH. A prospective study of cholesterol, apolipoproteins, and the risk of myocardial infarction. *N. Engl. J. Med.* 1991;325(6):373–381.

46. Goldbourt U, Yaari S, Medalie JH. Isolated low HDL cholesterol as a risk factor for coronary heart disease mortality. A 21-year follow-up of 8000 men. *Arterioscler.*

Thromb. Vasc. Biol. 1997;17(1):107–113.

47. Barter P et al. HDL cholesterol, very low levels of LDL cholesterol, and cardiovascular events. *N. Engl. J. Med.* 2007;357(13):1301–1310.

48. Huxley RR et al. Isolated low levels of high-density lipoprotein cholesterol are associated with an increased risk of coronary heart disease: an individual participant data meta-analysis of 23 studies in the Asia-Pacific region. *Circulation* 2011;124(19):2056–2064.

49. Holmes MV et al. Lipids, Lipoproteins, and Metabolites and Risk of Myocardial Infarction and Stroke. *J. Am. Coll. Cardiol.* 2018;71(6):620–632.

50. Chapman MJ et al. Raising high-density lipoprotein cholesterol with reduction of cardiovascular risk: the role of nicotinic acid--a position paper developed by the European Consensus Panel on HDL-C. *Curr Med Res Opin* 2004;20(8):1253–1268.

51. Gotto AM, Brinton EA. Assessing low levels of high-density lipoprotein cholesterol as a risk factor in coronary heart disease: a working group report and update. *J. Am. Coll. Cardiol.* 2004;43(5):717–724.

52. Maron DJ. The epidemiology of low levels of high-density lipoprotein cholesterol in patients with and without coronary artery disease. *Am. J. Cardiol.* 2000;86(12A):11L–14L.

53. Sharrett AR et al. Coronary heart disease prediction from lipoprotein cholesterol levels, triglycerides, lipoprotein(a), apolipoproteins A-I and B, and HDL density subfractions: The Atherosclerosis Risk in Communities (ARIC) Study. *Circulation* 2001;104(10):1108–1113.

54. Gordon DJ, Rifkind BM. High-density lipoprotein--the clinical implications of recent studies. *N. Engl. J. Med.* 1989;321(19):1311–1316.

55. Voight BF et al. Plasma HDL cholesterol and risk of myocardial infarction: a mendelian randomisation study. *Lancet* 2012;380(9841):572–580.

56. Frikke-Schmidt R et al. Association of loss-of-function mutations in the ABCA1 gene with high-density lipoprotein cholesterol levels and risk of ischemic heart disease. *JAMA* 2008;299(21):2524–2532.

57. CARDIoGRAMplusC4D Consortium et al. Large-scale association analysis identifies new risk loci for coronary artery disease. *Nat. Genet.* 2013;45(1):25–33.

58. White J et al. Association of Lipid Fractions With Risks for Coronary Artery Disease and Diabetes. *JAMA Cardiol* 2016;1(6):692–699.

59. Willer CJ et al. Discovery and refinement of loci associated with lipid levels. *Nat. Genet.* 2013;45(11):1274–1283.

60. Schaefer JR. Lipid management for the prevention of cardiovascular disease. *Curr. Pharm. Des.* 2011;17(9):852–860.

61. Briel M et al. Association between change in high density lipoprotein cholesterol and cardiovascular disease morbidity and mortality: systematic review and meta-regression analysis. *BMJ* 2009;338:b92.

62. Grundy SM. Dyslipidaemia in 2015: Advances in treatment of dyslipidaemia. *Nat Rev Cardiol* 2016;13(2):74–75.

63. LaRosa JC, He J, Vupputuri S. Effect of statins on risk of coronary disease: a meta-analysis of randomized controlled trials. *JAMA* 1999;282(24):2340–2346.

64. Gadi R, Amanullah A, Figueredo VM. HDL-C: Does it matter? An update on novel HDL-directed pharmaco-therapeutic strategies. *Int. J. Cardiol.* 2013;167(3):646–655.

65. Kamanna VS, Kashyap ML. Mechanism of action of niacin. *Am. J. Cardiol.* 2008;101(8A):20B–26B.

66. Clofibrate and niacin in coronary heart disease. *JAMA* 1975;231(4):360–381.

67. AIM-HIGH Investigators et al. Niacin in patients with low HDL cholesterol levels receiving intensive statin therapy. *N. Engl. J. Med.* 2011;365(24):2255–2267.

68. Garg A et al. Role of Niacin in Current Clinical Practice: A Systematic Review. *Am. J. Med.* 2017;130(2):173–187.

69. Birjmohun RS, Hutten BA, Kastelein JJP, Stroes ESG. Efficacy and safety of high-density lipoprotein cholesterol-increasing compounds: a meta-analysis of randomized controlled trials. *J. Am. Coll. Cardiol.* 2005;45(2):185–197.

70. Guyton JR, Bays HE. Safety considerations with niacin therapy. *Am. J. Cardiol.* 2007;99(6A):22C–31C.

71. Wierzbicki AS, Viljoen A. Fibrates and niacin: is there a place for them in clinical practice? *Expert Opin Pharmacother* 2014;15(18):2673–2680.

72. Berthou L et al. Opposite regulation of human versus mouse apolipoprotein A-I by fibrates in human apolipoprotein A-I transgenic mice. *J. Clin. Invest.* 1996;97(11):2408–2416.

73. Staels B et al. Mechanism of action of fibrates on lipid and lipoprotein metabolism. *Circulation* 1998;98(19):2088–2093.

74. Jun M et al. Effects of fibrates on cardiovascular outcomes: a systematic review and meta-analysis. *Lancet* 2010;375(9729):1875–1884.

75. ACCORD Study Group et al. Effects of combination lipid therapy in type 2 diabetes

mellitus. *N. Engl. J. Med.* 2010;362(17):1563–1574.

76. Lee M, Saver JL, Towfighi A, Chow J, Ovbiagele B. Efficacy of fibrates for cardiovascular risk reduction in persons with atherogenic dyslipidemia: a meta-analysis. *Atherosclerosis* 2011;217(2):492–498.

77. Holmes MV, Smith GD. Dyslipidaemia: Revealing the effect of CETP inhibition in cardiovascular disease. *Nat Rev Cardiol* 2017;14(11):635–636.

78. Yamashita S, Hirano K, Sakai N, Matsuzawa Y. Molecular biology and pathophysiological aspects of plasma cholesteryl ester transfer protein. *Biochim. Biophys. Acta* 2000;1529(1-3):257–275.

79. Barter PJ et al. Cholesteryl ester transfer protein: a novel target for raising HDL and inhibiting atherosclerosis. *Arterioscler. Thromb. Vasc. Biol.* 2003;23(2):160–167.

80. Inazu A et al. Increased high-density lipoprotein levels caused by a common cholesteryl-ester transfer protein gene mutation. *N. Engl. J. Med.* 1990;323(18):1234–1238.

81. Johannsen TH, Frikke-Schmidt R, Schou J, Nordestgaard BG, Tybjaerg-Hansen A. Genetic inhibition of CETP, ischemic vascular disease and mortality, and possible adverse effects. *J. Am. Coll. Cardiol.* 2012;60(20):2041–2048.

82. Webb TR et al. Systematic Evaluation of Pleiotropy Identifies 6 Further Loci Associated With Coronary Artery Disease. *J. Am. Coll. Cardiol.* 2017;69(7):823–836.

83. Nomura A et al. Protein-Truncating Variants at the Cholesteryl Ester Transfer Protein Gene and Risk for Coronary Heart Disease. *Circ. Res.* 2017;121(1):81–88.

84. Barter PJ et al. Effects of torcetrapib in patients at high risk for coronary events. *N. Engl. J. Med.* 2007;357(21):2109–2122.

85. Schwartz GG et al. Effects of dalcetrapib in patients with a recent acute coronary syndrome. *N. Engl. J. Med.* 2012;367(22):2089–2099.

86. Lincoff AM et al. Evacetrapib and Cardiovascular Outcomes in High-Risk Vascular Disease. *N. Engl. J. Med.* 2017;376(20):1933–1942.

87. HPS3/TIMI55-REVEAL Collaborative Group. Effects of Anacetrapib in Patients with Atherosclerotic Vascular Disease. *N. Engl. J. Med.* 2017;377(13):1217–1227.

88. Tall AR, Rader DJ. Trials and Tribulations of CETP Inhibitors. *Circ. Res.* 2018;122(1):106–112.

89. Merck. Merck Provides Update on Anacetrapib Development Program [Internet]2017;http://investors.merck.com/news/press-release-details/2017/Merck-Provides-Update-on-Anacetrapib-Development-Program/default.aspx. cited

90. Rader DJ, Tall AR. The not-so-simple HDL story: Is it time to revise the HDL cholesterol hypothesis? *Nat. Med.* 2012;18(9):1344–1346.

91. Barter PJ, Rye K-A. Relationship between the concentration and antiatherogenic activity of high-density lipoproteins. *Curr. Opin. Lipidol.* 2006;17(4):399–403.

92. Sacks FM, Brewer HB. Petar Alaupovic: The father of lipoprotein classification based on apolipoprotein composition. *Arterioscler. Thromb. Vasc. Biol.* 2014;34(6):1111–1113.

93. Gustafson A, Alaupovic P, Furman RH. Studies of the composition and structure of serum lipoproteins: physical-chemical characterization of phospholipid-protein residues obtained from very-low-density human serum lipoproteins. *Biochim. Biophys. Acta* 1964;84:767–769.

94. Alaupovic P. Apoliproproteins and lipoproteins. *Atherosclerosis* 1971;13(2):141–146.

95. Alaupovic P, Lee DM, McConathy WJ. Studies on the composition and structure of plasma lipoproteins. Distribution of lipoprotein families in major density classes of normal human plasma lipoproteins. *Biochim. Biophys. Acta* 1972;260(4):689–707.

96. Kostner G, Alaupovic P. Studies of the composition and structure of plasma lipoproteins. Separation and quantification of the lipoprotein families occurring in the high density lipoproteins of human plasma. *Biochemistry* 1972;11(18):3419–3428.

97. Alaupovic P. Significance of apolipoproteins for structure, function, and classification of plasma lipoproteins. *Meth. Enzymol.* 1996;263:32–60.

98. Davidson WS, Shah AS. HDL Proteome Watch [Internet]. *httphomepages.uc.edudavidswmHDLproteome.html* http://homepages.uc.edu/~davidswm/HDLproteome.html. cited January 14, 2018

99. Vaisar T et al. Shotgun proteomics implicates protease inhibition and complement activation in the antiinflammatory properties of HDL. *J. Clin. Invest.* 2007;117(3):746–756.

100. Davidson WS et al. Proteomic analysis of defined HDL subpopulations reveals particle-specific protein clusters: relevance to antioxidative function. *Arterioscler. Thromb. Vasc. Biol.* 2009;29(6):870–876.

101. Rall SC, Weisgraber KH, Mahley RW. Human apolipoprotein E. The complete amino acid sequence. *J. Biol. Chem.* 1982;257(8):4171–4178.

102. van't Hooft F, Havel RJ. Metabolism of chromatographically separated rat serum lipoproteins specifically labeled with 125I-apolipoprotein E. *J. Biol. Chem.* 1981;256(8):3963–3968.

103. Mahley RW, Innerarity TL. Lipoprotein receptors and cholesterol homeostasis. *Biochim. Biophys. Acta* 1983;737(2):197–222.

104. Beisiegel U, Weber W, Ihrke G, Herz J, Stanley KK. The LDL-receptor-related protein, LRP, is an apolipoprotein E-binding protein. *Nature* 1989;341(6238):162–164.

105. Mahley RW, Weisgraber KH, Innerarity TL. Interaction of plasma lipoproteins containing apolipoproteins B and E with heparin and cell surface receptors. *Biochim. Biophys. Acta* 1979;575(1):81–91.

106. Futamura M et al. Two-step mechanism of binding of apolipoprotein E to heparin: implications for the kinetics of apolipoprotein E-heparan sulfate proteoglycan complex formation on cell surfaces. *J. Biol. Chem.* 2005;280(7):5414–5422.

107. Williams KJ, Chen K. Recent insights into factors affecting remnant lipoprotein uptake. *Curr. Opin. Lipidol.* 2010;21(3):218–228.

108. Gonzales JC, Gordts PLSM, Foley EM, Esko JD. Apolipoproteins E and AV mediate lipoprotein clearance by hepatic proteoglycans. *J. Clin. Invest.* 2013;123(6):2742–2751.

109. Bradley WA, Gianturco SH. ApoE is necessary and sufficient for the binding of large triglyceride-rich lipoproteins to the LDL receptor; apoB is unnecessary. *J. Lipid Res.* 1986;27(1):40–48.

110. Tomiyasu K, Walsh BW, Ikewaki K, Judge H, Sacks FM. Differential metabolism of human VLDL according to content of ApoE and ApoC-III. *Arterioscler. Thromb. Vasc. Biol.* 2001;21(9):1494–1500.

111. Zheng C, Khoo C, Ikewaki K, Sacks FM. Rapid turnover of apolipoprotein C-III-containing triglyceride-rich lipoproteins contributing to the formation of LDL subfractions. *J. Lipid Res.* 2007;48(5):1190–1203.

112. Murphy AJ et al. ApoE regulates hematopoietic stem cell proliferation, monocytosis, and monocyte accumulation in atherosclerotic lesions in mice. *J. Clin. Invest.* 2011;121(10):4138–4149.

113. Ali K, Middleton M, Puré E, Rader DJ. Apolipoprotein E suppresses the type I inflammatory response in vivo. *Circ. Res.* 2005;97(9):922–927.

114. Zhang H, Wu L-M, Wu J. Cross-talk between apolipoprotein E and cytokines. *Mediators Inflamm.* 2011;2011(4852):949072–10.

115. Yancey PG, Yu H, Linton MF, Fazio S. A pathway-dependent on apoE, ApoAI, and ABCA1 determines formation of buoyant high-density lipoprotein by macrophage foam cells. *Arterioscler. Thromb. Vasc. Biol.* 2007;27(5):1123–1131.

116. Huang ZH, Mazzone T. ApoE-dependent sterol efflux from macrophages is

modulated by scavenger receptor class B type I expression. *J. Lipid Res.* 2002;43(3):375–382.

117. Chroni A, Nieland TJF, Kypreos KE, Krieger M, Zannis VI. SR-BI mediates cholesterol efflux via its interactions with lipid-bound ApoE. Structural mutations in SR-BI diminish cholesterol efflux. *Biochemistry* 2005;44(39):13132–13143.

118. Zanotti I et al. Macrophage, but not systemic, apolipoprotein E is necessary for macrophage reverse cholesterol transport in vivo. *Arterioscler. Thromb. Vasc. Biol.* 2011;31(1):74–80.

119. Plump AS et al. Severe hypercholesterolemia and atherosclerosis in apolipoprotein E-deficient mice created by homologous recombination in ES cells. *Cell* 1992;71(2):343–353.

120. Linton MF, Atkinson JB, Fazio S. Prevention of atherosclerosis in apolipoprotein E-deficient mice by bone marrow transplantation. *Science* 1995;267(5200):1034–1037.

121. Innerarity TL, Pitas RE, Mahley RW. Receptor binding of cholesterol-induced high-density lipoproteins containing predominantly apoprotein E to cultured fibroblasts with mutations at the low-density lipoprotein receptor locus. *Biochemistry* 1980;19(18):4359–4365.

122. Hui DY, Innerarity TL, Mahley RW. Lipoprotein binding to canine hepatic membranes. Metabolically distinct apo-E and apo-B,E receptors. *J. Biol. Chem.* 1981;256(11):5646–5655.

123. Blum CB, Deckelbaum RJ, Witte LD, Tall AR, Cornicelli J. Role of apolipoprotein E-containing lipoproteins in abetalipoproteinemia. *J. Clin. Invest.* 1982;70(6):1157–1169.

124. Funke H et al. Uptake of apolipoprotein E-containing high density lipoproteins by hepatic parenchymal cells. *Arteriosclerosis* 1984;4(5):452–461.

125. Kypreos KE, Zannis VI. Pathway of biogenesis of apolipoprotein E-containing HDL in vivo with the participation of ABCA1 and LCAT. *Biochem. J.* 2007;403(2):359–367.

126. Mahley RW, Huang Y, Weisgraber KH. Putting cholesterol in its place: apoE and reverse cholesterol transport. *J. Clin. Invest.* 2006;116(5):1226–1229.

127. Koo C, Innerarity TL, Mahley RW. Obligatory role of cholesterol and apolipoprotein E in the formation of large cholesterol-enriched and receptor-active high density lipoproteins. *J. Biol. Chem.* 1985;260(22):11934–11943.

128. Settasatian N, Barter PJ, Rye K-A. Remodeling of apolipoprotein E-containing spherical reconstituted high density lipoproteins by phospholipid transfer protein. *J. Lipid Res.* 2008;49(1):115–126.

129. Ikewaki K, Rader DJ, Zech LA, Brewer HB. In vivo metabolism of apolipoproteins A-I and E in patients with abetalipoproteinemia: implications for the roles of apolipoproteins B and E in HDL metabolism. *J. Lipid Res.* 1994;35(10):1809–1819.

130. Mahley RW, Rall SC. Apolipoprotein E: far more than a lipid transport protein. *Annu Rev Genomics Hum Genet* 2000;1(1):507–537.

131. Weisgraber KH, Innerarity TL, Mahley RW. Abnormal lipoprotein receptor-binding activity of the human E apoprotein due to cysteine-arginine interchange at a single site. *J. Biol. Chem.* 1982;257(5):2518–2521.

132. Fredrickson DS, Levy RI, Lees RS. Fat transport in lipoproteins--an integrated approach to mechanisms and disorders. *N. Engl. J. Med.* 1967;276(4):215–25 contd.

133. Mahley RW, Huang Y, Rall SC. Pathogenesis of type III hyperlipoproteinemia (dysbetalipoproteinemia). Questions, quandaries, and paradoxes. *J. Lipid Res.* 1999;40(11):1933–1949.

134. Cullen P et al. Phenotype-dependent differences in apolipoprotein E metabolism and in cholesterol homeostasis in human monocyte-derived macrophages. *J. Clin. Invest.* 1998;101(8):1670–1677.

135. Okoro EU et al. Apolipoprotein E4 is deficient in inducing macrophage ABCA1 expression and stimulating the Sp1 signaling pathway. *PLoS ONE* 2012;7(9):e44430.

136. Miyata M, Smith JD. Apolipoprotein E allele-specific antioxidant activity and effects on cytotoxicity by oxidative insults and beta-amyloid peptides. *Nat. Genet.* 1996;14(1):55–61.

137. Jofre-Monseny L et al. Effects of apoE genotype on macrophage inflammation and heme oxygenase-1 expression. *Biochem. Biophys. Res. Commun.* 2007;357(1):319–324.

138. Song Y, Stampfer MJ, Liu S. Meta-analysis: apolipoprotein E genotypes and risk for coronary heart disease. *Ann. Intern. Med.* 2004;141(2):137–147.

139. Hospattankar AV, Brewer HB, Ronan R, Fairwell T. Amino acid sequence of human plasma apolipoprotein C-III from normolipidemic subjects. *FEBS Lett.* 1986;197(1-2):67–73.

140. Clavey V, Lestavel-Delattre S, Copin C, Bard JM, Fruchart JC. Modulation of lipoprotein B binding to the LDL receptor by exogenous lipids and apolipoproteins CI, CII, CIII, and E. *Arterioscler. Thromb. Vasc. Biol.* 1995;15(7):963–971.

141. Ginsberg HN et al. Apolipoprotein B metabolism in subjects with deficiency of apolipoproteins CIII and AI. Evidence that apolipoprotein CIII inhibits catabolism of triglyceride-rich lipoproteins by lipoprotein lipase in vivo. *J. Clin. Invest.* 1986;78(5):1287–1295.

142. Sehayek E, Eisenberg S. Mechanisms of inhibition by apolipoprotein C of apolipoprotein E-dependent cellular metabolism of human triglyceride-rich lipoproteins through the low density lipoprotein receptor pathway. *J. Biol. Chem.* 1991;266(27):18259–18267.

143. de Silva HV et al. Overexpression of human apolipoprotein C-III in transgenic mice results in an accumulation of apolipoprotein B48 remnants that is corrected by excess apolipoprotein E. *J. Biol. Chem.* 1994;269(3):2324–2335.

144. Aalto-Setälä K et al. Mechanism of hypertriglyceridemia in human apolipoprotein (apo) CIII transgenic mice. Diminished very low density lipoprotein fractional catabolic rate associated with increased apo CIII and reduced apo E on the particles. *J. Clin. Invest.* 1992;90(5):1889–1900.

145. Mendivil CO, Zheng C, Furtado J, Lel J, Sacks FM. Metabolism of very-low-density lipoprotein and low-density lipoprotein containing apolipoprotein C-III and not other small apolipoproteins. *Arterioscler. Thromb. Vasc. Biol.* 2010;30(2):239–245.

146. Kinnunen PK, Ehnolm C. Effect of serum and C-apoproteins from very low density lipoproteins on human postheparin plasma hepatic lipase. *FEBS Lett.* 1976;65(3):354–357.

147. Krauss RM, Herbert PN, Levy RI, Fredrickson DS. Further observations on the activation and inhibition of lipoprotein lipase by apolipoproteins. *Circ. Res.* 1973;33(4):403–411.

148. Larsson M, Vorrsjö E, Talmud P, Lookene A, Olivecrona G. Apolipoproteins C-I and C-III inhibit lipoprotein lipase activity by displacement of the enzyme from lipid droplets. *J. Biol. Chem.* 2013;288(47):33997–34008.

149. Ito Y, Azrolan N, O'Connell A, Walsh A, Breslow JL. Hypertriglyceridemia as a result of human apo CIII gene expression in transgenic mice. *Science* 1990;249(4970):790–793.

150. Maeda N et al. Targeted disruption of the apolipoprotein C-III gene in mice results in hypotriglyceridemia and protection from postprandial hypertriglyceridemia. *J. Biol. Chem.* 1994;269(38):23610–23616.

151. Pollin TI et al. A null mutation in human APOC3 confers a favorable plasma lipid profile and apparent cardioprotection. *Science* 2008;322(5908):1702–1705.

152. TG and HDL Working Group of the Exome Sequencing Project, National Heart, Lung, and Blood Institute et al. Loss-of-function mutations in APOC3, triglycerides, and coronary disease. *N. Engl. J. Med.* 2014;371(1):22–31.

153. Jørgensen AB, Frikke-Schmidt R, Nordestgaard BG, Tybjaerg-Hansen A. Loss-of-function mutations in APOC3 and risk of ischemic vascular disease. *N. Engl. J. Med.* 2014;371(1):32–41.

154. Gaudet D et al. Antisense Inhibition of Apolipoprotein C-III in Patients with Hypertriglyceridemia. *N. Engl. J. Med.* 2015;373(5):438–447.

155. Sacks FM. The crucial roles of apolipoproteins E and C-III in apoB lipoprotein metabolism in normolipidemia and hypertriglyceridemia. *Curr. Opin. Lipidol.* 2015;26(1):56–63.

156. Mendivil CO, Rimm EB, Furtado J, Chiuve SE, Sacks FM. Low-density lipoproteins containing apolipoprotein C-III and the risk of coronary heart disease. *Circulation* 2011;124(19):2065–2072.

157. Talayero B et al. Obesity Favors Apolipoprotein E and CIII-containing High-density Lipoprotein Subfractions Associated with Risk of Heart Disease. *J. Lipid Res.* 2014;55(10):2167–2177.

158. Jensen MK et al. HDL Subspecies Defined by Presence of Apolipoprotein C-III and Incident Coronary Heart Disease in Four Cohorts. *Circulation* 2017;:CIRCULATIONAHA.117.031276.

159. Aalto-Setälä K et al. Further characterization of the metabolic properties of triglyceride-rich lipoproteins from human and mouse apoC-III transgenic mice. *J. Lipid Res.* 1996;37(8):1802–1811.

160. Shelburne F, Hanks J, Meyers W, Quarfordt S. Effect of apoproteins on hepatic uptake of triglyceride emulsions in the rat. *J. Clin. Invest.* 1980;65(3):652–658.

161. Zheng C, Khoo C, Furtado J, Sacks FM. Apolipoprotein C-III and the metabolic basis for hypertriglyceridemia and the dense low-density lipoprotein phenotype. *Circulation* 2010;121(15):1722–1734.

162. Sacks FM, Alaupovic P, Moye LA. Effect of pravastatin on apolipoproteins B and C-III in very-low-density lipoproteins and low-density lipoproteins. *Am. J. Cardiol.* 2002;90(2):165–167.

163. Zheng C et al. Statins suppress apolipoprotein CIII-induced vascular endothelial cell activation and monocyte adhesion. *Eur. Heart J.* 2013;34(8):615–624.

164. Bagdade J, Barter P, Quiroga C, Alaupovic P. Effects of Torcetrapib and Statin Treatment on ApoC-III and Apoprotein-Defined Lipoprotein Subclasses (from the ILLUMINATE Trial). *Am. J. Cardiol.* 2017;119(11):1753–1756.

165. Blum CB et al. High density lipoprotein metabolism in man. *J. Clin. Invest.* 1977;60(4):795–807.

166. Tan MH et al. The effect of a high cholesterol and saturated fat diet on serum high-density lipoprotein-cholesterol, apoprotein A-I, and apoprotein E levels in normolipidemic humans. *Am. J. Clin. Nutr.* 1980;33(12):2559–2565.

167. Mensink RP, Zock PL, Kester ADM, Katan MB. Effects of dietary fatty acids and carbohydrates on the ratio of serum total to HDL cholesterol and on serum lipids and apolipoproteins: a meta-analysis of 60 controlled trials. *Am. J. Clin. Nutr.* 2003;77(5):1146–1155.

168. Mensink RP. *Effects of saturated fatty acids on serum lipids and lipoproteins: a systematic review and regression analysis*. World Health Organization; 2016:

169. Guasch-Ferré M et al. Dietary fat intake and risk of cardiovascular disease and all-cause mortality in a population at high risk of cardiovascular disease. *Am. J. Clin. Nutr.* 2015;102(6):1563–1573.

170. Wang DD et al. Association of Specific Dietary Fats With Total and Cause-Specific Mortality. *JAMA Intern Med* 2016;176(8):1134–1145.

171. Lichtenstein AH et al. Comparison of deuterated leucine, valine, and lysine in the measurement of human apolipoprotein A-I and B-100 kinetics. *J. Lipid Res.* 1990;31(9):1693–1701.

172. Schonfeld G, Frick MS, Bailey AP. Measurement of apolipoprotein A-I in rat high density lipoprotein and in rat plasma by radioimmunoassay. *J. Lipid Res.* 1976;17(1):25–29.

173. Desroches S et al. Apolipoprotein A-I, A-II, and VLDL-B-100 metabolism in men: comparison of a low-fat diet and a high-monounsaturated fatty acid diet. *J. Lipid Res.* 2004;45(12):2331–2338.

174. Wolf RN, Grundy SM. Influence of weight reduction on plasma lipoproteins in obese patients. *Arteriosclerosis* 1983;3(2):160–169.

175. Gylling H, Vega GL, Grundy SM. Physiologic mechanisms for reduced apolipoprotein A-I concentrations associated with low levels of high density lipoprotein cholesterol in patients with normal plasma lipids. *J. Lipid Res.* 1992;33(10):1527–1539.

176. Richard C, Couture P, Desroches S, Lichtenstein AH, Lamarche B. Effect of weight loss, independent of change in diet composition, on apolipoprotein AI kinetic in men with metabolic syndrome. *J. Lipid Res.* 2013;54(1):232–237.

177. Labonté M-È et al. Adding MUFA to a dietary portfolio of cholesterol-lowering foods reduces apoAI fractional catabolic rate in subjects with dyslipidaemia. *Br. J. Nutr.* 2013;110(3):426–436.

178. Richard C, Couture P, Desroches S, Lichtenstein AH, Lamarche B. Effect of an isoenergetic traditional Mediterranean diet on apolipoprotein A-I kinetic in men with metabolic syndrome. *Nutr J* 2013;12(1):76.

179. Brinton EA, Eisenberg S, Breslow JL. A low-fat diet decreases high density lipoprotein (HDL) cholesterol levels by decreasing HDL apolipoprotein transport rates. *J.*

Clin. Invest. 1990;85(1):144–151.

180. Matthan NR et al. Dietary hydrogenated fat increases high-density lipoprotein apoA-I catabolism and decreases low-density lipoprotein apoB-100 catabolism in hypercholesterolemic women. *Arterioscler. Thromb. Vasc. Biol.* 2004;24(6):1092–1097.

181. Vélez-Carrasco W et al. Dietary restriction of saturated fat and cholesterol decreases HDL ApoA-I secretion. *Arterioscler. Thromb. Vasc. Biol.* 1999;19(4):918–924.

182. Camus MC, Chapman MJ, Forgez P, Laplaud PM. Distribution and characterization of the serum lipoproteins and apoproteins in the mouse, Mus musculus. *J. Lipid Res.* 1983;24(9):1210–1228.

183. Caslake MJ, Farish E, Shepherd J. Metabolism of apolipoprotein A-I in healthy young adults. *Metab. Clin. Exp.* 1978;27(4):437–447.

184. Zech LA, Schaefer EJ, Bronzert TJ, Aamodt RL, Brewer HB. Metabolism of human apolipoproteins A-I and A-II: compartmental models. *J. Lipid Res.* 1983;24(1):60–71.

185. Brinton EA, Eisenberg S, Breslow JL. Increased apo A-I and apo A-II fractional catabolic rate in patients with low high density lipoprotein-cholesterol levels with or without hypertriglyceridemia. *J. Clin. Invest.* 1991;87(2):536–544.

186. Rader DJ, Castro G, Zech LA, Fruchart JC, Brewer HB. In vivo metabolism of apolipoprotein A-I on high density lipoprotein particles LpA-I and LpA-I,A-II. *J. Lipid Res.* 1991;32(11):1849–1859.

187. Ikewaki K et al. Evaluation of apoA-I kinetics in humans using simultaneous endogenous stable isotope and exogenous radiotracer methods. *J. Lipid Res.* 1993;34(12):2207–2215.

188. Thompson PD et al. Effect of prolonged exercise training without weight loss on high-density lipoprotein metabolism in overweight men. *Metab. Clin. Exp.* 1997;46(2):217–223.

189. De Oliveira E Silva ER et al. Alcohol consumption raises HDL cholesterol levels by increasing the transport rate of apolipoproteins A-I and A-II. *Circulation* 2000;102(19):2347–2352.

190. Mendivil CO, Furtado J, Morton AM, Wang L, Sacks FM. Novel Pathways of Apolipoprotein A-I Metabolism in High-Density Lipoprotein of Different Sizes in Humans. *Arterioscler. Thromb. Vasc. Biol.* 2016;36(1):156–165.

CHAPTER 2

Apolipoproteins E and CIII interact to regulate HDL metabolism and coronary

heart disease risk

Author Contributions

I performed all of the laboratory experiments with help from Liyun Wang and developed the kinetic models. Manja Koch analyzed the case-cohort study data and created Table 2.4, Table 2.5, Figure 2.8, and assisted with Table 2.1 and writing the manuscript. I interpreted all metabolic results and was responsible for all other Tables and Figures and writing the manuscript. Carlos Mendivil and Jeremy Furtado conceived and designed experiments. Anne Tjønneland and Kim Overvad had oversight of the Danish Diet, Cancer and Health study. Majken Jensen and Frank Sacks secured funding, conceived and designed experiments, interpreted all results and edited the manuscript. All authors discussed the results and provided input on the manuscript.

Abstract

Background: Subspecies of HDL contain apoE and/or apoCIII. Both proteins have

properties that could affect HDL metabolism. The relation between HDL metabolism and

risk of coronary heart disease (CHD) is not well understood.

Methods: Eighteen participants were given a bolus infusion of [D3]L-leucine to label

endogenously proteins on HDL. HDL was separated into subspecies containing apoE

and/or apoCIII, and then into four sizes. Metabolic rates for apoA-I in HDL subspecies

and sizes were determined by interactive modeling. The concentrations of apoE in HDL

that contain or lack apoCIII were measured in a prospective study in Denmark including

1,949 incident CHD cases during 9 years.

Results: HDL containing apoE but not apoCIII is disproportionately secreted into the

circulation; actively expands while circulating; and is quickly cleared. These are key

metabolic steps in reverse cholesterol transport, which may protect against

atherosclerosis. ApoCIII on HDL strongly attenuates these metabolic actions of HDL

apoE. In the epidemiological study, the relation between HDL apoE concentration and

CHD significantly differed depending whether apoCIII was present. HDL apoE was

associated significantly with lower risk of CHD only in the HDL subspecies lacking

apoCIII.

Conclusion: ApoE and apoCIII on HDL interact to affect metabolism and CHD. ApoE promotes metabolic steps in reverse cholesterol transport and is associated with lower risk of CHD. ApoCIII, when coexisting with apoE on HDL, abolishes these benefits. Therefore, differences in metabolism of HDL subspecies pertaining to reverse cholesterol transport are reflected in differences in association with CHD.

2.1. Introduction

Despite advances in research and clinical care, cardiovascular disease (CVD) remains the leading cause of mortality in the United States, accounting for about 1 in 3 deaths each year (1). Epidemiological studies unequivocally demonstrate a strong inverse relationship between HDL, measured by its cholesterol content (HDL-C) or by its primary protein apolipoprotein (apo) A-I, and risk of CVD (2, 3). HDL is thought to exert its cardio-protective effects, in part, by removing excess cholesterol from cells that are present in atherosclerosis and transporting it to the liver for excretion, a process known as reverse cholesterol transport. However, the failure of large-scale studies that raised HDL-C levels without reducing risk of coronary heart disease (CHD) (4-7) has stimulated research on the protein cargo on HDL and its ability to mediate HDL function.

It is becoming increasingly recognized that HDL is a heterogeneous particle system that carries a vast array of proteins with heterogeneous biological functions (8) involved in lipid metabolism, reverse cholesterol transport and other conditions. These resident proteins likely form distinct subpopulations, or subspecies, of HDL that may capture its functional relationships with cardiometabolic disease and relation to CHD more so than total HDL-C concentrations (9). However, little is known about the effect of these subspecies on HDL metabolism and CHD in humans.

ApoE affects the metabolism of apoB-containing lipoproteins, offering insights as to how it might affect HDL metabolism in humans. ApoE binds to LDL-receptor (-R) (10), LDL-R

related protein (LRP) (11), and heparin/heparan sulfate proteoglycans (12-15). In humans, VLDL and IDL that contain apoE are cleared from the circulation much more quickly than those without apoE (16, 17). Much less is known about apoE as a component of HDL. In vitro, apoE facilitates size expansion of HDL (18-20) due to its interaction with phospholipid polar head groups on HDL particles (21), which assist in enrichment of the HDL core with cholesterol ester. In mice, apoE promotes HDL biogenesis by interacting with ABCA1 independent of apoA-I (22). ApoE can also mediate holoparticle uptake of HDL into hepatocytes and other cells (23-25). Receptor binding studies in cultured human fibroblasts showed that HDL containing apoE from patients with abetalipoproteinemia (a condition in which no apoB-containing lipoproteins are synthesized) outcompeted radiolabeled LDL in binding to LDL-R, implying that apoE can effectively mediate HDL holoparticle uptake (26). Finally, Ikewaki et al (27) exogenously labeled apoA-I and apoE and reassociated them with autologous lipoproteins in patients with abetalipoproteinemia to assess whether apoE had an effect on apoA-I metabolism. They demonstrated that apoA-I on apoE-containing HDL was cleared from the circulation faster than apoA-I on HDL that does not contain apoE. This finding suggests that apoE may affect metabolism of native HDL in normal humans, in vivo.

ApoCIII delays clearance of apoB-containing lipoproteins, but little is known about its role in HDL metabolism. In vitro, apoCIII inhibits the binding of apoE and apoB to LDL-R and other receptors (28). In humans, VLDL and IDL that contain apoCIII are cleared more slowly from plasma than VLDL and IDL that do not contain apoCIII (29, 30).

Fibrates, which are PPARα agonists, lower plasma apoCIII as one of their actions on the lipoprotein system, and increase clearance not only of apoB-containing lipoproteins but also of HDL apoA-I (31). That reduction in plasma apoCIII is correlated with increased clearance of HDL apoA-I (31). These findings together offer a hypothesis that apoCIII slows HDL clearance, which could have important implications for CVD pathophysiology.

In addition to their individual roles, apoE and apoCIII act in opposition to modulate the clearance of apoB-containing lipoproteins. In fibroblasts, apoCIII inhibits the apoE-dependent uptake of VLDL by LDL-R (28, 32). Addition of apoCIII to apoE-enriched chylomicrons in rats results in a pronounced inhibition of clearance of hepatic chylomicron and triglyceride emulsions (33). In mice, overexpression of apoCIII reduces VLDL clearance, and this action is rescued by either exogenous apoE or genetic apoE overexpression (34). Similarly, co-expression of the *APOE* transgene in *APOC3* transgenic mice eliminates the hypertriglyceridemia caused by apoCIII (34, 35). Finally, in kinetic studies of human VLDL and IDL, apoCIII overrides the increased clearance promoted by apoE (17, 30, 36). It is unknown if apoE and apoCIII function similarly on HDL.

The clinical implications of apoE on HDL are still poorly defined, potentially due to the presence of other proteins obscuring its true effect. Among 5 proteins on HDL found to differ in control subjects and participants with coronary artery disease (CAD), apoE was discovered to be the most abundant protein in HDL isolated from atherosclerotic lesions

(37) suggesting an important role of apoE in HDL in atherosclerosis pathophysiology. The few studies available examining the relation of apoE in HDL to CVD outcomes were together inconclusive (38, 39). In previous work in the Nurses' Health Study, the Health Professionals Follow-Up Study, the Multi-Ethnic Study of Atherosclerosis, and the Danish Diet, Cancer and Health study, four large prospective cohort studies, we found that the association of HDL with CHD risk was modified by the presence of apoCIII (40). HDL containing apoCIII was associated with higher risk of CHD, whereas HDL not containing apoCIII was associated with lower CHD risk.

The aims of this study were to determine if apoE and/or apoCIII has effects on human HDL metabolism, and whether the effects on metabolism had clinical counterparts in CHD risk. We hypothesized that HDL containing apoE would participate in reverse cholesterol transport, a hallmark of HDL antiatherogenic function. We considered crucial aspects of reverse cholesterol transport to be a) evidence of size expansion followed by b) increased clearance rates from the circulation. We also hypothesized that HDL containing apoCIII would have an attenuated clearance rate in vivo. Clinically, we hypothesized that apoE in HDL would be inversely related to incident CHD, and that apoCIII would mitigate this protective effect. We carried out these aims in a metabolic study in humans and a prospective case-cohort study nested in a large community-based sample.

2.2. Methods

Study population and design: For the metabolic study, we recruited adults between 23-70 years old who had low HDL-C (<45 mg/dL for men, <55 mg/dL for women) and high BMI (25-35 kg/m^2). Exclusion criteria included HDL-C (<20 mg/dL), LDL-C (>160 mg/dL), TG (>500 mg/dL), and use of lipid lowering medications or hormone replacement therapy, diabetes, and E2/E2 or E4/E4 apoE genotypes. In total, 63 individuals were screened, 24 completed part or all of the study, and 18 were analyzed.

The association of apoE in HDL and incident CHD was investigated in 3,639 participants that were part of a previous case-cohort study nested in the in the Danish Diet, Cancer, and Health study. As described in detail previously, the Diet, Cancer, and Health (DCH) study is an ongoing prospective study initiated in 1993-1997 when 57,053 Danish born residents, aged 50 to 65 years without record of cancer diagnosis in the Danish Cancer Registry, participated in a clinical examination and detailed lifestyle survey (60).

This case-cohort study included all confirmed incident cases of CHD between study entry and May 2008 (n=2,063) and a random subcohort (n=1,824) of individuals from the original DCH cohort who were free of CHD at baseline. After exclusion of participants for whom information on our main biochemical exposures was missing, the case-cohort included 1,946 participants with incident CHD and 1,750 participants of the random subcohort. Due to the case-cohort design, 57 participants with incident CHD are also part of the random subcohort.

The baseline examination included anthropometric and blood pressure measurements performed by trained laboratory technicians from Brigham and Women's Hospital. Participants completed self-administered questionnaires requesting information on participant's age, sex, years of education, smoking status, alcohol consumption, and history of hypertension and diabetes. Average alcohol consumption over the previous year (g/d) was calculated based on reported alcoholic beverages (beer, wine, spirits and mixed drinks) assessed with a validated food-frequency questionnaire mailed to the study participants before the visit to the study center. Blood was sampled at baseline in the study clinics in Aarhus and Copenhagen and plasma samples were stored at −150°C.

Dietary protocol: The participants of the metabolic study received a healthy high unsaturated fat diet (45% carbohydrate, 40% fat [10% sat, 23% mono, 7% poly], 15% protein, 180 mg cholesterol per day) for 28 days prior to the kinetic study. The diet was formulated by the Center for Clinical Investigation nutrition research unit of Brigham and Women's Hospital in Boston, MA. Participants picked up all their food to take home on Monday, Wednesday, and Friday at the study site. All food and beverages were provided, and participants were not allowed to eat any other food, but were allowed diet soda, coffee, and tea. Alcoholic beverages were not included or permitted. Physical activity was not monitored, but participants were asked not to alter their usual physical activity pattern. Participants were weighed during food pickups and dietitians adjusted

the amount of food to prevent changes in weight. These procedures have been used in our previous studies (17, 30, 41).

Infusion Protocol: On the morning of Day 29, participants in the metabolic study were admitted to the Clinical and Translational Science Center (CTSC) at Brigham & Women's Hospital. Participants were given intravenously a bolus of (5,5,5-D3) L-leucine (Cambridge Isotope Laboratories, Cambridge, MA) at a dose of 10 mg/kg, administered in a volume of 150 mL at 15 mL/minute. Blood was sampled at 0, 0.5, 1, 1.5, 2, 3, 4, 6, 8, 10, 12, 14, 16, 18, 22, 46, 70, and 94 hours post-infusion into chilled tubes that had been stored in the cold room. Plasma was separated immediately in a refrigerated centrifuge and aliquoted into tubes containing phenylmethanesulfonyl fluoride, gentamicin, benzamidine, and a protease inhibitor cocktail (all from Sigma). Aliquots were stored at -80°C until lipoprotein separation began after a mean time of 12 months (range 1 to 24 months).

HDL subspecies separation using immunoaffinity column chromatography: These methods have been described in detail (9). Briefly, thawed plasma from each time point was incubated with Sepharose 4B immunoaffinity columns (Bio-Rad) containing affinity purified polyclonal antibodies to apoA-I (Academy Biomedical). The apoA-I containing bound lipoproteins were eluted with 3M sodium thiocyanate, and immediately desalted in PBS. This procedure was repeated with the unbound lipoproteins to improve recovery of apoA-I. Then, apoA-I containing lipoproteins were incubated in an anti-apoE immunoaffinity column (Academy Biomedical) to separate HDL into two subspecies:

HDL not containing apoE (E-), and HDL containing apoE (E+). In the last ten participants, an additional immunoaffinity separation using anti-apoCIII (Academy Biomedical) columns produced four subspecies: HDL not containing apoE or apoCIII (E-CIII-), HDL containing apoCIII but not apoE (E-CIII+), HDL containing apoE but not apoCIII (E+CIII-), and HDL containing both apoE and apoCIII (E+CIII+). Repeat incubation of unbound HDL to apoE or apoCIII columns was not needed. Efficiency of columns was measured and determined to be 90% for apoA-I, 99% for apoE, and 98-99% for apoCIII. There were no differences in size or subspecies distribution comparing the HDL that bound to the anti-apoA-I antibody resin and that which did not.

HDL size separation and apoA-I purification: These methods have been described in detail (41). Briefly, HDL subspecies were separated by size using non-denaturing polyacrylamide gel electrophoresis (PAGE) on a 4-30% gradient gel (Jule Biotechnologies) into four sizes: alpha-1 (9.5-12.2nm), alpha-2 (8.2-9.5nm), alpha-3 (7.1-8.2nm), and prebeta (<7.1nm) and then electrophoretically transferred to a 0.45 micrometer polyvinylidene difluoride (PVDF) membrane. The membranes were then stained with 0.2% amido black. HDL of each size were excised from PVDF membranes and eluted overnight at 4°C in Tris-SDS-Triton-X. ApoA-I from each HDL size was purified using SDS-PAGE in a 4-20% gradient, transferred to a PVDF membrane and stained with 0.2% amido black. Excised apoA-I bands underwent amino acid hydrolysis and derivatization to heptafluorobutyric acid esters. Measurements of tracer enrichment were performed by gas chromatography/single-ion monitoring mass spectrometry as previously described (17).

<u>Tracer enrichment and pool size:</u> The apoA-I tracer enrichment at each time point was defined as area under the curve (AUC) of D3-leucine / (AUC of D3-leucine + AUC of D0-leucine). ApoA-I concentration of each HDL subspecies was measured at each time point using SDS-PAGE band densitometry, corrected to plasma total apoA-I values determined by ELISA. ApoA-I pool size was determined by multiplying apoA-I concentration by plasma volume, which was assumed to be 4.4% of ideal body weight (calculated by using a BMI of 25 kg/m^2). Because all participants were overweight, we adjusted the plasma volume using the following formula: Adjusted plasma volume = ideal body weight * 0.044 + excess weight * 0.010 (61).

To facilitate workflow, we evaluated the importance of early and late time points which do not affect ascertainment of the critical parts of the enrichment curve (the rise to peak enrichment and the descending slope). Time points 0.5, 1.5, 70, and 94 hours were later omitted from laboratory separation after determining they did not affect fitted curves or the fractional catabolic rates.
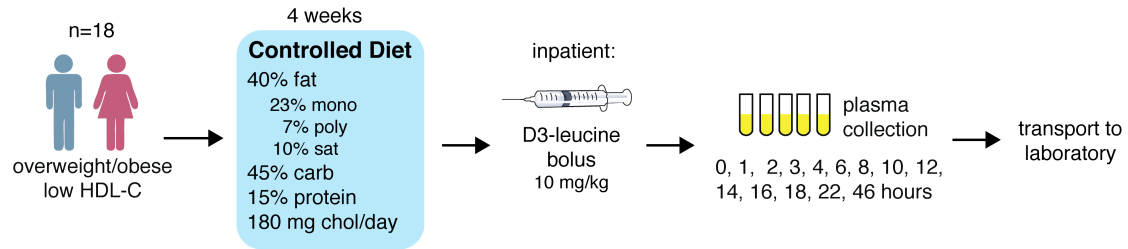
Pool sizes of plasma total apoA-I were calculated by summing the pool sizes of the E+ and E- subspecies. Tracer enrichments of plasma total apoA-I at each time point were constructed by summing the enrichments of apoA-I in the E+ and E- subspecies, weighting them by relative pool size. Pool sizes of apoA-I in the CIII- and CIII+ subspecies were determined by summing the pool sizes in the relevant subspecies: E-CIII- and E+CIII- to make CIII-; E-CIII+ and E+CIII+ to make CIII+. Tracer enrichments

of apoA-I in the CIII- and CIII+ subspecies were constructed by summing the enrichments of apoA-I in the relevant subfractions (see above) and weighting them by relative pool size.

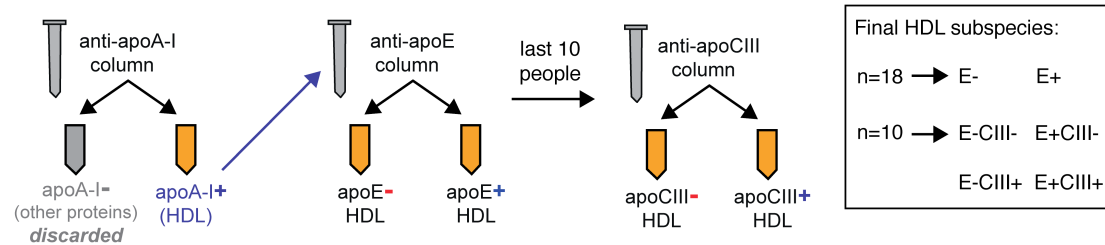These methods are summarized in **Figure 2.1**.

Model development and kinetic analysis: Compartmental modeling was performed using SAAM-II (The Epsilon Group, Charlottesville, VA) (43). We constructed models using prior knowledge about human HDL physiology (41). The input is a forcing function using free plasma leucine isotopic enrichment. The model outputs were rate constants (in pools/hour, converted to pools/day) and flux measurements (in mg/hour, converted to mg/day), each with a standard deviation and 95% confidence interval. For each HDL subspecies, we chose the most parsimonious model that had the most favorable statistics. Fractional catabolic rates (FCRs) for a specific HDL subspecies were calculated by summing all the rate constants out of the compartment for that subspecies. All models were initially established by using the average data of the subjects, and then the data for each subject were modeled individually. For a full description of the modeling process, please see **Chapter 4**.

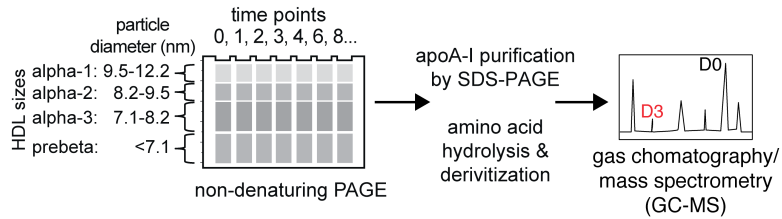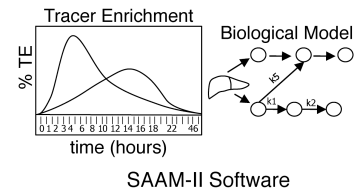**Figure 2.1:** Overview of clinical protocol and laboratory methods.

Plasma lipid and apolipoprotein measurements: Plasma concentrations of lipids and apolipoproteins were measured at time zero of the infusion protocol. Total plasma cholesterol and triglycerides were measured using an enzymatic assay (Thermo Scientific). HDL-C was measured as above in the supernatant of plasma after the precipitation of apoB-containing lipoproteins with dextran sulfate (50,000 MW, Genzyme). LDL-C was estimated using the Friedewald equation (62). ELISA using affinity-purified antibodies (Academy Bio-Medical Co.) was performed to measure plasma concentrations of apoA-I, apoE, apoCIII, and apoB. HDL subspecies according to apoCIII were measured in plasma samples stored at -80°C. A sandwich ELISA approach was applied as previously described (63). ELISA plates were read with a BioTek Synergy HT 96-well plate reader controlled by Gen5 1.10 software. All assays were completed in triplicate, and any sample with an intra-assay coefficient of variation >15% was repeated. Final data were exported to Microsoft Excel for analysis and database management.

Molar ratios: HDL subspecies were generated using immunoaffinity column chromatography as described above. Cholesterol content of each subspecies was measured using a commercially available enzymatic assay as described above. The concentrations of apoA-I, apoE, and apoCIII on each HDL subspecies were determined by sandwich ELISA (9). The molar ratios of apoE:apoA-I and apoCIII:apoA-I were calculated using the molecular weights of the three apolipoproteins. Cholesterol ratios were determined by dividing the cholesterol content of each subspecies by the plasma apoA-I concentration.

ApoE genotyping: We performed genotyping on buffy coat samples using the ABI

PRISM 7900HT Sequence Detection System (Applied Biosystems, Foster City, CA), in

384-well format. The 5' nuclease assay (TaqMan®) was used to distinguish the two

alleles of a gene. PCR amplification was carried out on 5-20ng DNA using 1 X

TaqMan® universal PCR master mix (No Amp-erase UNG) in a 5ml reaction volume.

Amplification conditions on an AB 9700 dual plate thermal cycler (Applied Biosystems,

Foster City, CA) were as follows: 1 cycle of 95°C for 10min, followed by 50 cycles of

92°C for 15s and 60°C for 1 min. TaqMan® assays were ordered using the ABI Assays-

on-Demand service.

CHD assessment: Information on CHD (non-fatal myocardial infarction [MI] and fatal

coronary heart disease) during follow-up until 2008 was obtained as previously

described (64). Briefly, the unique personal identification number assigned to all Danish

citizens in the Danish Civil Registration System allowed identification of hospital

discharges in the Danish National Register of Patients and the Cause of Death

Register. Registers provided information on first-time discharge diagnosis of MI

(International Classification of Diseases [ICD], 8th revision codes 410 to 410.99; and

ICD 10th revision codes I21.0-I21.9) and diagnosis of sudden cardiac death diagnosis

(ICD 8: 427.27 or ICD 10: I46.0-I46.9) if the cardiac arrest after validation was believed

to be caused by an MI. The diagnosis of registered MIs was verified with hospital

medical records (65) which were reviewed in accordance with current guidelines (66).

This registry has a high degree of validity in recorded MIs (65).

Statistical analysis: The results are presented as means $\pm$ SEM unless otherwise specified. Paired t tests were used to compare two parameters in the same participants (for example, apoA-I pool sizes, FCRs, and fluxes in HDL containing or not containing apoE). Overall differences in FCRs, fluxes, and pool sizes across the four HDL subspecies were examined using a mixed effects model with HDL subspecies as a fixed factor and participant ID as a random factor. Tests to compare HDL subspecies were carried out independently in each HDL size. Significance was denoted as $p<0.05$ unless otherwise specified. All statistical analysis was performed using Stata 14 (College Station, TX) or GraphPad Prism 7 (La Jolla, CA). This study had greater than 90% power to detect significant ($p<0.05$) differences in FCR between apoE-containing and non-apoE-containing subspecies.

We evaluated the baseline characteristics of participants with incident CHD during the follow-up period and the random subcohort separately. Wilcoxon rank-sum tests and chi-square tests were performed to compare continuous and categorical characteristics of cases and controls. Spearman correlation coefficients were used to evaluate the association of apoE in HDL containing or not containing apoCIII with HDL, apoCIII, HDL containing or not containing apoCIII, apoB and triglycerides. We estimated hazard ratios (HRs) and 95% confidence intervals (CI) for CHD using Cox proportional hazards regression with standard inverse probability weights and age used as the underlying time scale and stratification by sex. To account for oversampling of cases, female non-cases were given a weight of 24,658/917 and male non-cases were given a weight of

55

28,785/842 corresponding to the number of men or women in the full cohort (sex-specific counts of non-cases in the overall cohort divided by the sex-specific counts of non-cases in the random subcohort). We assessed the proportionality of hazards over time (here: age) by including an interaction term of the HDL subspecies with age as a covariate. Apolipoprotein measures were modeled continuous (log_2-transformed) and as quintiles based on the distribution of the subcohort. Wald tests for trend were performed with apolipoprotein variables modeled as the median of each quintile. We first adjusted for laboratory batch, smoking status (never; former; current <15, 15-24, ≥ 25 g/day), education (missing, <8; 8-10; >10 years), alcohol intake (nondrinker; drinker <5, 5-9, 10-19, 20-39, ≥40 g/alcohol/day), BMI (<25; 25-<30; >30 kg/m2), and self-reported diagnosis of hypertension, and self-reported diagnosis of diabetes at baseline. In subsequent models, we additionally adjusted for HDL, apoCIII, triglycerides, and apoB. Models included apoE in HDL containing apoCIII and HDL not containing apoCIII simultaneously and likelihood ratio tests were used to assess slope heterogeneity of the two HDL subspecies containing or not containing apoCIII with the null hypothesis of them being equal. All analyses were performed using STATA 12.1 statistical software (StataCorp, College Station, TX)

Study approval: The study was performed in accordance with the principles of the Declaration of Helsinki and all participants gave written informed consent. Procedures of the metabolic study were approved by the Human Subjects Committees at Brigham and Women's Hospital. The Danish Diet, Cancer and Health study was approved by the

National Committee on Health Research Ethics and the Danish Data Protection Agency
(KF 01-116/96).

2.3. Results

For the metabolic study, we enrolled 18 adults (9 male and 9 female; **Table 2.1**).

Participants had low HDL-C (<45 mg/dL for males, <55 mg/dL for females), and were

overweight (BMI $\geq$25 kg/m^2). The median apoA-I concentration in plasma was 100

mg/dL. Plasma concentrations of apoE and apoCIII were normal. We studied apoA-I-

containing HDL subspecies containing apoE (E+) or not containing apoE (E-) in all 18

participants, and HDL subspecies containing apoE and/or apoCIII in a subset of 10

participants (4 male, 6 female).

ApoA-I metabolism of four HDL sizes: After administering a high unsaturated fat control

diet for four weeks, we infused study participants with a bolus of tri-deuterated leucine

(5,5,5-D3 L-leucine, D3-leucine), and isolated and purified apoA-I from plasma collected

over time (**Figure 2.1**). To compare with the metabolism of a human population we have

previously studied (41), we first modeled the metabolism of plasma apoA-I in four sizes

of HDL (**Figure 2.2**). Alpha-2 and alpha-3, large and medium size HDL (42), are the

major size fractions of HDL in these participants, accounting for about 75% of total

apoA-I mass (**Figure 2.2A**). Discoidal prebeta HDL comprises about 10% of plasma

apoA-I. We modeled the tracer enrichment curves and masses using SAAM-II, a

commercially available modeling software (43). We found that the model that

Table 2.1: Characteristics of participants in the metabolic study (A.M.M.) and the case-cohort study (M.K.) nested in the Danish Diet, Cancer and Health study.

| Variable | Metabolic study[A] | | Case-cohort study[B] | | |
	Full set with HDL E+, E- measurement (N=18)	Subset with HDL apoE and/or apoCIII measurement (N=10)	Random subcohort (N=1,750)	CHD (N=1,946)	P for difference
Age, y	49 (23, 70)	49 (23, 70)	56 (51, 64)	59 (51, 65)	<0.001
Male	9 (50)	4 (40)	933 (53)	1,419 (73)	<0.001
Current smoker	NA	NA	662 (38)	1070 (55)	<0.001
Alcohol intake, g/day[C]	0	0	14 (1, 66)	14 (0.2, 69)	0.69
BMI, kg/m^2	30 (26, 36)	31 (26, 36)	26 (20, 33)	27 (21, 35)	<0.001
Hypertension[D]	3 (17%)	2 (20%)	259 (15)	498 (26)	<0.001
Diabetes[D]	0 (0)	0 (0)	31 (2)	107 (6)	<0.001
LDL-C[E], mg/dL	117 (59, 184)	106 (59, 147)	137 (87, 197)	151 (92, 210)	<0.001
HDL-C, mg/dL	45 (24, 54)	46 (24, 54)	52 (27, 90)	46 (24, 89)	<0.001
Triglycerides, mg/dL	112 (50, 271)	80 (62, 262)	81 (36, 237)	108 (43, 304)	<0.001
HDL-ApoA-I[F], mg/dL	100 (73, 147)	111 (73, 147)	136 (78, 224)	134 (74, 230)	0.04
Plasma apoCIII[G], mg/dL	8 (3.5, 13.5)	8 (3.5, 13.5)	11 (4, 23)	11 (4, 24)	0.76
Plasma apoE, mg/dL	6.0 (4.0, 9.5)	6.5 (4.0, 9.5)	NA	NA	
ApoE genotype			NA	NA	
E3/E3	9 (50)	4 (40)			
E2/E3	1 (6)	0 (0)			
E4/E3	6 (33)	4 (40)			
E2/E4	2 (11)	2 (20)			

[A]Median (range) or N (%). [B]Median (5th and 95th percentiles) or N (%). [C]N=3 missing. [D]Self-reported physician diagnosis of hypertension or diabetes. [E]N=95 missing in random subcohort and N=984 missing in CHD cases. [F]The concentration of HDL was quantified based on apoA-I levels, the major apolipoprotein component of HDL. [G]N=1 missing in random cohort.
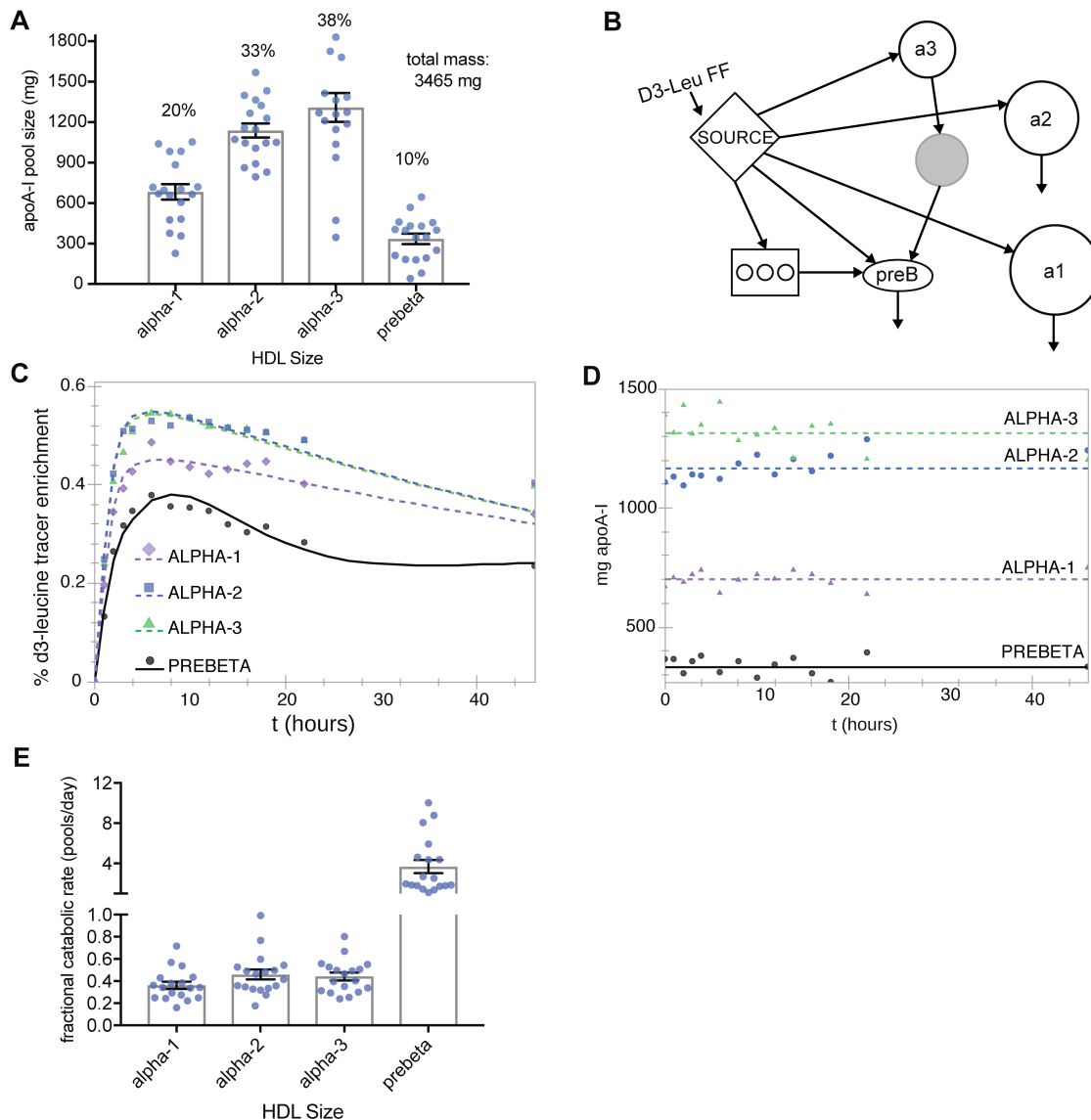
Figure 2.2: ApoA-I metabolism on four sizes of HDL (n=18). (A) Left: mean pool size of plasma apoA-I for four sizes of HDL, calculated from SDS-PAGE band densitometry corrected to plasma apoA-I concentrations measured by ELISA. Error bars = SEM. Numbers above bars: Mean percent plasma apoA-I distribution across HDL sizes. **(B)** Compartmental model used in SAAM-II with the greatest parsimony ("bare minimum model"). Plasma D3-leucine enrichment, the precursor to protein synthesis, is modeled

(Figure 2.2 continued)

as a forcing function (FF) input to the liver or intestine ("Source" compartment). Circles

represent each HDL size (from large to small: a1 = alpha-1, a2 = alpha-2, a3 = alpha-3,

preB = prebeta). Arrows between compartments represent transfer of apoA-I. Arrows

out of compartments represent clearance of apoA-I from plasma. The rectangle with

interior circles represents an intravascular delay compartment used for synthesis,

assembly, and secretion of apoA-I. The gray circle represents a non-sampled

remodeling compartment to generate prebeta HDL from alpha-3 HDL such as by the

action of SR-B1 or hepatic TG lipase. **(C)** SAAM-II model fit of mean tracer enrichment

in HDL apoA-I for each HDL size. The tracer enrichments were generated by averaging

all participants' enrichments at each time point. **(D)** SAAM-II model fit of mean apoA-I

mass (pool size) for each HDL size. The masses were the averages of all participants'

masses at each time point. Masses were measured from SDS-PAGE band

densitometry corrected to plasma apoA-I concentrations measured by ELISA. **(E)** Mean

apoA-I fractional catabolic rates (representing protein turnover) for each HDL size. A

value of 0.4 represents 40% of the protein pool turned over each day. Each dot

represents a single participant. Error bars = SEM.

provided excellent fits to the data is characterized by direct secretion of all four sizes of

HDL and size contraction from alpha-3 to prebeta, representing prebeta generation

(**Figure 2.2B**). We called this the "bare minimum model" due to its parsimony (for

additional information on model development, please see **Chapter 4**). The tracer

enrichment curves (**Figure 2.2C**) and pool sizes (**Figure 2.2D**) with SAAM-II model fits

are shown for the average of 18 people for four sizes of HDL. Fractional catabolic rates

(FCRs), representing turnover of apoA-I, were about 0.4 pools/day for apoA-I on alpha-

1, -2, and -3 HDL and 3.7 pools/day for prebeta (**Figure 2.2E, Table 2.2**). These results

are consistent with those in a previous report in a separate group of humans (41).

ApoA-I metabolism on HDL containing or not containing apoE: To model the tracer

enrichments and pool sizes of apoA-I of the HDL subspecies, we started with the

previous well-characterized "bare minimum model" for plasma apoA-I across four HDL

sizes (**Figure 2.3A, Figure 2.2B**). However, the apoA-I of E+ HDL required size

expansion from prebeta to alpha-1 and alpha-2 to fit the tracer enrichment curves

(**Figure 2.3B**). This flux pathway was not needed to fit E- HDL. **Figure 2.3C** shows the

tracer enrichment curves and model fits of apoA-I tracer enrichments on E- HDL and E+

HDL. Compared to E- HDL, the tracer enrichment curves of apoA-I in E+ HDL had

steeper slopes to and from the peak, generally indicative of faster turnover. The FCR of

apoA-I on E+ HDL was about 8, 4, and 4 times faster than that of E- HDL for alpha 1, 2,

and 3 respectively ($p \leq 0.001$ for all, paired t-test), and not significantly different for

prebeta HDL (p=0.13) (**Figure 2.3D** and **Table 2.2)**. Only about 4% of apoA-I HDL

Table 2.2: Concentration, percent distribution, and mass ratios of HDL-C and apoA-I across four HDL subspecies (n=10).

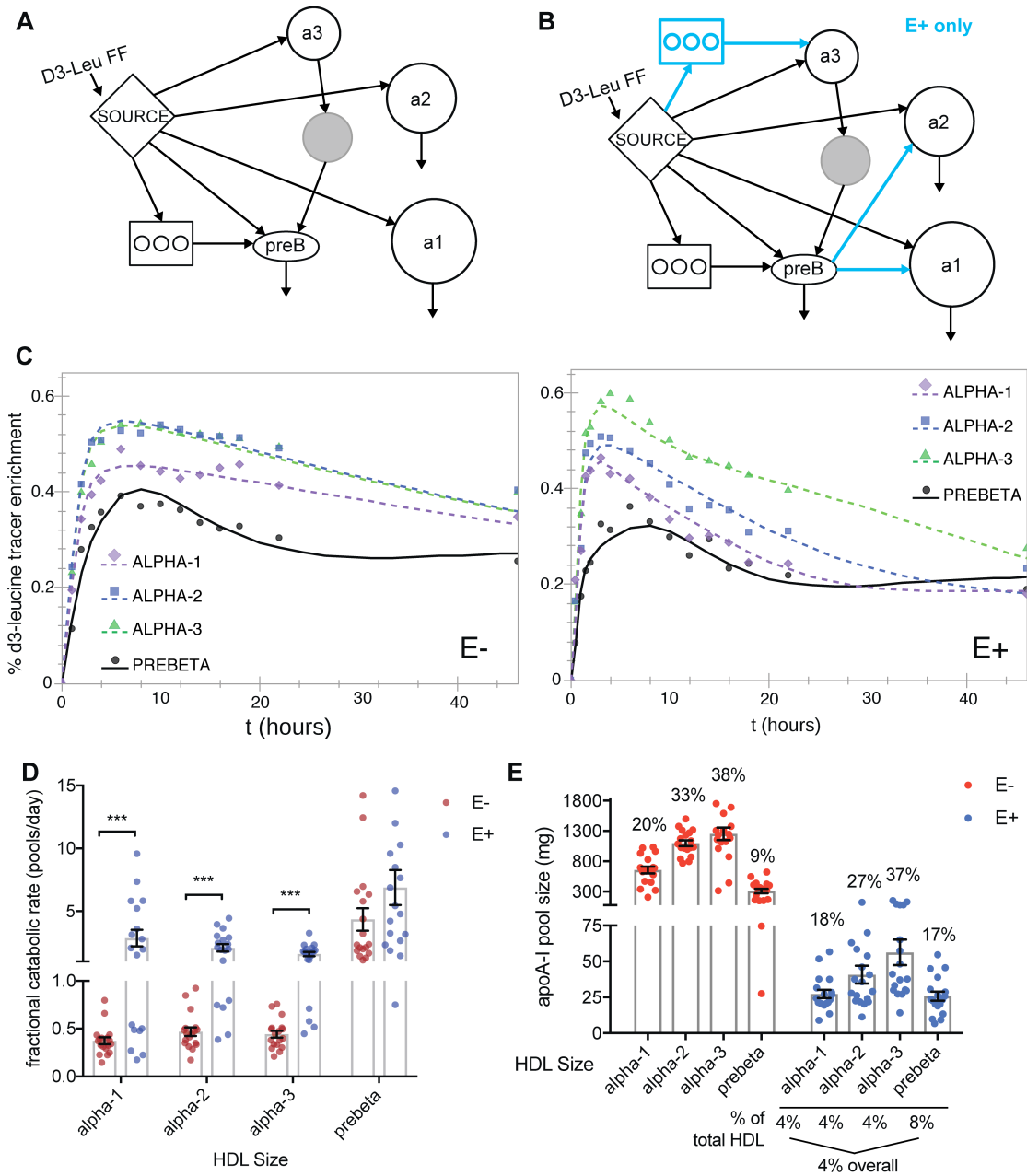|	HDL-C (mg/dl)				apoA-I (mg/dl)				HDL-C : apoA-I ratio
	Mean	SEM	% of total	SEM	Mean	SEM	% of total	SEM	
E-CIII-	33	3	82%	7%	101	7	91%	6%	0.3
E-CIII+	3	0.3	8%	1%	6	1	6%	1%	0.5
E+CIII-	2	0.2	5%	0.5%	2	0.4	2%	0.4%	0.8
E+CIII+	2	0.2	5%	0.4%	1	0.2	1%	0.1%	1.3
Sum	40		100%		112		100%		0.4

Figure 2.3: The metabolism of HDL based on presence or absence of apoE (n=18).

Figure 2.3 (cont.): The metabolism of HDL based on presence or absence of apoE (n=18). (A) HDL not containing apoE (E-). Compartmental model used in SAAM-II with the greatest parsimony ("bare minimum model"). Plasma D3-leucine enrichment, the precursor to protein synthesis, is modeled as a forcing function (FF) input to the liver or intestine ("Source" compartment). Circles represent each HDL size (from large to small: a1 = alpha-1, a2 = alpha-2, a3 = alpha-3, preB = prebeta). Arrows between compartments represent transfer of apoA-I. Arrows out of compartments represent clearance of apoA-I from plasma. Rectangles with interior circles represent intravascular delay compartments used for lipoprotein synthesis, assembly, and secretion. The gray circle represents a non-sampled remodeling compartment to generate prebeta HDL from alpha-3 HDL. **(B) HDL containing apoE (E+).** Modifications to the bare minimum model from Figure 2A, showing additional size expansion and intravascular delay pathways used in modeling tracer enrichment of apoA-I in HDL containing apoE (E+) (shown in blue). **(C)** Model fit of apoA-I tracer enrichments in HDL not containing apoE (E-) (left) and HDL containing apoE (E+) (right). The tracer enrichments for each HDL size were generated by averaging all participants' enrichments at each time point. **(D)** Mean apoA-I fractional catabolic rates, representing protein turnover, in HDL not containing apoE (E-) or containing (E+). Each dot represents a single participant (n=18). Error bars = SEM. ***: p<0.005 for E+ vs. E-, Student's paired two-sided *t*-test. **(E)** Mean pool sizes (masses) of apoA-I in HDL not containing apoE (E-) and HDL containing apoE (E+). Each dot represents a single participant. Numbers above bars represent percent of total pool size (mass) in that subspecies. Bottom right corner: percent of apoA-I mass on E+ HDL by size and overall. Error bars = SEM.

contained apoE (**Figure 2.3E**). The size distributions for apoA-I in E+ and E- HDL were similar.

ApoA-I on HDL containing or not containing apoCIII: We also wanted to determine if there was a unique effect of apoCIII on HDL metabolism (as was seen with apoE) (**Figure 2.4**). We used the same "bare minimum model" established for E- HDL (**Figure 2.3A**, **Figure 2.2B**) to model the tracer enrichment curves for apoA-I in CIII- (**Figure 2.4A**) and CIII+ (**Figure 2.4B**) HDL. The enrichment curves for both subspecies appeared similar and were both visually similar to those of plasma apoA-I and E- HDL (**Figure 2.2C**, **Figure 2.3C**). Corroborating these visual findings, the apoA-I FCRs shown in Figure 4C and summarized in Supplemental Table 1 were not significantly different between CIII- and CIII+ HDL (p-value for two-tailed paired *t* test not significant across each size) and were similar to those of plasma apoA-I and E- HDL (**Figure 2.2E**, **Figure 2.3D**). As with the E+ subspecies, a small percentage of apoA-I resides on HDL that contains apoCIII, and the size distributions for apoA-I on CIII+ and CIII- HDL were relatively similar (**Figure 2.4D**). Taken together, these results demonstrated no clear difference in apoA-I metabolism between HDL containing apoCIII and HDL not containing apoCIII.

HDL speciation according to presence of apoE and/or apoCIII: Because we hypothesized that apoE and CIII have antagonistic effects on HDL metabolism, we studied the metabolism of apoA-I on the four subspecies with and without apoE and/or apoCIII: E-CIII-, E+CIII-, E-CIII+, and E+CIII+. **Figure 2.5** describes the distribution of
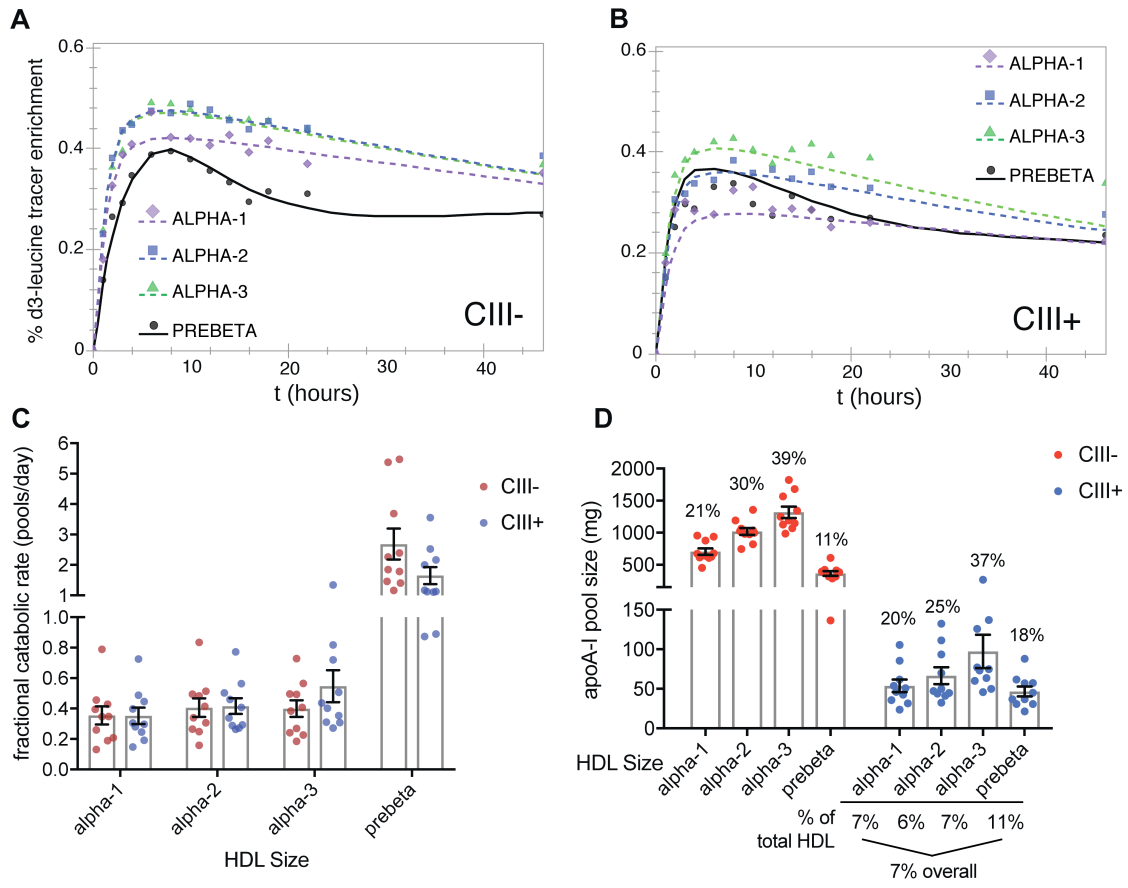
Figure 2.4: The metabolism of HDL based on presence or absence of apoCIII (n=10).

Figure 2.4 (continued): The metabolism of HDL based on presence or absence of apoCIII (n=10). (A) Model fit in SAAM-II of average tracer enrichment in HDL not containing apoCIII (CIII-). The tracer enrichments were generated by averaging all participants' enrichments at each time point. The model used was the "bare minimum model" (Figure 2A). **(B)** Model fit in SAAM-II of average tracer enrichment in HDL containing apoCIII (CIII+). The tracer enrichments were generated by averaging all participants' enrichments at each time point. The model used was the "bare minimum model" (Figure 2A). **(C)** Mean plasma apoA-I fractional catabolic rates on HDL not containing apoCIII (CIII-) and containing apoCIII (CIII+). Each dot represents a single participant. Error bars = SEM. All comparisons between sizes not significant (p>0.05) by Student's paired two-sided *t*-test. **(D)** Mean pool sizes of apoA-I in HDL not containing apoCIII (CIII-) and HDL containing apoCIII (CIII+). Each dot represents an individual participant. Numbers above bars represent percent of total pool size in that subspecies. Bottom right corner: percent of apoA-I mass on CIII+ HDL by size and overall. Error bars = SEM.
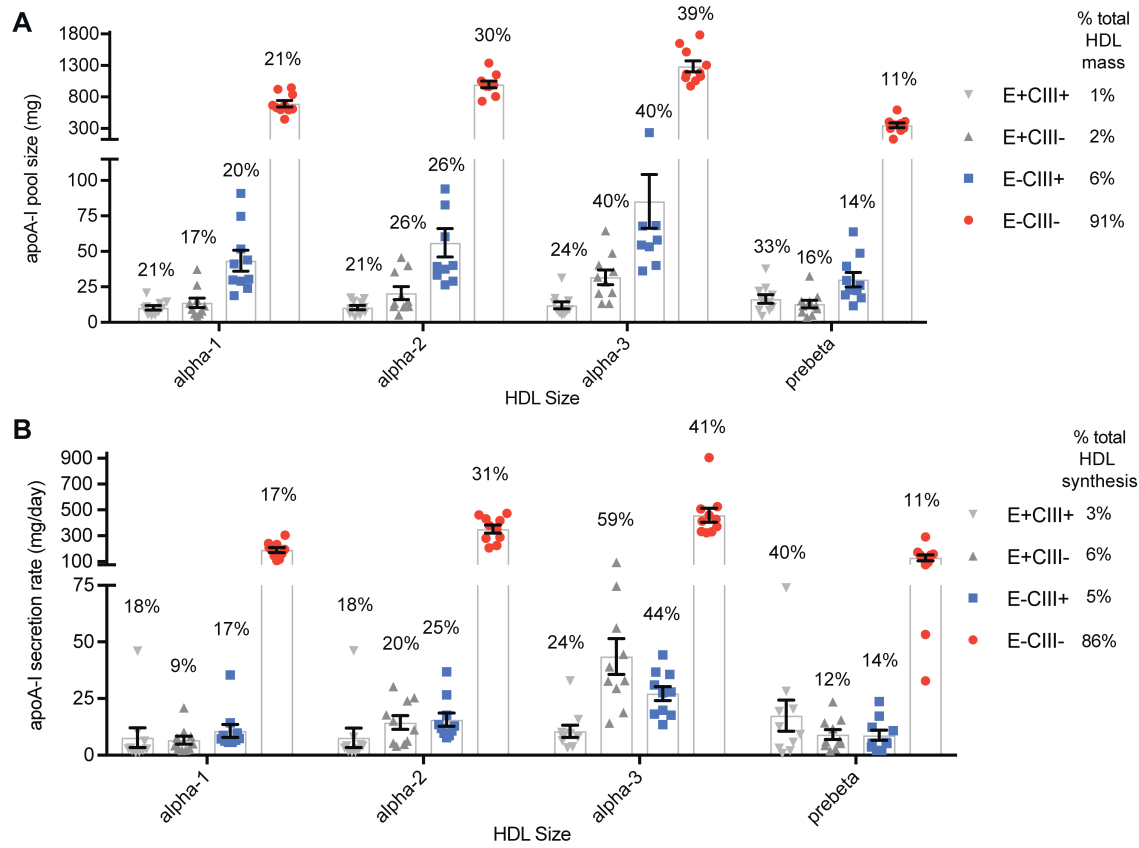
Figure 2.5: Plasma pool size and secretion rates of HDL subspecies containing apoE and/or apoCIII (n=10).

Figure 2.5 (continued): Plasma pool size and secretion rates of HDL subspecies containing apoE and/or apoCIII (n=10). (A) Mean plasma apoA-I pool size, calculated by SDS-PAGE densitometry corrected to plasma apoA-I concentrations measured by ELISA. Each point represents an individual participant. Numbers over bars represent the percent of pool size for each subspecies. Error bars = SEM. Right: Percent of total HDL mass. E+CIII+: HDL containing apoE and apoCIII. E+CIII-: HDL containing apoE but not apoCIII. E-CIII+: HDL containing apoCIII but not apoE. E-CIII-: HDL not containing apoE or apoCIII. **(B)** Mean plasma apoA-I secretion rates in four HDL subspecies defined by presence or absence of apoE or apoCIII, determined by SAAM-II modeling software. Each point represents an individual participant. Numbers over bars represent the percent of total apoA-I secretion (synthesis) for each subspecies. Error bars = SEM. Right: Percent of total HDL secretion (synthesis).

apoA-I mass and secretion across the four subspecies each separated into four sizes. The majority of apoA-I mass was in E-CIII- HDL (91%), followed by 6% in E-CIII+, 2% in E+CIII-, and 1% in E+CIII+ (**Figure 2.5A**). Consistent with these values, the majority of HDL-C is found on E-CIII- HDL (82%), followed by 8% in E-CIII+, 5% in E+CIII-, and 5% in E+CIII+ (**Table 2.3**). The intra-subspecies size distribution was roughly similar across the subspecies, except for E+CIII+, which had a disproportionate amount of apoA-I on prebeta (33% of E+CIII+ mass vs. 16%, 14%, and 11% in the other three subspecies). The majority of apoA-I was secreted on E-CIII- HDL (86%), consistent with its large pool size (**Figure 2.5B**). E-CIII+ received 5% of total apoA-I secretion, E+CIII- received 6%, and E+CIII+ received 3%. The percent distribution of apoA-I secretion onto each size was similar by subspecies, with alpha-2 and alpha-3 HDL having the most apoA-I synthesis per day. E+CIII- HDL had a disproportionate amount of apoA-I secretion (6% of total apoA-I secretion vs. 2% of total apoA-I mass), as did E+CIII+ (3% of total apoA-I secretion vs. 1% of total apoA-I mass). **Figure A3.1** illustrates these model-derived rates and pool sizes for the four HDL subspecies divided into four sizes. We also calculated molar ratios of apolipoproteins on each HDL subspecies, aggregating all sizes together. There was about 1 apoE to each apoA-I on E+CIII-, 2 apoCIII per apoA-I on E-CIII+, and about 2.5 apoE and 5 apoCIII per apoA-I on E+CIII+. These values are consistent with what has been reported previously in a separate group of participants (9).

We then modeled the apoA-I tracer enrichment in each subspecies, using the average enrichment data of 10 participants (**Figure 2.6A**). Tracer enrichments of apoA-I in all
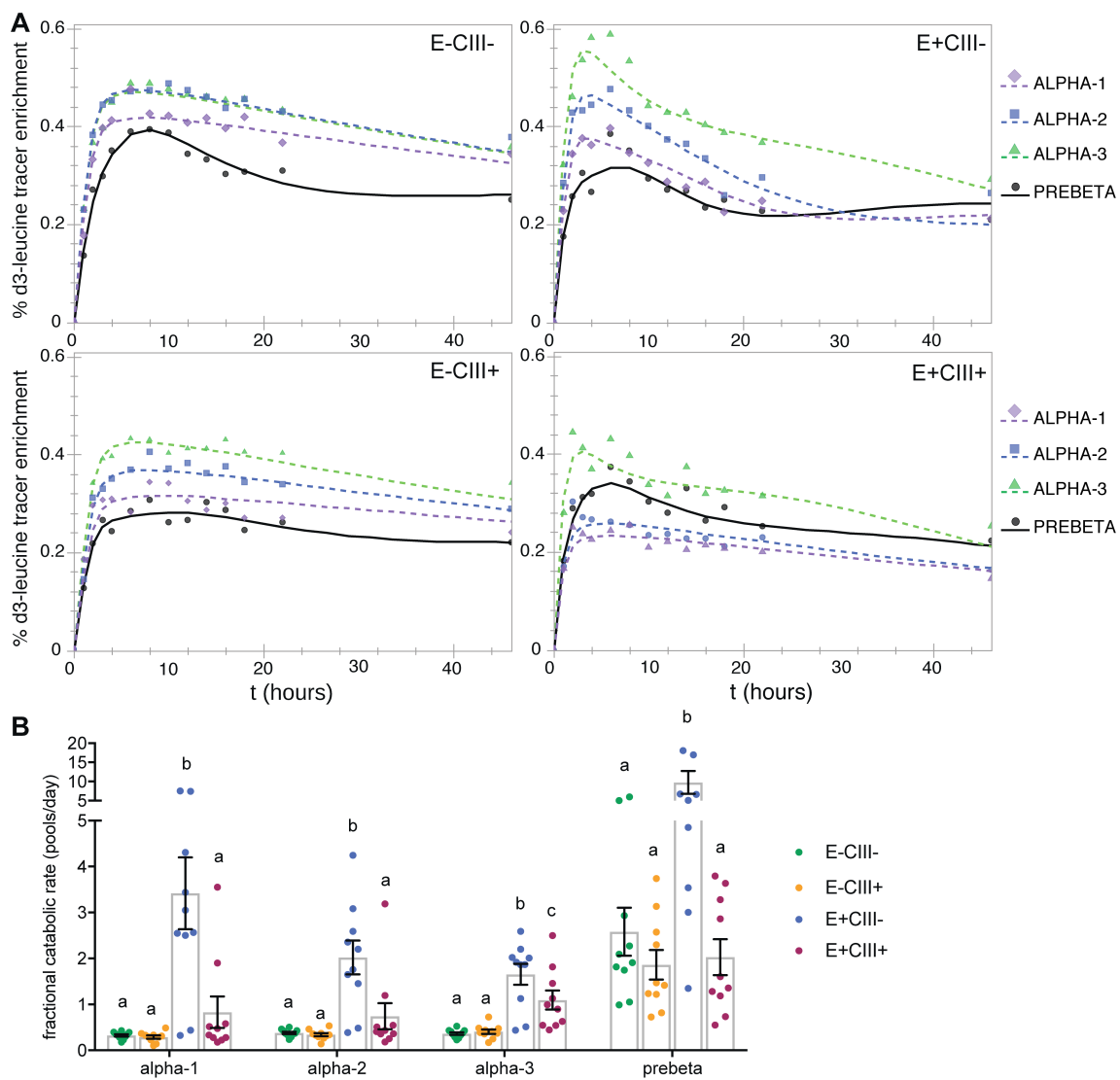
Figure 2.6: Interaction between apoE and apoCIII on HDL: Model fit for apoA-I tracer enrichments and apoA-I FCRs (pools/day) in four HDL subspecies each separated into four HDL sizes (n=10).

Figure 2.6 (continued): Interaction between apoE and apoCIII on HDL: Model fit for apoA-I tracer enrichments and apoA-I FCRs (pools/day) in four HDL subspecies each separated into four HDL sizes (n=10). (A) Model fit and mean tracer enrichments. The % D3-leucine tracer enrichments [D3-leucine/(D3-leucine + unlabeled leucine)*100] were computed by averaging all participants' enrichments (n=10) at each time point and modeling them as a single participant. Points = data; Lines = model fit. The "bare minimum model", as shown in Figure 2.2A, was used for E-CIII-, E-CIII+, and E+CIII+ (defined in Figure 2.5). The complex model, as shown in Figure 2.2B, was used for E+CIII- only. **(B)** ApoA-I fractional catabolic rates, representing protein turnover. Each point represents a single participant (n=10). A value of 1 = 100% of protein pool turned over per day. Horizontal lines in bars = mean. Error bars = SEM. Within each HDL size, different letters above means refer to statistically different means (p<0.005 vs. all other subspecies as assessed by mixed effects model). Specifically, the FCR of E+C-III- subspecies in each size is significantly faster than that of the other subspecies, whereas the FCR of E+C-III+ is not significantly higher, suggesting an interaction between the two apolipoproteins on HDL. One outlier is not shown for visual purposes (E+CIII- prebeta, value 31 pools/day) but was included in the statistical analysis.

sizes and subspecies of HDL appeared in circulation at about the same time, as we

reported previously (41). In all subspecies, tracer enrichment of apoA-I in the smallest

prebeta HDL peaked later than the larger alpha sizes, indicating that prebeta could not

be a pure precursor to any larger HDL, a major principle of reverse cholesterol

transport. Notably, apoA-I in the E+CIII- subspecies had faster rises and steeper

descending slopes in tracer enrichments compared to the other subspecies, suggestive

of faster HDL turnover.

The final models used in SAAM-II are shown in **Figure 2.3A-B**. The model with the

greatest parsimony, the "bare minimum model," is characterized by direct secretion of

all HDL sizes from the source compartment, an intravascular delay compartment for the

prebeta fraction, no size conversion of a smaller to a larger HDL, and size contraction

only from alpha-3 to prebeta HDL (**Figure 2.3A**). This model had satisfactory visual fit

and was statistically suitable (the majority of parameter values estimated by SAAM-II

had 95% confidence intervals excluding zero) for all subspecies and sizes except for the

E+CIII-, which required a more complex model (**Figure 2.3B**). This subspecies uniquely

required size expansion pathways from prebeta HDL to alpha-2 and alpha-1 to fit the

data. These size expansion pathways both improved the visual fit and reduced the

weighted residual sum of squares (WRSS) enough to justify their addition, as

determined by a significant result by F test (**Figure 2.7**). The final models also had

excellent apoA-I mass fits, and the masses from SAAM-II modeling correlated highly to

those measured in SDS-PAGE band quantification (**Figure A3.2**). Model development

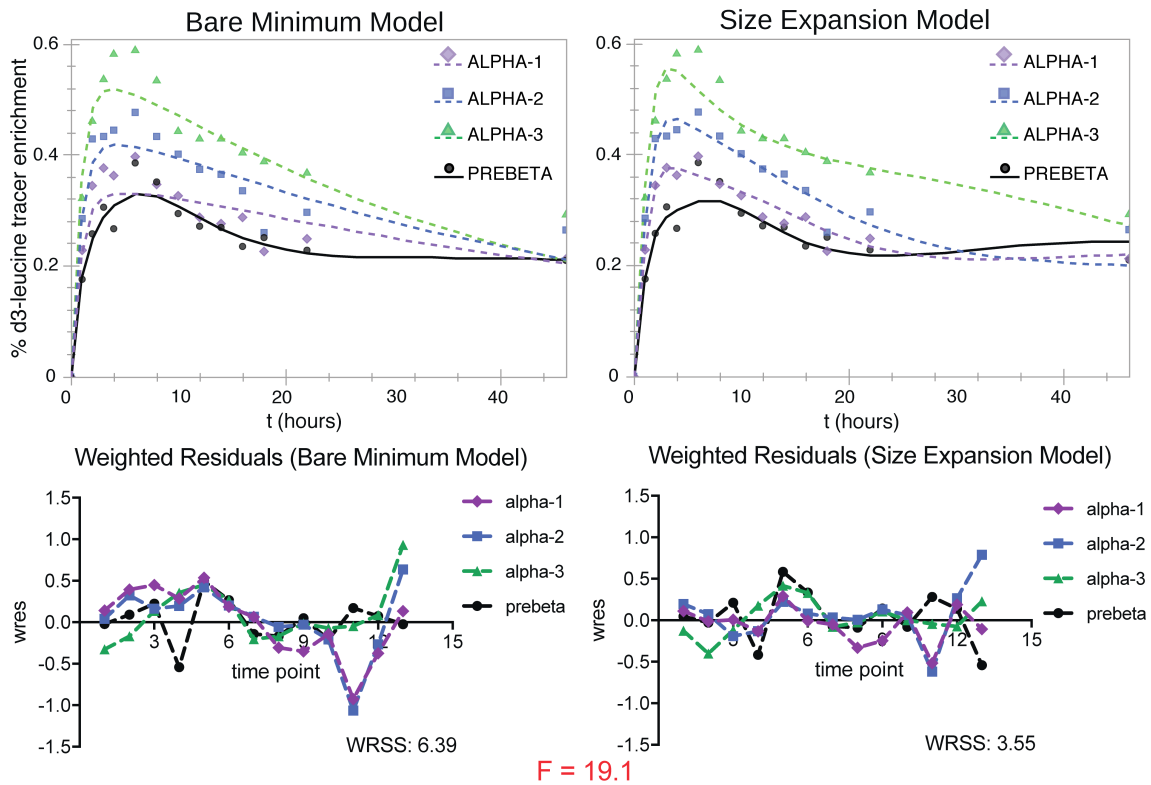is described in detail in **Chapter 4**.

Figure 2.7: Justification for use of a more complex model that includes size expansion for the HDL E+CIII- subspecies. Shown are model fits of the average apoA-I tracer enrichments in HDL E+CIII-, using the bare minimum model (left, shown in Figure 2A) vs. complex model featuring size expansion (right, shown in Figure 2B) (n=10). Weighted residuals (wres) for each time point (13 in total, 1 hour to 46 hours) are shown below with WRSS and value for F-statistic (comparison of models: p<0.001). The highly significantly lower WRSS for the size expansion model used for HDL E+CIII- indicates that the additional pathways for size expansion are needed to optimize the fit of the model to the data.

Fractional catabolic rates: After establishing the final models using the average tracer enrichment and pool sizes of 10 participants, we then modeled the apoA-I tracer enrichment and pool sizes of each participant in the study to calculate clearance rates (**Figure 2.6B**). Uniquely, apoA-I on E+CIII- was cleared 2-11 times faster than E-CIII-, E-CIII+, and E+CIII+ depending on the size (p<0.001 for all comparisons). These accelerated turnover rates contributed to the disproportionately greater flux of apoA-I in the E+CIII- subspecies relative to its share of the apoA-I pool size (**Figure 2.5A-B**). Importantly, FCRs for apoA-I on E+CIII+ were significantly slower than on E+CIII-. E+CIII+ had slightly faster turnover rates than on E-CIII+ and E-CIII-, though it was only significant in the small alpha-3 size. FCRs for apoA-I on E-CIII- and E-CIII+ were similar. Altogether, these results demonstrate an interaction between apoE and apoCIII on the clearance rate of HDL apoA-I.

Subgroup analyses: **Table 2.3** is a breakdown of apoA-I FCR, pool size, and flux in each subspecies by sex, race, apoE genotype, and BMI (overweight vs. obese). We did not test for statistical significance due to small sample size, but we report the following potentially interesting findings: the average male apoA-I FCR was higher than the average female apoA-I FCR, and the apoE2/E4 genotype had lower apoA-I clearance rates than apoE3/E3 in the E+ subspecies.

Association of apoE in HDL containing or not containing apoCIII and risk for CHD: We then wanted to determine if differences in metabolism among these HDL subspecies corresponded to differences in risk of CHD. We used a case-cohort study nested within

75

Table 2.3: Effect of covariates on FCRs, pool size, and secretion rates of apoA-I in HDL subspecies (n=10).

	Fractional catabolic rate (pools/day)[A]															
	Sex				Race				ApoE Genotype						BMI (kg/m^2)	
	Male[B]		Female[C]		White[C]		Black[B]		E3/E3[B]		E4/E3[B]		E2/E4[D]		<30[E]		>30[E]
HDL	Mean	SEM	Mean	SEM	Mean	SEM	Mean	SEM	Mean	SEM	Mean	SEM	Mean	SEM	Mean	SEM	Mean	SEM
E-CIII-	0.64	0.04	0.44	0.02	0.52	0.02	0.53	0.06	0.56	0.05	0.48	0.04	0.51	0.04	0.55	0.04	0.50	0.04
E-CIII+	0.60	0.09	0.47	0.04	0.57	0.07	0.46	0.05	0.54	0.02	0.54	0.10	0.48	0.05	0.51	0.02	0.54	0.09
E+CIII-	2.89	0.42	2.41	0.22	2.93	0.24	2.23	0.42	2.91	0.28	3.06	0.13	1.05	0.08	2.91	0.25	2.29	0.35
E+CIII+	1.57	0.34	1.06	0.26	1.56	0.35	0.82	0.09	1.33	0.28	1.44	0.36	0.77	0.10	1.72	0.35	0.81	0.12

	Plasma mass (mg)[F]															
	Sex				Race				ApoE Genotype						BMI (kg/m^2)	
	Male		Female		White		Black		E3/E3		E4/E3		E2/E4		<30		>30
HDL	Mean	SEM	Mean	SEM	Mean	SEM	Mean	SEM	Mean	SEM	Mean	SEM	Mean	SEM	Mean	SEM	Mean	SEM
E-CIII-	2967	101	3194	150	3038	162	3201	77	3336	170	2940	97	2965	1	3237	164	2970	84
E-CIII+	165	23	208	30	147	16	256	30	180	14	190	41	214	18	164	16	217	35
E+CIII-	59	10	71	10	45	4	98	8	53	4	61	12	105	2	50	4	83	11
E+CIII+	42	6	44	5	40	5	49	6	40	5	44	6	50	6	43	5	44	6

	Flux (mg/day)[G]															
	Sex				Race				ApoE Genotype						BMI (kg/m^2)	
	Male		Female		White		Black		E3/E3		E4/E3		E2/E4		<30		>30
HDL	Mean	SEM	Mean	SEM	Mean	SEM	Mean	SEM	Mean	SEM	Mean	SEM	Mean	SEM	Mean	SEM	Mean	SEM
E-CIII-	1922	172	1393	74	1530	55	1716	222	1870	176	1389	75	1504	118	1763	171	1446	98
E-CIII+	88	9	90	7	81	9	103	4	98	10	78	7	95	1	87	11	92	3
E+CIII-	138	20	168	27	129	14	198	31	160	22	177	30	109	6	150	21	163	28
E+CIII+	67	21	42	8	35	1	64	18	48	8	66	21	33	0	74	18	30	3

[A]FCRs for each HDL size are weighted by respective pool size and combined into a "total" FCR for each subspecies.
[B]n=4. [C]n=6. [D]n=2. [E]n=5. [F]Pool sizes are calculated from SAAM-II. [G]Total amount cleared from plasma each day.

the Danish Diet, Cancer and Health study including 1,750 participants selected randomly at baseline and 1,946 participants with incident CHD cases during a median follow-up of 9 years (**Table 2.1**). The median levels of apoA-I in each HDL subspecies were not different in the random subcohort versus in the participants who developed CHD, and the concentration of apoE in each HDL subspecies correlated moderately with other lipoprotein measurements (**Table 2.4**). In multivariable adjusted regression analysis, the concentration of apoE in unfractionated HDL was not statistically significantly associated with CHD risk (**Table 2.5**). The hazard ratio (HR) for CHD across extreme quintiles of apoE in unfractionated HDL was 0.97 (95% CI 0.66, 1.41; p-trend=0.88). Next, we investigated if the concentration of apoE in separate subspecies of HDL containing or not containing apoCIII was differentially related to incident CHD **(Figure 2.8, Table 2.5)**. In multivariable regression analysis, adjusting for potential confounders, the risk for CHD across extreme quintiles of apoE in HDL that contained apoCIII was not statistically significantly higher (HR 1.29 [95% CI 0.86, 1.93]; p-trend=0.25). In contrast, in HDL not containing apoCIII, the concentration of apoE was inversely related to risk of CHD. The risk of CHD was 34% lower in participants in the highest quintile compared to participants in the lowest quintile of apoE levels in the subspecies of HDL not containing apoCIII (HR 0.66 [95% CI 0.48, 0.89]; p-trend=0.01). The regression coefficients of apoE in the two HDL subspecies containing and not containing apoCIII and CHD risk were statistically significantly different (p-heterogeneity=0.02)

Table 2.4: Concentrations[A] of apoE in HDL[B] that contains apoCIII and apoE in HDL that does not contain apoCIII, and Spearman correlations with apolipoproteins and triglycerides in the random subcohort, n=1750. **Table author: Manja Koch**

	Random subcohort (n=1,750)	CHD (n=1,946)	Random subcohort					
			ApoE in HDL		*ApoE in HDL that contains apoCIII*		*ApoE in HDL that does not contain apoCIII*	
			r	p	r	p	r	p
HDL-ApoA-I, mg/dL	136 (78, 224)	134 (74, 230)	0.160	<0.001	0.108	<0.001	0.137	<0.001
ApoCIII[C], mg/dL	11 (4, 23)	11 (4, 24)	0.040	0.098	0.153	<0.001	-0.039	0.100
ApoE in HDL, mg/dL	2 (1, 5)	2 (1, 7)						
ApoE in HDL that contains apoCIII, mg/dL	1 (0.2, 3)	1 (0.3, 4)						
ApoE in HDL that does not contain apoCIII, mg/dL	1 (0.3, 3)	1 (0.3, 3)						
HDL that contains apoCIII, mg/dL	11 (4, 26)	11 (4, 28)	0.064	0.007	0.149	<0.001	-0.001	0.976
HDL that does not contain apoCIII, mg/dL	123 (71, 202)	122 (67, 211)	0.162	<0.001	0.094	<0.001	0.145	<0.001
ApoB, mg/dL	88 (48, 146)	98 (54, 167)	-0.069	0.004	0.018	0.453	-0.113	<0.001
Triglycerides, mg/dL	81 (36, 237)	108 (43, 304)	0.021	0.373	0.193	<0.001	-0.133	<0.001

[A]Median (5th and 95th percentiles). [B]The concentration of HDL was quantified based on apoA-I levels, the major apolipoprotein component of HDL. [C]n=1749.

Table 2.5: Hazard Ratios (HRs)[A] and 95% confidence intervals of CHD according to quintiles of the concentration of apoE in unfractionated HDL[B] or the concentration of apoE in HDL subspecies in participants of the Danish Diet Cancer and Health study, n=3639. **Table author: Manja Koch**

	Q1	Q2	Q3	Q4	Q5	P trend	Per log$_2$ increase[C]	P heterogeneity[D]
ApoE in HDL								
Median levels in sub-cohort, mg/dL	0.93	1.48	1.95	2.67	4.27			
Number of CHD cases	352	359	378	390	467			
Unadjusted	1 (ref)	0.90 (0.69, 1.19)	0.82 (0.61, 1.09)	0.83 (0.62, 1.12)	0.91 (0.65, 1.28)	0.81	0.95 (0.83, 1.08)	
Multivariable-adjusted[E]	1 (ref)	0.99 (0.74, 1.33)	0.92 (0.67, 1.26)	0.91 (0.67, 1.25)	0.97 (0.66, 1.41)	0.88	0.93 (0.81, 1.08)	
Plus HDL	1 (ref)	1.01 (0.75, 1.36)	0.94 (0.68, 1.29)	0.95 (0.69, 1.31)	1.07 (0.73, 1.56)	0.71	0.97 (0.84, 1.13)	
Plus HDL and apoCIII[F]	1 (ref)	0.99 (0.74, 1.34)	0.90 (0.66, 1.25)	0.90 (0.65, 1.25)	0.97 (0.66, 1.42)	0.88	0.93 (0.80, 1.08)	
Plus HDL, apoCIII, triglycerides, apoB[G]	1 (ref)	0.99 (0.73, 1.33)	0.86 (0.62, 1.19)	0.88 (0.63, 1.21)	0.94 (0.63, 1.38)	0.79	0.90 (0.77, 1.05)	
ApoE in HDL that contains apoCIII								
Median levels in sub-cohort, mg/dL	0.31	0.53	0.75	1.03	1.86			
Number of CHD cases	256	249	316	437	688			
Unadjusted	1 (ref)	1.07 (0.80, 1.44)	1.19 (0.86, 1.64)	1.31 (0.94, 1.82)	1.40 (0.96, 2.03)	0.08	1.14 (1.00, 1.29)	0.01
Multivariable-adjusted[E]	1 (ref)	1.02 (0.74, 1.41)	1.16 (0.82, 1.64)	1.34 (0.94, 1.91)	1.29 (0.86, 1.93)	0.25	1.12 (0.98, 1.28)	0.02
Plus HDL	1 (ref)	1.03 (0.75, 1.42)	1.18 (0.83, 1.67)	1.37 (0.96, 1.95)	1.32 (0.88, 1.97)	0.22	1.13 (0.99, 1.29)	0.03
Plus HDL and apoCIII[F]	1 (ref)	0.99 (0.71, 1.36)	1.11 (0.78, 1.57)	1.24 (0.86, 1.78)	1.16 (0.77, 1.76)	0.54	1.08 (0.94, 1.24)	0.05
Plus HDL, apoCIII, triglycerides, apoB[G]	1 (ref)	0.94 (0.68, 1.30)	1.00 (0.70, 1.42)	1.09 (0.76, 1.58)	1.02 (0.67, 1.55)	0.86	1.03 (0.89, 1.18)	0.18
ApoE in HDL that does not contain apoCIII								
Median levels in sub-cohort, mg/dL	0.44	0.72	1.00	1.40	2.19			
Number of CHD cases	416	407	358	341	424			
Unadjusted	1 (ref)	0.84 (0.64, 1.10)	0.79 (0.60, 1.04)	0.61 (0.46, 0.82)	0.66 (0.49, 0.89)	<0.01	0.88 (0.79, 0.98)	
Multivariable-adjusted[E]	1 (ref)	0.77 (0.58, 1.02)	0.79 (0.59, 1.05)	0.63 (0.46, 0.85)	0.66 (0.48, 0.89)	0.01	0.88 (0.78, 0.98)	

Table 2.5 (continued)

	Q1	Q2	Q3	Q4	Q5	P trend	Per $\log_2$ increase[C]
Plus HDL and apoCIII[F]	1 (ref)	0.78 (0.59, 1.04)	0.80 (0.60, 1.07)	0.64 (0.47, 0.88)	0.68 (0.49, 0.93)	0.02	0.89 (0.79, 1.00)
Plus HDL, apoCIII, triglycerides, apoB[G]	1 (ref)	0.80 (0.60, 1.06)	0.80 (0.59, 1.07)	0.68 (0.50, 0.93)	0.68 (0.49, 0.94)	0.02	0.90 (0.80, 1.01)

[A]Hazard Ratios (HRs) obtained from Cox proportional hazard regression models with age used as the underlying time scale, adjusted for laboratory batch and stratification by sex.

[B]The concentration of HDL was quantified based on apoA-I levels, the major apolipoprotein component of HDL.

[C]Equivalent to doubling in apoE.

[D]We tested for equality of the regression coefficients for apoE in HDL containing apoCIII and apoE in HDL not containing apoCIII (p heterogeneity).

[E]ApoE in HDL containing or not containing apoCIII are simultaneously included in all models. The multivariable model was adjusted for laboratory batch, smoking status (never; former; current <15, 15-24, ≥ 25 g/day), education (missing, <8; 8-10; >10 years), alcohol intake (nondrinker; drinker <5, 5-9, 10-19, 20-39, ≥40 g/alcohol/day), BMI (<25; 25-<30; >30 kg/m^2), and self-reported diagnosis of hypertension, and self-reported diagnosis of diabetes at baseline.

[F]n=3638. [G]n

ApoE in HDL

p trend = 0.88

**ApoE in HDL
containing apoCIII**

p trend = 0.25

**ApoE in HDL
not containing apoCIII**

p trend = 0.01

HR (95% CI) for CHD

Q1 Q2 Q3 Q4 Q5   Q1 Q2 Q3 Q4 Q5   Q1 Q2 Q3 Q4 Q5
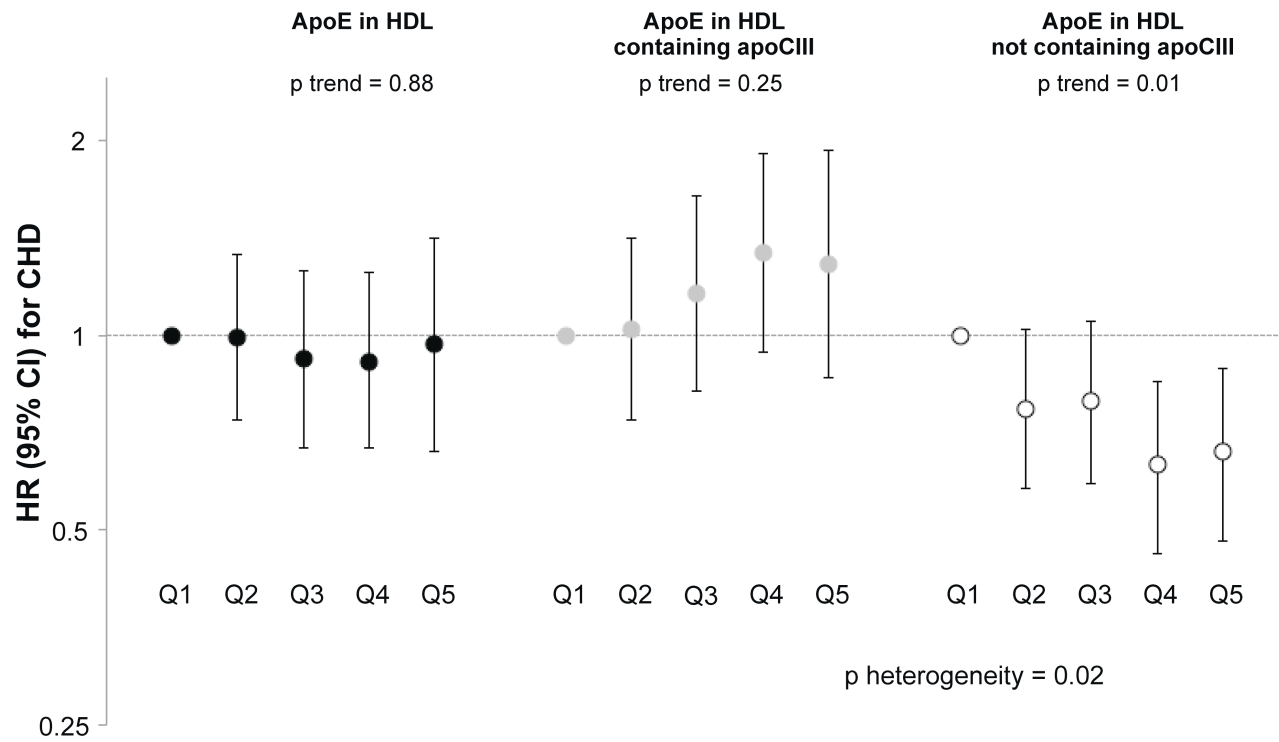
p heterogeneity = 0.02

Figure 2.8: HDL apoE and apoCIII interacts with coronary heart disease (CHD) (Figure author: Manja Koch).

Figure 2.8 (continued): HDL apoE and apoCIII interacts with coronary heart disease (CHD) (Figure author: Manja Koch). Hazard Ratios (HRs) and 95% confidence intervals of CHD are shown according to quintiles of apoE concentration in unfractionated HDL and in HDL containing or not containing apoCIII in participants of the Danish Diet Cancer and Health study (n=3635). HRs were adjusted for laboratory batch, smoking status (never; former; current <15, 15-24, ≥ 25 g/day), education (missing, <8; 8-10; >10 years), alcohol intake (nondrinker; drinker <5, 5-9, 10-19, 20-39, ≥40 g/alcohol/day), BMI (<25; 25-<30; >30 kg/m^2), self-reported diagnosis of hypertension, and self-reported diagnosis of diabetes at baseline obtained from Cox proportional hazard regression models with standard inverse probability weights and age used as underlying time scale and stratification by sex. The concentration of HDL was quantified by apoA-I levels. ApoE concentration in HDL containing or not containing apoCIII were simultaneously included in the model. Equality of the regression coefficients was tested for apoE in HDL containing apoCIII and apoE in HDL not containing apoCIII (p heterogeneity = 0.02). The significant heterogeneity test indicates that the association with CHD is different for HDL apoE concentration depending on the presence or absence of apoCIII on the HDL.

Additional adjustment for factors involved in the pathophysiology of CHD including HDL-apoA-I, apoCIII, plasma triglycerides, and apoB (**Table 2.5**) did not affect the results. ApoE in total (unfractionated) HDL was unrelated to risk of CHD (p trend = 0.79). The concentration of apoE in HDL was inversely associated with CHD risk only in HDL not containing apoCIII (p for trend = 0.02 in HDL containing apoCIII versus p=0.86 in HDL not containing apoCIII).

2.4.   Discussion

This study is the first in humans to link the impact of an apolipoprotein on HDL physiology to risk of CHD. The central metabolic findings are that a subspecies of HDL that contains apoE but not apoCIII uniquely participates in classical pathways of reverse cholesterol transport – disproportionately high secretion into plasma, size expansion most likely by taking up cholesterol (the major lipid component of the HDL core), size contraction at least in part by selective cholesterol ester uptake by the liver and potentially via actions of lipoprotein lipase (LPL) and hepatic lipase (HL) to generate prebeta HDL, and increased clearance rates from the circulation. These pathways are not evident for the HDL that does not contain apoE. We also found that apoCIII robustly attenuates the size expansion pathway and high clearance rate.

We interpreted the metabolic results to mean greater reverse cholesterol transport for only the HDL subspecies that contains apoE but not apoCIII. Next, we studied whether these metabolic indicators of reverse cholesterol transport corresponded to lower rates of clinical CHD outcomes for HDL containing apoE, which might be attenuated when

apoCIII is also present. The results of the epidemiology study match closely with the metabolism study. In a large prospective population-based study, the apoE concentration of HDL is inversely related to the risk of CHD but only in the major HDL subspecies that does not contain apoCIII **(Figure 2.8)**. Interestingly, early work by Mahley and colleagues (44) showed that increasing the amount of apoE in phospholipid disks exponentially increased their affinity for LDL receptors on human fibroblasts, which provides an additional mechanistic explanation for these findings. In contrast, the apoE concentration was not associated with CHD in the subspecies of HDL that contains apoCIII, indicating that no amount of apoE in a physiological range can overcome the effect of the apoCIII also present. We demonstrate for the first time a close correspondence between metabolic properties of HDL subspecies defined by specific protein content that presumptively affects reverse cholesterol transport, and the prediction by these HDL subspecies and proteins of risk of CHD in a population (**Figure 2.9**).

We found disproportionate apoA-I secretion and HDL-C content in E+CIII- and E+CIII+ HDL relative to their respective pool sizes (**Figure 2.3B, Table 2.3**). This disproportionate flux in synthesis is supported by the ability of apoE to activate ABCA1 (45, 46), which is present on hepatocytes and is an essential mediator in HDL biogenesis. This has also been studied in a mimetic peptide derived from the C-terminal domain of apoE, which stimulated ABCA1-mediated efflux from cultured macrophages and nascent HDL formation (47). Furthermore, LPL could contribute to the formation of
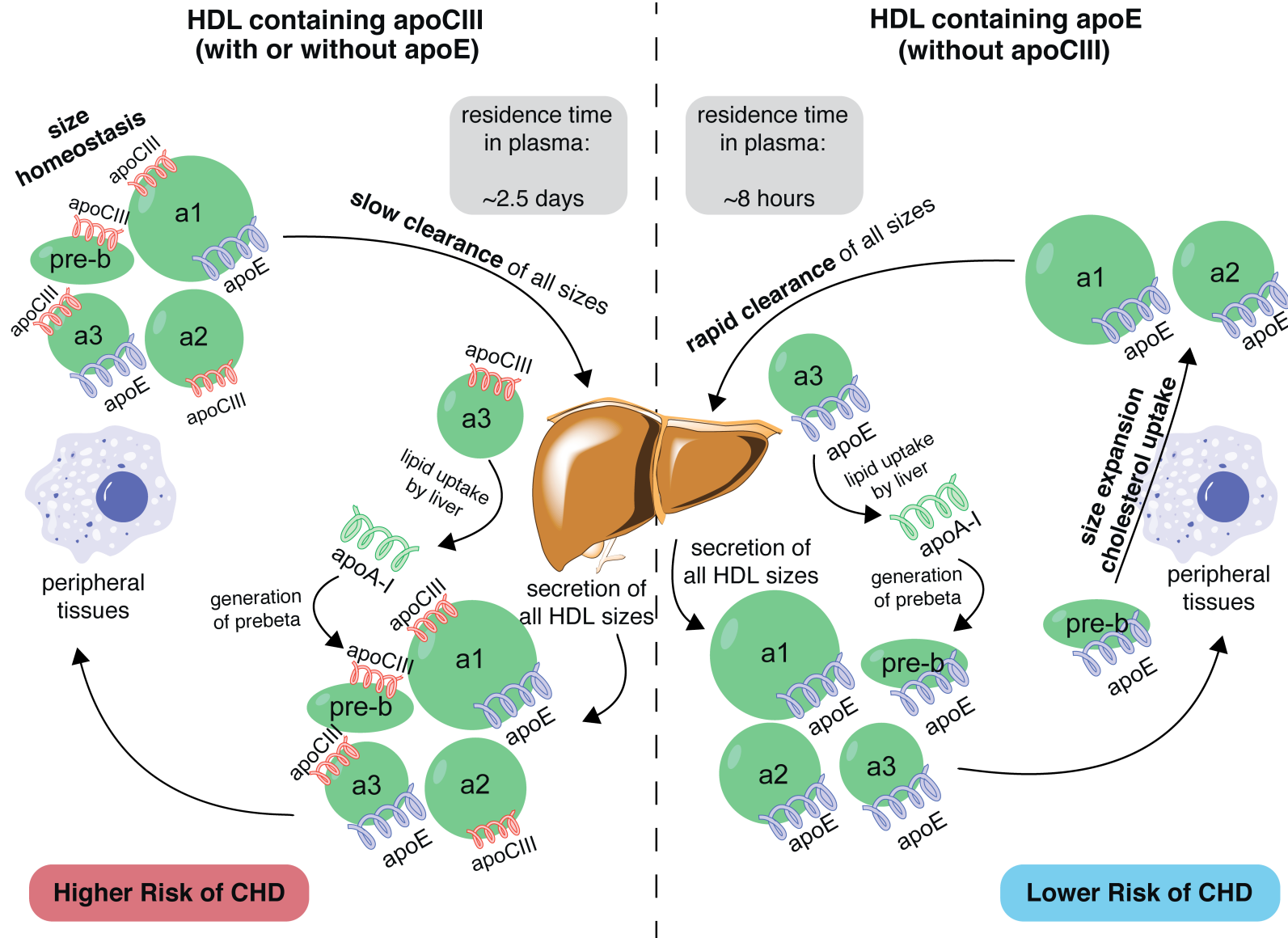
Figure 2.9: Integrated model of metabolism and epidemiology showing an adverse interaction between apoE and apoCIII.

Figure 2.9 (continued): Integrated model of metabolism and epidemiology showing an adverse interaction between apoE and apoCIII. <u>Left panel:</u> The liver secretes HDL containing both apoE and apoCIII (E+CIII+) or HDL containing apoCIII but not apoE (E-CIII+) across a range of HDL sizes. These HDL subspecies do not experience significant size expansion that increases the size category. Upon arrival at the liver, either the lipids are cleared and prebeta generated, or the particles are cleared slowly from circulation (residence time: approximately 2.5 days). These HDL subspecies are associated with a higher risk of CHD. <u>Right panel:</u> The liver secretes HDL containing apoE but not apoCIII (E+CIII-) across a range of sizes. This HDL subspecies experiences size expansion from discoidal prebeta to larger alpha sizes, due to efflux of cholesterol from peripheral tissues. Upon arrival at the liver, either the lipids are cleared and prebeta generated, or the particles are cleared rapidly from the circulation (residence time: ~8 hours). This HDL subspecies is associated with a lower risk of CHD.

HDL by transferring surface protein and lipid from remnant chylomicrons and VLDL to newly synthesized HDL particles (48, 49).

Our models suggest that HDL containing apoE participates in size expansion of HDL more so than HDL that does not contain apoE, likely due to increased cholesterol incorporation into the core of the particle, which is supported and confirmed by evidence in vitro and in animal models. Structural investigations have shown that apoE has a different conformation on HDL than does apoA-I, and that this conformation facilitates lipid incorporation into the particle (21, 45, 50). ApoA-I-containing HDL from CETP-deficient humans is able to accommodate only a limited amount of cholesterol ester, which is greatly increased when apoE is present (51). In mice lacking apoA-I, adenoviral-mediated expression of apoE promoted the secretion of discoidal HDL which was converted to spherical (alpha) HDL by lecithin-cholesterol acyl transferase (LCAT), indicating size expansion (22). In canine serum depleted of apoE, coincubation of cholesterol-loaded J774 macrophages with exogenous human apoA-I modestly increased the concentration of all sizes of HDL, whereas exogenous apoE robustly increased mainly larger HDL, again potentially reflecting size expansion. Of note, incubation with exogenous human apoCIII did not result in an increase in concentration of any HDL size (19). Our results support these findings, given that we saw evidence of size expansion in E+CIII- HDL, but not in E-CIII+ or E+CIII+ (**Figure 2.7**; for more details, the reader is referred to **Chapter 4**).

Consistent with the role of apoE as a high affinity liver receptor ligand (13, 15, 52), we found that the subspecies of HDL containing apoE has a much shorter residence time in the circulation than the subspecies of HDL that does not contain apoE, about 8 hours compared to 2.5 days, with the assumption that apoA-I kinetics recapitulate HDL particle kinetics (**Figure 2.3D**). The 8 hour residence time for apoA-I HDL containing apoE is similar to the residence time of apoE itself on HDL (53), suggesting apoE mediates holoparticle uptake and complete removal of the HDL particle on which it resides. HDL containing apoE could also interact with circulating HL to increase hydrolysis of HDL phospholipid and triglyceride to regenerate prebeta HDL (54).

Unlike apoE, apoCIII appears to have a minor if any role in apoA-I metabolism on its own, given that the metabolism of apoA-I on CIII+ HDL is similar to CIII- HDL (**Figure 2.4, Table 2.2**) and the metabolism of apoA-I on CIII+ HDL is similar to E-CIII- (**Figure 2.6, Table 2.2**). Importantly, however, the presence of apoCIII strongly abolishes the effect of apoE to increase clearance of HDL, as shown by comparing FCR in E+CIII+ compared to E+CIII- (**Figure 2.6B**). These opposing roles of apoE and apoCIII in humans have been shown in apoB-containing lipoproteins, in which E+CIII- VLDL and IDL are cleared rapidly, but E+CIII+ VLDL and IDL have attenuated clearance rates, although faster than E-CIII+ (17, 30, 36). This antagonistic effect has also been shown mechanistically in vitro (28, 32) and in animal models (33-35), in which exogenous or transgenic apoE is able to facilitate lipoprotein binding to LDL-R and lipoprotein uptake, and exogenous or transgenic apoCIII ablates this effect. Taken together, the effect of apoCIII on HDL metabolism manifests only when apoCIII coexists with apoE on HDL.

The metabolic evidence here supports and is supported by epidemiological evidence suggesting that apoCIII interferes with anti-atherogenic functions of HDL. When human HDL is separated into subspecies containing or not containing apoCIII, the concentration of HDL that contains apoCIII predicts higher risk of CHD, whereas HDL that does not contain apoCIII predicts lower risk (55). In our study, the inverse association of apoE in HDL with the risk of CHD was completely masked in HDL that contains apoCIII (**Figure 2.8, Table 2.5**). Findings from studies on the association of apoE in unfractionated HDL and CVD have been inconsistent. In a prospective nested case-control study (370 control participants, 418 cases) in a randomized, placebo controlled clinical trial of pravastatin in survivors of myocardial infarction, higher concentrations of apoE in HDL were associated with an increased risk for recurrent coronary events (38). In a cross-sectional setting, there were reduced levels of apoE in HDL isolated from the plasma of 40 coronary artery disease patients compared to 20 healthy subjects (56). In contrast, a clinical study revealed higher concentrations of apoE in a small and dense subfraction of HDL (HDL_3) from 7 patients with coronary artery disease compared to HDL_3 of 6 healthy control (37). Similarly, higher apoE levels in HDL were observed in 74 male coronary bypass patients compared to 78 apparently healthy male controls (57). These divergent results might be related to small sample sizes of some of the studies, cross-sectional study design, and lacking adjustment for potential confounders. As the concentration of apoE or apoCIII in HDL might be influenced by disease status, it is particularly important to study this association in

prospective studies in populations without CHD at baseline, as we did for the first time in the present study.

Strengths of our metabolic study include large sample size for a kinetic study, wide age range of study participants, and inclusion of men and women as well as white and black participants. Restriction of the study population to the low HDL, high BMI phenotype, frequently seen with the metabolic syndrome, is clinically relevant but restricts our ability to make conclusions about HDL metabolism in individuals with optimal body weight and high HDL-C. We restricted the use of medications that alter HDL levels (i.e. statins, estrogen replacement therapy) to ensure these were not study confounders. Our study participants received a high-unsaturated fat diet easy to adhere to with foods typical of the American population. Strengths of the prospective case-cohort study include the large sample size with minimal loss to follow-up, the population-based design, and the rigorous validation of CHD cases. Another cost-efficient study design often used to minimize the use of precious biological samples, but retaining the prospective setting, is the nested case-control design where matching of future cases to controls who remain free of disease can take care of important confounders such as smoking and age at the design phase. The main advantage of the present case-cohort study design is that the random subcohort can be used as a comparison group for multiple outcomes (58). In case-cohort studies, potential confounding must be addressed by comprehensive multivariable adjustments. A recent study showed that both designs yield comparable results to full cohort analyses, especially if inverse probability weighting is applied (59). Our study extends the ongoing discussion about HDL heterogeneity and provides

evidence that apoE is involved in HDL's cardioprotective activities. Unfortunately, no apoE genotype data was available for this analysis and future studies should evaluate if apoE isoforms provide further insight in the association of apoE in HDL and risk of CHD. However, the proportion of HDL carrying apoE did not differ by apoE genotype in a previous study (39).

This study in humans is the first to show that apolipoproteins, present at small concentrations in HDL, can strongly influence the metabolism of HDL in plasma and interact to affect CHD risk. A unique subspecies of HDL that contains apoE but not apoCIII behaves entirely differently from other HDL. High secretion, coupled with size expansion and rapid clearance, of HDL containing apoE but not apoCIII, suggests an HDL particle especially active in reverse cholesterol transport hypothesized to protect against atherosclerosis and points to a potential therapeutic target. However, apoE on HDL is unable to overcome the metabolic influence of apoCIII also present on HDL. These metabolic findings map closely with our finding that HDL apoE is associated with lower CHD risk, but only so on HDL that does not contain apoCIII, and ineffective when apoCIII is present. It is important to note that we only studied this subspecies in overweight and obese individuals with low HDL-C, where the concentration of E+CIII- HDL is quite low in plasma. It is plausible that lean, healthy individuals with presumably higher HDL functionality have greater amounts of E+CIII- HDL. HDL subspecies, because they are based on functional properties of the associated proteins, are more likely to have a causal role in atherosclerosis and CHD events and should be explored in further studies.

2.5 Acknowledgments

2.6 References

1. Writing Group Members et al. Heart Disease and Stroke Statistics-2016 Update: A Report From the American Heart Association. *Circulation* 2016;133(4):e38–360.

2. Gordon T, Castelli WP, Hjortland MC, Kannel WB, Dawber TR. High density lipoprotein as a protective factor against coronary heart disease. The Framingham Study. *Am. J. Med.* 1977;62(5):707–714.

3. Thompson A, Danesh J. Associations between apolipoprotein B, apolipoprotein AI, the apolipoprotein B/AI ratio and coronary heart disease: a literature-based meta-

analysis of prospective studies. *J. Intern. Med.* 2006;259(5):481–492.

4. Barter PJ et al. Effects of torcetrapib in patients at high risk for coronary events. *N. Engl. J. Med.* 2007;357(21):2109–2122.

5. Schwartz GG et al. Effects of dalcetrapib in patients with a recent acute coronary syndrome. *N. Engl. J. Med.* 2012;367(22):2089–2099.

6. AIM-HIGH Investigators et al. Niacin in patients with low HDL cholesterol levels receiving intensive statin therapy. *N. Engl. J. Med.* 2011;365(24):2255–2267.

7. Lincoff AM et al. Evacetrapib and Cardiovascular Outcomes in High-Risk Vascular Disease. *N. Engl. J. Med.* 2017;376(20):1933–1942.

8. Gordon SM, Deng J, Lu LJ, Davidson WS. Proteomic characterization of human plasma high density lipoprotein fractionated by gel filtration chromatography. *J. Proteome Res.* 2010;9(10):5239–5249.

9. Talayero B et al. Obesity Favors Apolipoprotein E and CIII-containing High-density Lipoprotein Subfractions Associated with Risk of Heart Disease. *J. Lipid Res.* [published online ahead of print: June 25, 2014]; doi:10.1194/jlr.M042333

10. Mahley RW, Innerarity TL. Lipoprotein receptors and cholesterol homeostasis. *Biochim. Biophys. Acta* 1983;737(2):197–222.

11. Beisiegel U, Weber W, Ihrke G, Herz J, Stanley KK. The LDL-receptor-related protein, LRP, is an apolipoprotein E-binding protein. *Nature* 1989;341(6238):162–164.

12. Mahley RW, Weisgraber KH, Innerarity TL. Interaction of plasma lipoproteins containing apolipoproteins B and E with heparin and cell surface receptors. *Biochim. Biophys. Acta* 1979;575(1):81–91.

13. Futamura M et al. Two-step mechanism of binding of apolipoprotein E to heparin: implications for the kinetics of apolipoprotein E-heparan sulfate proteoglycan complex formation on cell surfaces. *J. Biol. Chem.* 2005;280(7):5414–5422.

14. Williams KJ, Chen K. Recent insights into factors affecting remnant lipoprotein uptake. *Curr. Opin. Lipidol.* 2010;21(3):218–228.

15. Gonzales JC, Gordts PLSM, Foley EM, Esko JD. Apolipoproteins E and AV mediate lipoprotein clearance by hepatic proteoglycans. *J. Clin. Invest.* 2013;123(6):2742–2751.

16. Tomiyasu K, Walsh BW, Ikewaki K, Judge H, Sacks FM. Differential metabolism of human VLDL according to content of ApoE and ApoC-III. *Arterioscler. Thromb. Vasc. Biol.* 2001;21(9):1494–1500.

17. Zheng C, Khoo C, Ikewaki K, Sacks FM. Rapid turnover of apolipoprotein C-III-containing triglyceride-rich lipoproteins contributing to the formation of LDL subfractions.

J. Lipid Res. 2007;48(5):1190–1203.

18. Mahley RW, Huang Y, Weisgraber KH. Putting cholesterol in its place: apoE and reverse cholesterol transport. *J. Clin. Invest.* 2006;116(5):1226–1229.

19. Koo C, Innerarity TL, Mahley RW. Obligatory role of cholesterol and apolipoprotein E in the formation of large cholesterol-enriched and receptor-active high density lipoproteins. *J. Biol. Chem.* 1985;260(22):11934–11943.

20. Settasatian N, Barter PJ, Rye K-A. Remodeling of apolipoprotein E-containing spherical reconstituted high density lipoproteins by phospholipid transfer protein. *J. Lipid Res.* 2008;49(1):115–126.

21. Peters-Libeu CA, Newhouse Y, Hatters DM, Weisgraber KH. Model of biologically active apolipoprotein E bound to dipalmitoylphosphatidylcholine. *J. Biol. Chem.* 2006;281(2):1073–1079.

22. Kypreos KE, Zannis VI. Pathway of biogenesis of apolipoprotein E-containing HDL in vivo with the participation of ABCA1 and LCAT. *Biochem. J.* 2007;403(2):359–367.

23. Innerarity TL, Pitas RE, Mahley RW. Receptor binding of cholesterol-induced high-density lipoproteins containing predominantly apoprotein E to cultured fibroblasts with mutations at the low-density lipoprotein receptor locus. *Biochemistry* 1980;19(18):4359–4365.

24. Hui DY, Innerarity TL, Mahley RW. Lipoprotein binding to canine hepatic membranes. Metabolically distinct apo-E and apo-B,E receptors. *J. Biol. Chem.* 1981;256(11):5646–5655.

25. Funke H et al. Uptake of apolipoprotein E-containing high density lipoproteins by hepatic parenchymal cells. *Arteriosclerosis* 1984;4(5):452–461.

26. Blum CB, Deckelbaum RJ, Witte LD, Tall AR, Cornicelli J. Role of apolipoprotein E-containing lipoproteins in abetalipoproteinemia. *J. Clin. Invest.* 1982;70(6):1157–1169.

27. Ikewaki K, Rader DJ, Zech LA, Brewer HB. In vivo metabolism of apolipoproteins A-I and E in patients with abetalipoproteinemia: implications for the roles of apolipoproteins B and E in HDL metabolism. *J. Lipid Res.* 1994;35(10):1809–1819.

28. Clavey V, Lestavel-Delattre S, Copin C, Bard JM, Fruchart JC. Modulation of lipoprotein B binding to the LDL receptor by exogenous lipids and apolipoproteins CI, CII, CIII, and E. *Arterioscler. Thromb. Vasc. Biol.* 1995;15(7):963–971.

29. Sacks FM. The crucial roles of apolipoproteins E and C-III in apoB lipoprotein metabolism in normolipidemia and hypertriglyceridemia. *Curr. Opin. Lipidol.* 2015;26(1):56–63.

30. Mendivil CO, Zheng C, Furtado J, Lel J, Sacks FM. Metabolism of very-low-density

lipoprotein and low-density lipoprotein containing apolipoprotein C-III and not other small apolipoproteins. *Arterioscler. Thromb. Vasc. Biol.* 2010;30(2):239–245.

31. Watts GF et al. Differential regulation of lipoprotein kinetics by atorvastatin and fenofibrate in subjects with the metabolic syndrome. *Diabetes* 2003;52(3):803–811.

32. Sehayek E, Eisenberg S. Mechanisms of inhibition by apolipoprotein C of apolipoprotein E-dependent cellular metabolism of human triglyceride-rich lipoproteins through the low density lipoprotein receptor pathway. *J. Biol. Chem.* 1991;266(27):18259–18267.

33. Shelburne F, Hanks J, Meyers W, Quarfordt S. Effect of apoproteins on hepatic uptake of triglyceride emulsions in the rat. *J. Clin. Invest.* 1980;65(3):652–658.

34. de Silva HV et al. Overexpression of human apolipoprotein C-III in transgenic mice results in an accumulation of apolipoprotein B48 remnants that is corrected by excess apolipoprotein E. *J. Biol. Chem.* 1994;269(3):2324–2335.

35. Aalto-Setälä K et al. Further characterization of the metabolic properties of triglyceride-rich lipoproteins from human and mouse apoC-III transgenic mice. *J. Lipid Res.* 1996;37(8):1802–1811.

36. Zheng C, Khoo C, Furtado J, Sacks FM. Apolipoprotein C-III and the metabolic basis for hypertriglyceridemia and the dense low-density lipoprotein phenotype. *Circulation* 2010;121(15):1722–1734.

37. Vaisar T et al. Shotgun proteomics implicates protease inhibition and complement activation in the antiinflammatory properties of HDL. *J. Clin. Invest.* 2007;117(3):746–756.

38. Sacks FM et al. VLDL, apolipoproteins B, CIII, and E, and risk of recurrent coronary events in the Cholesterol and Recurrent Events (CARE) trial. *Circulation* 2000;102(16):1886–1892.

39. Wilson HM, Patel JC, Russell D, Skinner ER. Alterations in the concentration of an apolipoprotein E-containing subfraction of plasma high density lipoprotein in coronary heart disease. *Clin. Chim. Acta* 1993;220(2):175–187.

40. Jensen MK et al. HDL Subspecies Defined by Presence of Apolipoprotein C-III and Incident Coronary Heart Disease in Four Cohorts. *Circulation* 2017;:CIRCULATIONAHA.117.031276.

41. Mendivil CO, Furtado J, Morton AM, Wang L, Sacks FM. Novel Pathways of Apolipoprotein A-I Metabolism in High-Density Lipoprotein of Different Sizes in Humans. *Arterioscler. Thromb. Vasc. Biol.* 2016;36(1):156–165.

42. Rosenson RS et al. HDL measures, particle heterogeneity, proposed nomenclature, and relation to atherosclerotic cardiovascular events. *Clin. Chem.* 2011;57(3):392–410.

43. Barrett PH et al. SAAM II: Simulation, Analysis, and Modeling Software for tracer and pharmacokinetic studies. *Metab. Clin. Exp.* 1998;47(4):484–492.

44. Innerarity TL, Pitas RE, Mahley RW. Binding of arginine-rich (E) apoprotein after recombination with phospholipid vesicles to the low density lipoprotein receptors of fibroblasts. *J. Biol. Chem.* 1979;254(10):4186–4190.

45. Vedhachalam C et al. The C-terminal lipid-binding domain of apolipoprotein E is a highly efficient mediator of ABCA1-dependent cholesterol efflux that promotes the assembly of high-density lipoproteins. *Biochemistry* 2007;46(10):2583–2593.

46. Zannis VI et al. Discrete roles of apoA-I and apoE in the biogenesis of HDL species: lessons learned from gene transfer studies in different mouse models. *Ann. Med.* 2008;40 Suppl 1(sup1):14–28.

47. Hafiane A, Bielicki JK, Johansson JO, Genest J. Apolipoprotein E derived HDL mimetic peptide ATI-5261 promotes nascent HDL formation and reverse cholesterol transport in vitro. *Biochim. Biophys. Acta* 2014;1842(10):1498–1512.

48. Patsch JR, Gotto AM, Olivercrona T, Eisenberg S. Formation of high density lipoprotein2-like particles during lipolysis of very low density lipoproteins in vitro. *Proc. Natl. Acad. Sci. U.S.A.* 1978;75(9):4519–4523.

49. Cheung MC, Sibley SD, Palmer JP, Oram JF, Brunzell JD. Lipoprotein lipase and hepatic lipase: their relationship with HDL subspecies Lp(A-I) and Lp(A-I,A-II). *J. Lipid Res.* 2003;44(8):1552–1558.

50. Davidson WS, Silva RAGD. Apolipoprotein structural organization in high density lipoproteins: belts, bundles, hinges and hairpins. *Curr. Opin. Lipidol.* 2005;16(3):295–300.

51. Matsuura F, Wang N, Chen W, Jiang X-C, Tall AR. HDL from CETP-deficient subjects shows enhanced ability to promote cholesterol efflux from macrophages in an apoE- and ABCG1-dependent pathway. *J. Clin. Invest.* 2006;116(5):1435–1442.

52. Mahley RW. Apolipoprotein E: cholesterol transport protein with expanding role in cell biology. *Science* 1988;240(4852):622–630.

53. Singh SA et al. Multiple apolipoprotein kinetics measured in human HDL by high-resolution/accurate mass parallel reaction monitoring. *J. Lipid Res.* 2016;57(4):714–728.

54. Hime NJ, Drew KJ, Hahn C, Barter PJ, Rye K-A. Apolipoprotein E enhances hepatic lipase-mediated hydrolysis of reconstituted high-density lipoprotein phospholipid and triacylglycerol in an isoform-dependent manner. *Biochemistry* 2004;43(38):12306–12314.

55. Jensen MK, Rimm EB, Furtado JD, Sacks FM. Apolipoprotein C-III as a Potential

Modulator of the Association Between HDL-Cholesterol and Incident Coronary Heart Disease. *J Am Heart Assoc* 2012;1(2):jah3–e000232–jah3–e000232.

56. Riwanto M et al. Altered activation of endothelial anti- and proapoptotic pathways by high-density lipoprotein from patients with coronary artery disease: role of high-density lipoprotein-proteome remodeling. *Circulation* 2013;127(8):891–904.

57. Chivot L et al. Logistic discriminant analysis of lipids and apolipoproteins in a population of coronary bypass patients and the significance of apolipoproteins C-III and E. *Atherosclerosis* 1990;82(3):205–211.

58. Prentice RL. A case-cohort design for epidemiologic cohort studies and disease prevention trials. *Biometrika* 1986;73(1):1–11.

59. Kim RS. A new comparison of nested case-control and case-cohort designs and methods. *Eur. J. Epidemiol.* 2015;30(3):197–207.

60. Tjønneland A et al. Study design, exposure variables, and socioeconomic determinants of participation in Diet, Cancer and Health: a population-based prospective cohort study of 57,053 men and women in Denmark. *Scand J Public Health* 2007;35(4):432–441.

61. Nikkilä EA, Kekki M. Plasma triglyceride metabolism in thyroid disease. *J. Clin. Invest.* 1972;51(8):2103–2114.

62. Friedewald WT, Levy RI, Fredrickson DS. Estimation of the concentration of low-density lipoprotein cholesterol in plasma, without use of the preparative ultracentrifuge. *Clin. Chem.* 1972;18(6):499–502.

63. Mendivil CO, Rimm EB, Furtado J, Chiuve SE, Sacks FM. Low-density lipoproteins containing apolipoprotein C-III and the risk of coronary heart disease. *Circulation* 2011;124(19):2065–2072.

64. Jensen MK et al. Obesity, behavioral lifestyle factors, and risk of acute coronary events. *Circulation* 2008;117(24):3062–3069.

65. Joensen AM et al. Predictive values of acute coronary syndrome discharge diagnoses differed in the Danish National Patient Registry. *J Clin Epidemiol* 2009;62(2):188–194.

66. Luepker RV et al. Case definitions for acute coronary heart disease in epidemiology and clinical research studies: a statement from the AHA Council on Epidemiology and Prevention; AHA Statistics Committee; World Heart Federation Council on Epidemiology and Prevention; the European Society of Cardiology Working Group on Epidemiology and Prevention; Centers for Disease Control and Prevention; and the National Heart, Lung, and Blood Institute. *Circulation* 2003;108(20):2543–2549.

CHAPTER 3

Dietary unsaturated fat increases metabolic pathways in reverse cholesterol transport via HDL containing apoE

Allyson M. Morton, Carlos O. Mendivil, Jeremy D. Furtado, Frank M. Sacks

Abstract

Background: HDL that contains apoE is a subspecies especially active in steps in reverse cholesterol transport, a process that brings cholesterol from peripheral cells to the liver. Here we studied the effect of dietary unsaturated fat compared to carbohydrate on HDL containing apoE. We hypothesized that its metabolism is enhanced, as a mechanism by which unsaturated fat protects against coronary heart disease.

Methods: We enrolled nine adults who were overweight or obese and had low HDL-C ($\leq$45 mg/dl for men, $\leq$55 mg/dl for women) in a crossover study of a high-unsaturated fat diet and a high carbohydrate diet. A metabolic tracer study was done after each diet period.

Results: High dietary unsaturated fat compared to carbohydrate increased the synthesis rate of HDL containing apoE by 2 to 3 fold, increased its flux from small to large particles, and increased generation of small from large HDL. HDL containing apoE is cleared quickly from the circulation, and even more so during unsaturated fat intake. These effects occurred only in participants who had the apoE3/E3 genotype, and not in apoE heterozygotes. The high-unsaturated fat diet did not affect the metabolism of HDL lacking apoE.

Conclusions: Dietary unsaturated fat compared to carbohydrate increases the secretion and clearance of HDL subspecies containing apoE, and renders them more biologically

active in metabolic pathways that involve reverse cholesterol transport. HDL containing

apoE may be a relevant mechanism to consider in development of HDL treatments.

3.1.   Introduction

A major function of HDL is to bring cholesterol from peripheral cells to the liver, either directly or via transfer to apoB-containing lipoproteins, a process called reverse cholesterol transport. Size expansion of HDL is a hallmark of reverse cholesterol transport because it happens when circulating plasma HDL takes up cholesterol from cells and esterifies it, increasing in size. There is evidence for reverse cholesterol transport in humans, primates, and mouse models. For example, a synthetic small HDL particle composed of phospholipid and apoA-I injected in humans increases its size over 24 hours as it circulates by taking up cholesterol (1). Small HDL particles, prepared by column chromatography or by delipidation and injected into monkeys, increase to larger sizes (2, 3). Cholesterol ester in loaded macrophages injected in mice appears in the feces, a process dependent on the presence of HDL (4, 5). This and other evidence (6, 7) supports a hypothesis that size expansion by reverse cholesterol transport is a functioning pathway by which excess cholesterol in peripheral cells can be transferred to HDL and then delivered to the liver for secretion into bile or for redistribution to other tissues via lipoprotein secretion.

Until recently, size expansion of endogenous circulating HDL has never been directly observed or measured in humans. We adapted metabolic tracer methods and compartmental modeling used in our studies of apoB metabolism to find that size expansion occurs but only in minor pathways comprising a minority of total apoA-I flux (8). The rest of plasma apoA-I HDL flux occurs within stable size ranges from 7 to 12 nm. HDL could expand by any small size HDL that is available to take up cholesterol, or

size expansion could occur in HDL subspecies that have proteins that have been shown to promote cholesterol uptake and size expansion, and therefore be a target for treatments. However, size expansion of HDL can be useful in reverse cholesterol transport only if the expanded HDL particle has a means for efficient delivery of its cholesterol to the liver where it can perform its homeostatic role.

ApoE is a prime candidate for this hypothesis, because it facilitates all the steps of reverse cholesterol transport: HDL biogenesis, size expansion presumably by cholesterol uptake, regeneration of small HDL by selective cholesterol uptake by the liver, and holoparticle clearance by the liver of size-expanded HDL. First, HDL apoE increases HDL biogenesis in vitro by interacting with ABCA1 (9). HDL containing apoE is a subspecies accounting for 5-10% of total plasma apoA-I and has a relatively rapid secretion rate compared to HDL not containing apoE (ref. (10), **Chapter 2**). Second, apoE facilitates size expansion in vitro by interacting with LCAT (9, 11-13), and apoE enhances HDL size expansion in vivo in humans (ref. (10), **Chapter 2**). Finally, evidence in vitro and in animal models suggests that apoE facilitates removal of cholesterol-containing HDL from the body (14-17). This is due to the ability of apoE to bind to various liver receptors, including low density lipoprotein (LDL)-receptor (-R) (18), LDL-R related protein (LRP) (19), and heparin/heparan sulfate proteoglycans (20-23). In abetalipoproteinemia, in which HDL is the main plasma lipoprotein, apoA-I on apoE-containing HDL is cleared from the circulation faster than apoA-I on HDL that does not contain apoE (24). In normal humans, we have shown that HDL containing apoE is cleared from the circulation 5-10 times faster than HDL not containing apoE (ref. (10),

Chapter 2). Given these findings, we investigated whether this apoE-dependent, apparently protective process could be increased by an intervention such as dietary unsaturated fat.

Dietary fat increases plasma HDL-C concentration when it replaces carbohydrates or protein in the diet (25, 26). In 1990, the first dietary trial to study human HDL metabolism concluded that saturated fat, when it replaces carbohydrates in the diet, increases HDL-C by promoting the synthesis of plasma total apoA-I (27). A later study in 1999 confirmed this important finding (28). However, it is not known whether the increased apoA-I synthesis is coupled to increased flux through reverse cholesterol transport pathways such as those involving apoE. We hypothesized that dietary unsaturated fat enhances these putatively beneficial pathways. Up to now, a mechanistic link involving HDL metabolism has not been demonstrated between an HDL cholesterol raising treatment and prevention of atherosclerosis and cardiovascular disease (29).

3.2. Methods

Eligibility Criteria: We recruited adults between 21-75 years old who had low HDL-C ($\leq$45 mg/dl for men, $\leq$55 mg/dl for women) and high body-mass index (25-35 kg/m^2). Exclusion criteria included HDL-C (<20 mg/dl), LDL-C (>190 mg/dl), TG (>500 mg/dl), use of lipid lowering medications or hormone replacement therapy, history of diabetes, and E2/E2, E2/E4, or E4/E4 apoE genotypes.

Dietary Protocol & Infusion Protocol: A schema of the study protocol is shown in **Figure 3.1**. The participants received two diets in a random (variable order) crossover design: a high-unsaturated fat diet (45% carbohydrate, 40% fat [10% saturated, 23% monounsaturated, 7% polyunsaturated], 15% protein, 180 mg cholesterol per day) and a low fat diet (65% carbohydrate, 20% fat [10% saturated, 8% monounsaturated, 7% polyunsaturated], 15% protein, 90 mg cholesterol per day), each for 28 days. The diets were both designed to be healthy, heavily featuring vegetable oils, nuts, and whole grains. Registered dieticians formulated the diets at the Center for Clinical Investigation nutrition research unit of Brigham and Women's Hospital in Boston, MA. Participants picked up all their food to take home on Monday, Wednesday, and Friday at the study site. All food and beverages were provided, and participants were not allowed to eat any other food, but were allowed diet soda, coffee, and tea. Alcoholic beverages were not included or permitted. Participants were asked not to alter their usual physical activity pattern. Participants were weighed during food pickups and dietitians adjusted the amount of food to prevent changes in weight (**Figure 3.2**). These procedures have been used in our previous studies (8, 10, 30, 31).

After four weeks on the first diet, participants were admitted to the Clinical and Translational Science Center at Brigham and Women's Hospital for a bolus infusion of $[5,5,5-^2H_3]$-L-leucine (D3-leucine), an amino acid isotope tracer (Cambridge Isotope Laboratories, Cambridge, MA), at a dose of 10 mg/kg of body weight, administered in a volume of 150 ml over 10 minutes. Blood was taken right before the infusion (time 0) and at regular time points following the infusion up to 94 hours (0.5, 1, 1.5, 2, 3, 4, 6, 8,
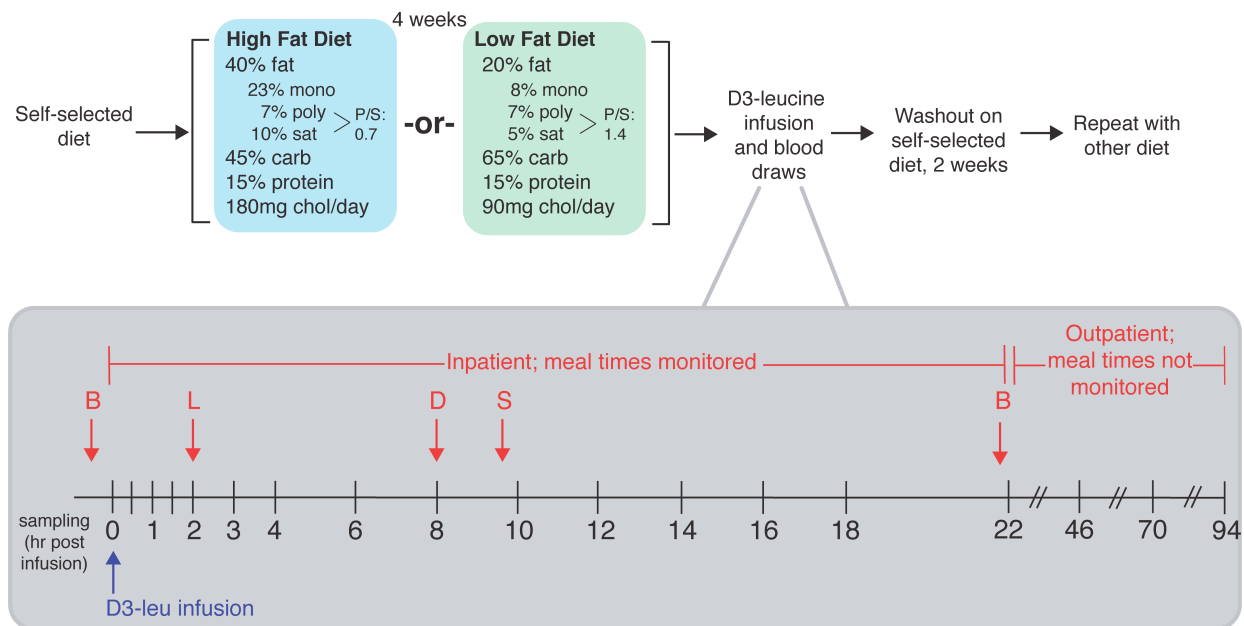
Figure 3.1: Overview of dietary intervention and sampling protocol. After screening, study participants were instructed to continue on their usual diet ("self-selected diet") prior to the study period, upon which they were randomized to either receive a high-unsaturated fat or low fat diet for four weeks. After four weeks on either the high-unsaturated fat or low fat diet, subjects were admitted to the hospital on the morning of Day 29 for the infusion protocol. They were instructed to eat the prescribed study breakfast (B) before coming to the hospital. At 10am (time 0) they received the bolus infusion of d3-leucine. Samples were collected at 0, 0.5, 1, 1.5, 2, 3, 4, 6, 8, 10, 12, 14, 16, 18, and 22 hours post-infusion while the study participants were in the hospital. Participants also ate lunch (L), dinner (D), and a snack (S) in the hospital. After the 22 hour sample was collected, participants were released from the hospital with their remaining study meals and were instructed to return to the hospital at 10am for the next 3 days for the remaining blood draws (46, 70, 94 hours). Before receiving the alternate diet and repeating the study protocol, they were instructed to return to their usual diet for a washout period of three weeks. mono = monounsaturated fat; poly = polyunsaturated fat; sat = saturated fat; carb = carbohydrate; chol = cholesterol
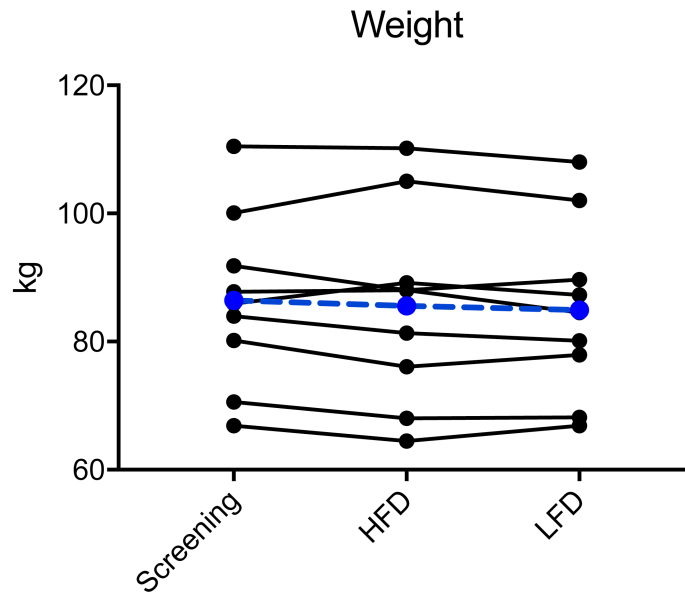
Figure 3.2: No change in body weight during dietary intervention period. Weight was measured at screening and following 4 weeks on high fat diet (HFD) and low fat diet (LFD). Mean value (n=9) shown in blue dashed line.

10, 12, 14, 16, 18, 22, 46, 70, 94 hours post infusion), and stored in chilled tubes that had been stored at 4°C. Up to 22 hours, participants received a low-leucine diet in the hospital as an inpatient so as to promote the incorporation of tracer leucine, rather than dietary leucine, into synthesized proteins. Following the 22-hour time point, participants were released from the hospital with the remaining study meals and instructed to return every morning for the next three days, up to 94 hours. After the completion of the last time point, participants were instructed to return to their normal diet for a washout period of 2 weeks before restarting the protocol with the second diet.

Collected plasma was separated immediately in a refrigerated centrifuge and aliquoted into tubes containing phenylmethanesulfonyl fluoride, gentamicin, benzamidine, and a protease inhibitor cocktail (all from Sigma). Aliquots were immediately placed into storage at -80°C until lipoprotein separation began after a median time of 3.5 months (range 1 to 18 months).

HDL subspecies separation using immunoaffinity column chromatography: These methods have been described in detail (32). Briefly, thawed plasma from each time point was incubated with Sepharose 4B immunoaffinity columns (Bio-Rad) containing affinity purified polyclonal antibodies to apoA-I (Academy Biomedical). The apoA-I containing bound lipoproteins were eluted with 3M sodium thiocyanate, and immediately desalted in PBS. This procedure was repeated with the unbound lipoproteins to improve recovery of apoA-I. Then, apoA-I containing lipoproteins were incubated in an anti-apoE immunoaffinity column (Academy Biomedical) to separate HDL into two subspecies:

HDL not containing apoE (E-), and HDL containing apoE (E+). Repeat incubation of unbound HDL to apoE columns was not needed. Efficiency of columns was measured and determined to be 90% for apoA-I and 99% for apoE. There were no differences in size or subspecies distribution comparing the HDL that bound to the anti-apoA-I antibody resin and that which did not.

HDL size separation and apoA-I purification: These methods have been described in detail (8). Briefly, HDL was separated by using non-denaturing polyacrylamide gel electrophoresis (PAGE) on a 4-30% gradient gel (Jule Biotechnologies) into four sizes, from largest to smallest: alpha-1 (9.5-12.2nm), alpha-2 (8.2-9.5nm), alpha-3 (7.1-8.2nm), and prebeta (<7.1nm) and then electrophoretically transferred to a 0.45 micrometer polyvinylidene difluoride (PVDF) membrane. The membranes were then stained with 0.2% amido black. HDL of each size were excised from PVDF membranes and eluted overnight at 4°C in Tris-SDS-Triton-X. ApoA-I from each HDL size was purified using SDS-PAGE in a 4-20% gradient, transferred to a PVDF membrane and stained with 0.2% amido black. Excised apoA-I bands underwent amino acid hydrolysis and derivatization to heptafluorobutyric acid esters. Measurements of tracer enrichment were performed by gas chromatography/single-ion monitoring mass spectrometry as previously described (30). Investigators and laboratory technicians were blinded to the diet allocation of each sample during laboratory separation and purification.

Tracer enrichment and pool size: The apoA-I tracer enrichment at each time point was defined as area under the curve (AUC) of D3-leucine / (AUC of D3-leucine + AUC of

D0-leucine). ApoA-I concentration of each HDL subspecies was measured at each time

point using SDS-PAGE band densitometry, corrected to plasma total apoA-I values

determined by ELISA. ApoA-I pool size was determined by multiplying apoA-I

concentration by plasma volume, which was assumed to be 4.4% of ideal body weight

(calculated using a BMI of 25 kg/m^2). Because all participants were overweight, we

adjusted the plasma volume using the following formula: Adjusted plasma volume =

ideal body weight $\times$ 0.044 + excess weight $\times$ 0.010 (33).

Model development and kinetic analysis: Compartmental modeling was performed using

SAAM-II (The Epsilon Group, Charlottesville, VA) (34). We constructed models using

prior knowledge about human HDL physiology (8, 10). The input was a forcing function

using free plasma leucine isotopic enrichment. The model outputs were rate constants

(in pools/hour, converted to pools/day) and flux measurements (in mg/hour, converted

to mg/day), each with a standard deviation and 95% confidence interval. For each HDL

subspecies, we chose the most parsimonious model (fewest number of parameters), on

the condition that it had favorable statistics (95% confidence intervals for parameter

estimations that excluded zero). Fractional catabolic rates (FCRs) for a specific HDL

subspecies were calculated by summing all the rate constants out of the compartment

for that subspecies. All models were initially established by using the average data of

the participants, following which the data for each participant was modeled individually

to achieve population statistics. For more information on model development, the reader

is referred to **Chapter 4**.

Plasma lipid and apolipoprotein measurements: Plasma lipid concentrations were measured at screening and the eighteen-hour time point of the infusion protocol, 8.5 hours after dinner. Cholesterol and triglycerides were measured using an enzymatic assay (Thermo Scientific). HDL-C was measured in the supernatant of plasma after the precipitation of apoB-containing lipoproteins with dextran sulfate (50,000 MW, Genzyme). LDL-C was estimated using the Friedewald equation (35). ELISA using affinity-purified antibodies (Academy Bio-Medical Co.) was performed to measure fasting plasma concentrations of apoA-I, apoE, apoCIII, and apoB. ELISA plates were read with a BioTek Synergy HT 96-well plate reader controlled by Gen5 1.10 software. All assays were completed in triplicate, and any sample with an intra-assay coefficient of variation >15% was repeated. Final data were exported to GraphPad Prism for analysis and database management.

ApoE Genotyping: We performed genotyping on buffy coat samples using the ABI PRISM 7900HT Sequence Detection System (Applied Biosystems, Foster City, CA), in 384-well format. The 5' nuclease assay (TaqMan®) was used to distinguish the two alleles of a gene. PCR amplification was carried out on 5-20ng DNA using 1 X TaqMan® universal PCR master mix (No Amp-erase UNG) in a 5 ml reaction volume. Amplification conditions on an AB 9700 dual plate thermal cycler (Applied Biosystems, Foster City, CA) were as follows: 1 cycle of 95°C for 10 minutes, followed by 50 cycles of 92°C for 15 seconds and 60°C for 1 minute. TaqMan® assays were ordered using the ABI Assays-on-Demand service.

Statistics: The results are presented as means $\pm$ SEM unless otherwise specified.

Paired two-tailed t tests were used to compare two parameters in the same participants (for example, apoA-I fractional catabolic rates in HDL containing vs. not containing apoE, or apoA-I pool sizes in HDL containing apoE on a high fat vs. low fat diet). Tests to compare HDL subspecies were carried out independently in each HDL size. Significance was denoted as $p<0.05$ unless otherwise specified. All statistical analysis was performed using GraphPad Prism 7 (La Jolla, CA). This study had greater than 90% power to detect significant ($p<0.05$) within-person differences between the diets in secretion rates, size expansion flux, and fractional catabolic rates of both HDL subspecies.

Study Approval: The study was performed in accordance with the principles of the Declaration of Helsinki and all procedures were approved by the Human Subjects Committee at Brigham and Women's Hospital. All participants gave written informed consent.

3.3. Results

Nine participants completed the dietary intervention and tracer infusion protocol (**Figure 3.1**). The characteristics of the participants are shown in **Table 3.1.** The average age was 47 years and all participants were overweight or obese (average BMI 29 kg/m^2). Total cholesterol was 199 mg/dl and all participants had low HDL-C (average 41 mg/dl). Mean triglycerides were 151 mg/dl, with a large range of 50-260 mg/dl. Six participants had the E3/E3 genotype; two had E4/E3; and one had E2/E3.

Table 3.1: Characteristics of study participants at screening (n=9).

ID	Age	Sex	Race	BMI (kg/m^2)	Weight (kg)	Total cholesterol (mg/dl)	LDL-C (mg/dl)	HDL-C (mg/dl)	TG (mg/dl)	ApoE genotype
1	68	male	White	30	84	215	136	45	169	E4/E3
2	51	male	White	30	100	159	102	38	95	E3/E3
3	59	female	White/His.	29	67	247	174	47	129	E2/E3
4	34	female	White	28	71	222	125	45	260	E3/E3
5	58	male	White	29	88	206	118	34	271	E4/E3
6	31	male	White	28	80	256	184	36	182	E3/E3
7	33	female	Black	30	86	142	95	37	50	E3/E3
8	39	male	White	32	110	176	103	45	138	E3/E3
9	48	male	Black	30	92	171	116	42	64	E3/E3
Mean	47			29	86	199	128	41	151	
SD	13			1	14	40	32	5	78	

Figure 3.3 shows the effect of the two study diets on fasting lipids and apolipoproteins. Both diets significantly reduced total cholesterol (**Figure 3.3a**) and LDL-cholesterol (**Figure 3.3b**) by 25-30% compared to levels at the screening visit when study participants were eating self-selected diets ($p \leq 0.001$ for both diets). The changes on each diet were not significantly different from each other ($p=0.68$ for total cholesterol, $p=0.91$ for LDL-C). There were no differences in HDL-C compared to screening ($p=0.89$ for HFD; $p=0.19$ for LFD). HDL-C was 5% higher on the high- compared to the low-fat diet ($p=0.076$) (**Figure 3.3c**), whereas apoA-I was 7% lower ($P=0.09$). Both diets reduced plasma triglycerides (**Figure 3.3d**) by about 30% ($p<0.05$ for both; $p=0.80$ between diets). The diets did not significantly affect plasma concentrations of apoE, apoCIII, or apoB (**Figure 3.3e-h**).

Figure 3.4 shows the effect of diet on HDL apoA-I metabolism. The most parsimonious model used to fit the data in SAAM-II, the "bare minimum model," (ref. (10), **Chapter 2**) is shown in **Figure 3a**. It is characterized by a D3-leucine forcing function ("FF") to model the precursor amino acid enrichment, which feeds into the "Source" compartment (representing liver or intestinal synthesis of apoA-I). Each HDL size is secreted into plasma directly, represented by four separate compartments. The smallest HDL size, prebeta, also receives input from a "delay" compartment (representing time spent outside the plasma, for example in interstitial fluid or lymph) and from a remodeling compartment originating from alpha-3 (presumably representing recycling and remodeling of HDL apoA-I by the liver during cholesterol uptake). Each HDL size is
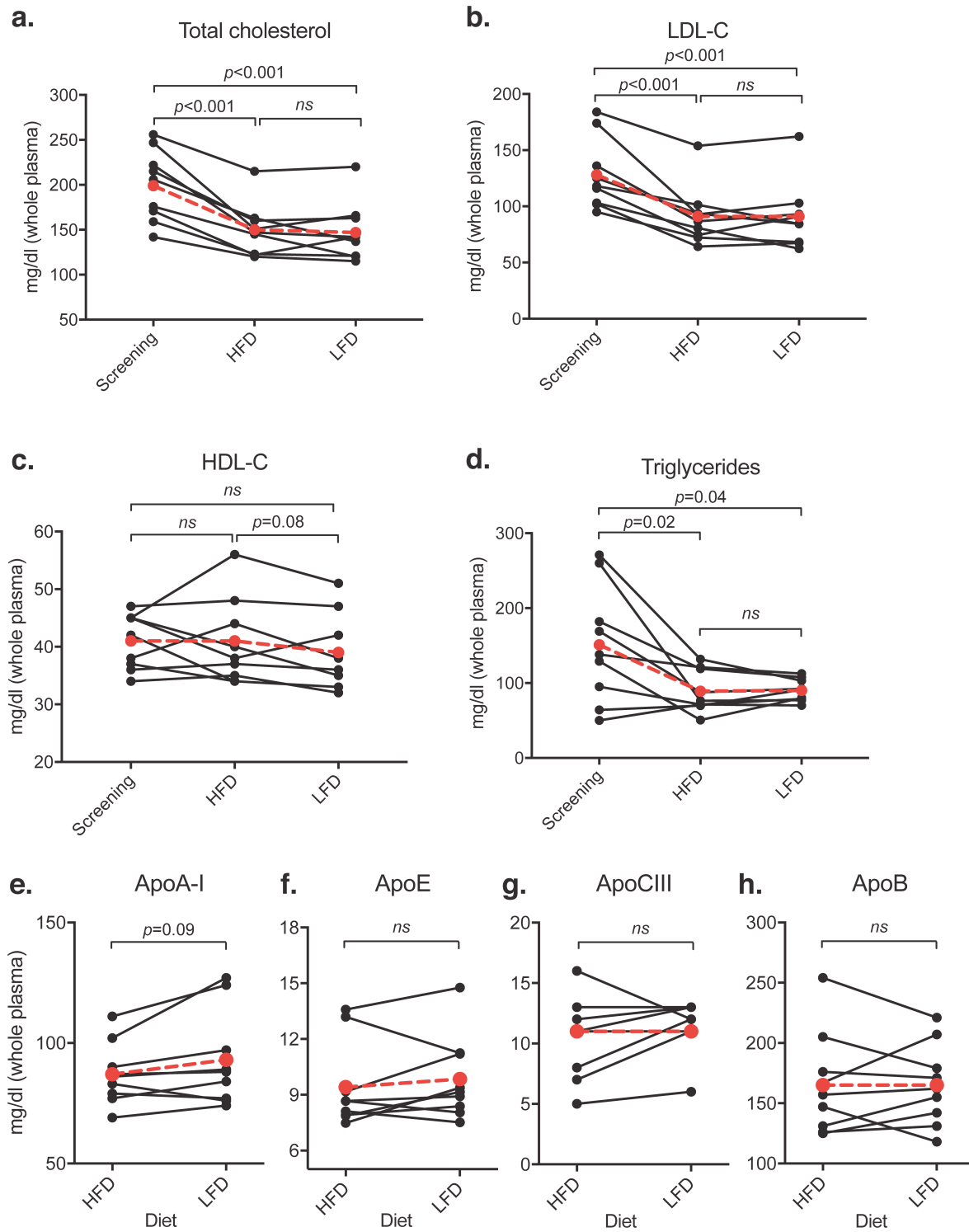
Figure 3.3: Effect of diet on fasting concentrations of plasma lipids and apolipoproteins.

Figure 3.3 (continued): Effect of diet on fasting concentrations of plasma lipids and apolipoproteins. Values (mg/dl) were measured at each study participant's screening visit (lipids only) and following completion of each dietary intervention. HFD = high fat diet; LFD = low fat diet. Mean value (n=9) shown in thicker colored circle and dotted red line. P-value shown for paired two-tailed t-test. ns = not significant ($p>0.15$). **(A)** Total cholesterol. **(B)** LDL-cholesterol. **(C)** HDL-cholesterol. **(D)** Triglycerides. **(E)** ApoA-I. **(F)** ApoE. **(G)** ApoCIII. **(H)** ApoB.
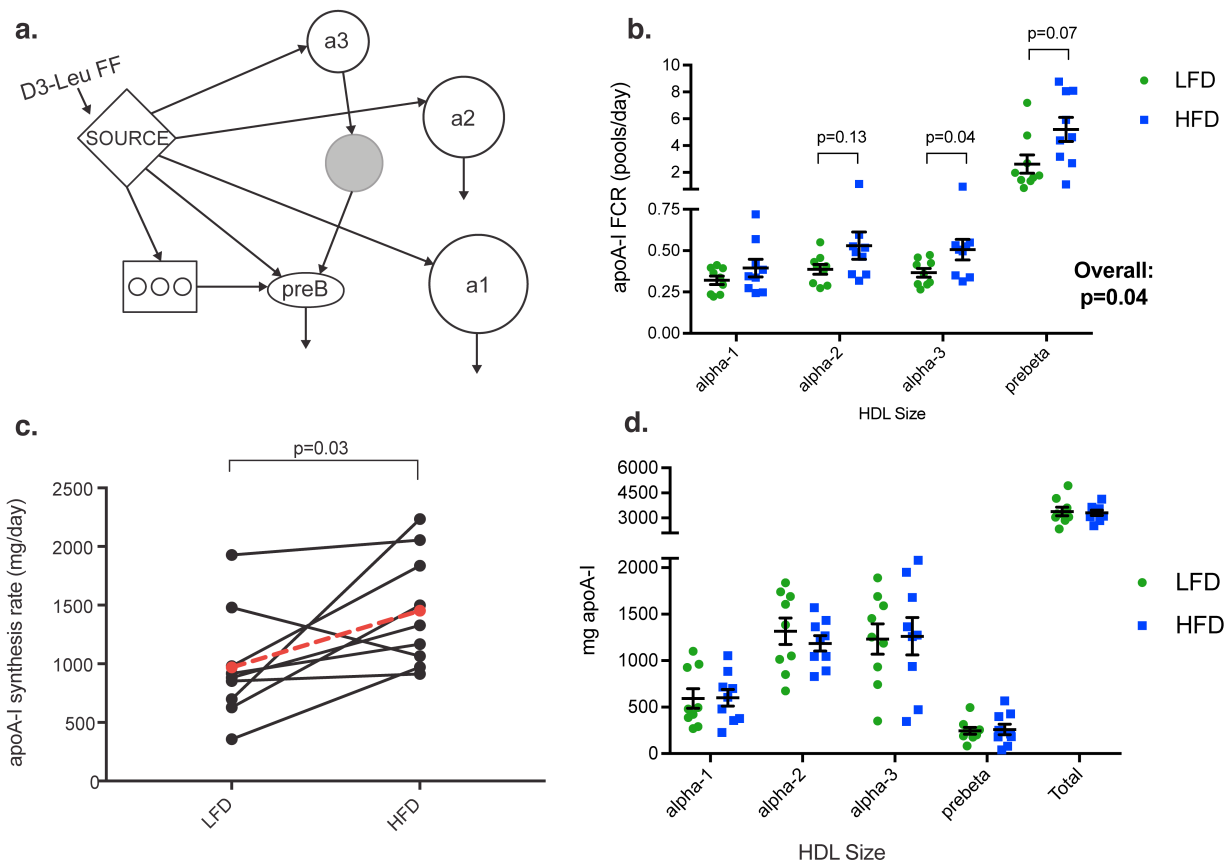
Figure 3.4: Dietary unsaturated fat increases the synthesis and clearance rates of HDL apoA-I (n=9).

Figure 3.4 (continued): Dietary unsaturated fat increases the synthesis and clearance rates of HDL apoA-I (n=9). HFD = high fat diet; LFD = low fat diet. P-value shown for paired two-tailed t-test. **(A)** SAAM-II compartmental model ("bare minimum model"). Plasma D3-leucine enrichment, the precursor, is modeled as a forcing function (FF) input to the liver or intestine ("Source" compartment). Circles represent each HDL size. Lines represent transfer of apoA-I from one compartment to another. Rectangles represent intravascular delay compartments used for lipoprotein synthesis, assembly, and secretion. The gray circle represents a non-sampled remodeling compartment to generate prebeta HDL. See **Chapter 2** and **Chapter 4**. **(B)** Fractional catabolic rates (FCR, pools/day) across four sizes of HDL. Mean value shown. Error bars = SEM. **(C)** Synthesis rates (mg/day). Mean value (n=9) shown in thicker colored circle and dotted red line. **(D)** Plasma apoA-I pool size (mg) across four sizes of HDL and total. Mean value shown. Error bars = SEM.

directly cleared from circulation. This model provided excellent visual fits for both diets as well as low standard deviations for each parameter value (data not shown). The high fat diet increased clearance of HDL apoA-I (p=0.04 overall) (**Figure 3.4b**). Concomitantly, we found that the high fat diet increased overall apoA-I synthesis rates by about 50% (p=0.03) (**Figure 3.4c**). These two metabolic processes led to approximately equal pool sizes on the diets (**Figure 3.4d**).

Figure 3.5 shows the models and model fits of the D3-leucine tracer enrichment of apoA-I on four sizes of HDL either containing apoE or not containing apoE. We started with the most parsimonious "bare minimum" model (**Figures 3.5a, 3.4a, Chapters 2, 4**) This model fit the apoA-I tracer enrichments of apoA-I on HDL not containing apoE (E-), showing excellent visual fits as well as low standard deviations for each parameter value. Adjustments to the "bare minimum" model are shown in **Figure 3.5b** (ref (10), **Chapters 2, 4**). This model had size expansion pathways from prebeta HDL to the larger alpha-2 and alpha-1 sizes, and an intravascular delay compartment feeding into alpha-3 synthesis. These additional pathways were necessary to fit the apoA-I tracer enrichments in HDL containing apoE (E+).

Figure 3.5c shows the mean (n=9) D3-leucine tracer enrichment and SAAM-II model fit for apoA-I on four sizes of HDL either containing apoE (E+) or not containing apoE (E-) across two diets. The latest time points (70 and 94 hours) were removed from the analysis for visual purposes after determining that they did not affect fitting of the
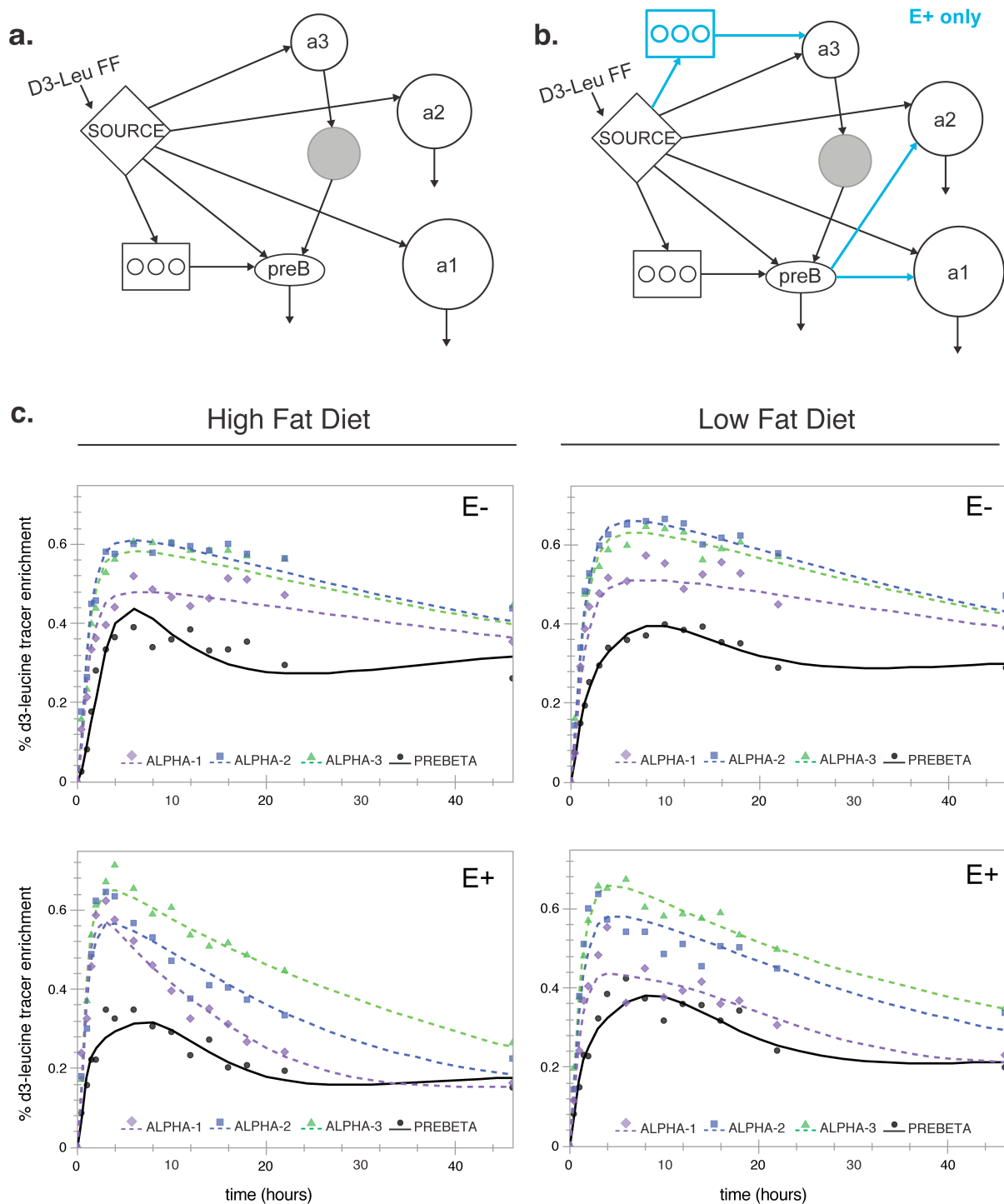
Figure 3.5: Model fit for apoA-I tracer enrichments for each HDL subspecies across two diets.

Figure 3.5 (continued): Model fit for apoA-I tracer enrichments for each HDL subspecies across two diets. (A) SAAM-II compartmental model ("bare minimum model"). See **Figure 3.4a**, **Chapter 4**. **(B)** Modifications to the "bare minimum model." Blue arrows and delay compartment represent additional pathways for the E+ subspecies only. **(C)** Model fit for the average (n=9) apoA-I tracer enrichment on four sizes of HDL, across each HDL subspecies and diet. The % d3-leucine tracer enrichments [d3-leucine/(d3-leucine + d0-leucine)*100] were generated by averaging all participants' enrichments (n=9) at each time point and modeling them as a single participant. Points = data; Lines = model fit.

descending slope of the tracer enrichment curve. All sizes of HDL appeared in circulation around the same time. HDL E+ reached peak enrichment around 4-6 hours, and HDL E- at about 8-10 hours. Compared to apoA-I on E- HDL, apoA-I on E+ HDL had steeper ascending and descending slopes from the peak tracer enrichment, generally indicative of faster FCR. These faster rates are confirmed in **Figure 3.6**. On both diets, apoA-I on HDL containing apoE was cleared from the circulation about ten times more quickly than HDL not containing apoE, except on the smallest prebeta HDL (**Figure 3.6a-b**). When considering all sizes together, the overall difference in clearance was highly significant (p=0.001 for both diets). The effect of diet was striking on HDL containing apoE (E+) (**Figure 3.6c**). The high fat diet significantly increased apoA-I FCR on the larger HDL sizes by about 250% (p=0.03 for alpha-1, p=0.005 for alpha-2), and over all sizes (p=0.057). In contrast, HDL not containing apoE had a 37% faster FCR of on the high fat diet, but it was not significant (p=0.12) **(Figure 3.6d)**.

Figure 3.7 shows the effect of diet on the distribution of apoA-I mass and synthesis rates across four sizes of HDL (from large to small: alpha-1, alpha-2, alpha-3, prebeta) either containing apoE or not containing apoE. About 5% of apoA-I was present on HDL containing apoE, irrespective of diet (**Figure 3.7a**). About 70% of apoA-I was on the middle HDL sizes (alpha-2 and alpha-3), regardless of diet or subspecies. HDL containing apoE had slightly more apoA-I on the two smaller sizes (alpha-3 and prebeta) than HDL not containing apoE (p=0.04 for HFD, p=0.11 for LFD). Overall, there was no effect of diet on apoA-I pool size. The percent distribution of apoA-I across sizes and subspecies was similar in the two diets (data not shown).
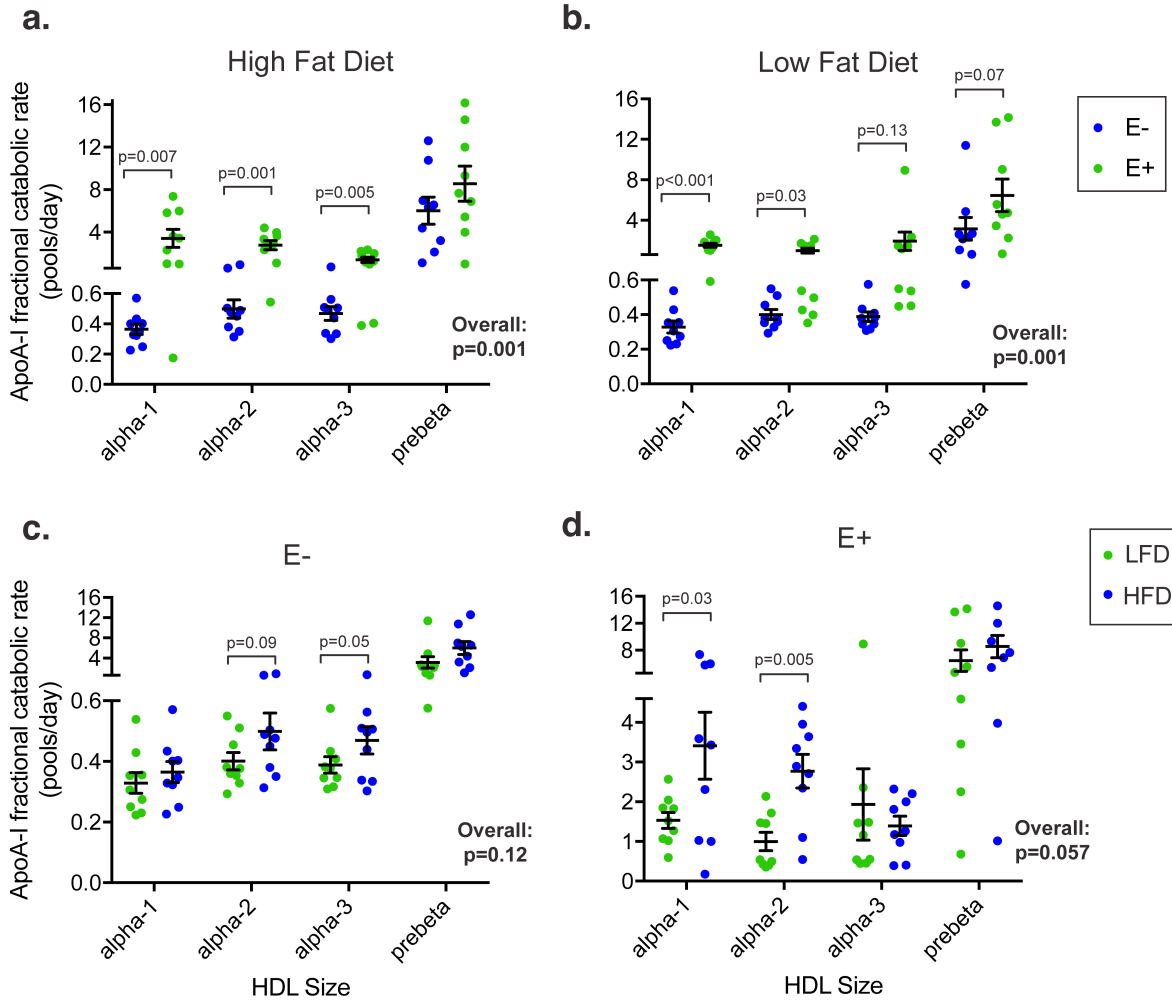
Figure 3.6: Dietary unsaturated fat increases the clearance rates of the larger sizes (alpha-1 and alpha-2) of HDL containing apoE (E+).

Figure 3.6 (continued): Dietary unsaturated fat increases the clearance rates of the larger sizes (alpha-1 and alpha-2) of HDL containing apoE (E+). ApoA-I fractional catabolic (turnover) rates (FCRs) in pools/day for are shown for each HDL subspecies across two diets. Each point is an individual study participant (n=9 for all). Black bar = mean, error bars = SEM. LFD = low fat diet; HFD = high fat diet. P-value shown for paired two-tailed t-test. Overall p-value for comparison considering all sizes together is shown on each graph. **(A)** Comparison of apoA-I FCRs on subspecies of HDL containing apoE (E+) or not containing apoE (E-) in the context of a high fat diet. **(B)** Comparison of apoA-I FCRs on subspecies of HDL containing apoE (E+) or not containing apoE (E-) in the context of a low fat diet. **(C)** Comparison of apoA-I FCRs across two diets only among the subspecies of HDL not containing apoE (E-). **(D)** Comparison of apoA-I FCRs across two diets only among the subspecies of HDL containing apoE (E+).
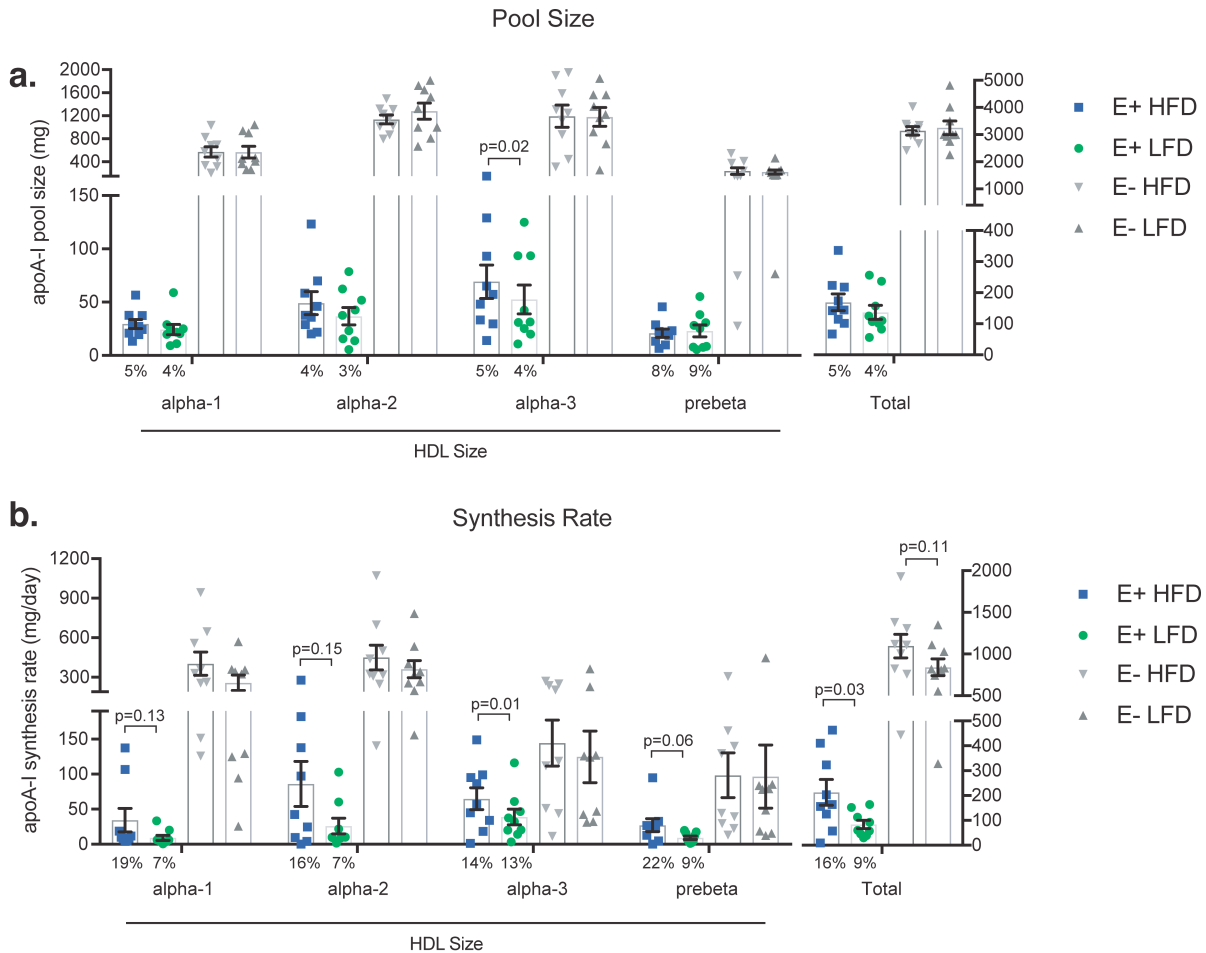
Figure 3.7: Dietary unsaturated fat increases the synthesis of HDL containing apoE (E+). Mean plasma apoA-I pool sizes and synthesis rates are shown in four sizes of HDL subspecies containing apoE (E+) or not containing apoE (E-), across two diets (HFD = high fat diet; LFD = low fat diet). Error bars = SEM. P-value shown for paired two-tailed t-test. **(A)** Mean absolute pool size of apoA-I (mg) and percent of apoA-I on E+ HDL. **(B)** Mean absolute synthesis rate of apoA-I (mg/day) and percent of apoA-I synthesized on E+ HDL per day.

The high fat diet significantly increased the synthesis of apoA-I on HDL containing apoE by about 250% (p=0.03 when considering all sizes together) (**Figure 3.7b**). The high-fat diet also tended to increase the synthesis of apoA-I on HDL not containing apoE by about 30% (p=0.11 when considering all sizes together). Relative to its pool size, a disproportionate amount of apoA-I synthesis occurred on HDL containing apoE, especially on the high fat diet (16% of total apoA-I synthesis vs. 5% of total apoA-I pool size).

Figure 3.8 illustrates the effect of diet on HDL apoA-I flux in the E+ subspecies via synthesis, size interconversion, and clearance pathways. The high fat diet significantly increased the synthesis rate by about 250% (p=0.03) (**Figure 3.8a, Figure 3.7b**). Increased synthesis was evident in each size subfraction. The high fat diet tended to increase size expansion from prebeta to alpha-2 (p=0.09), and size contraction from alpha-3 to prebeta (p=0.01) (**Figure 3.8b**). The high fat diet also increased the clearance of alpha-1 by about 200% (p=0.09) and of alpha-2 by about 400% (p=0.04) (**Figure 3.8c**). The high fat diet weakly increased apoA-I synthesis in E- HDL, but it was not significant (30% higher vs. LFD, p=0.11, data not shown).

The data from Figures 3, 5, 6, and 7 is tabulated in **Table A3.1**.

ApoE genotype analysis: Our study participants included six E3/E3, as well as two E4/E3, one E2/E3, and one E2/E4 participant completed the dietary intervention trial but whose data was excluded from the main analysis due to the genotype violating study
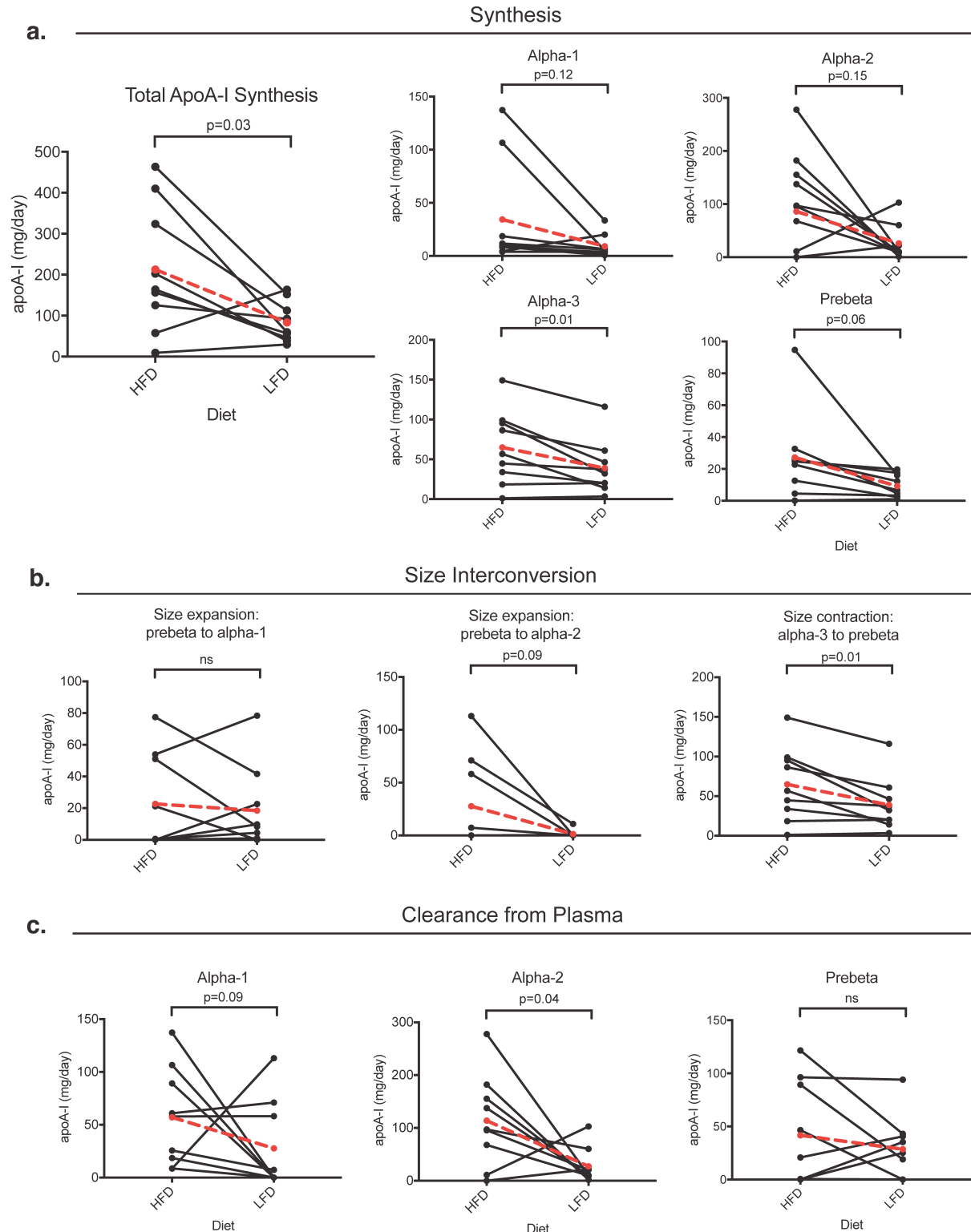
Figure 3.8: Dietary unsaturated fat increases apoA-I flux through synthesis, size expansion, size contraction and clearance pathways in HDL containing apoE (E+).

Figure 3.8 (continued): Dietary unsaturated fat increases apoA-I flux through synthesis, size expansion, size contraction and clearance pathways in HDL containing apoE (E+). Individual values shown, with mean value (n=9) in larger point and dotted red line. HFD = high fat diet, LFD = low fat diet. P-value shown for paired two-tailed t-test. **(A)** Pathways from the source compartment to each HDL size, representing synthesis and secretion from the liver (or small intestine) and appearance in plasma. **(B)** Pathways between HDL sizes, representing HDL size expansion or contraction. The source size and destination size are indicated above each graph. **(C)** Clearance of apoA-I on each HDL size from plasma. Note that all of alpha-3 is converted to prebeta and is thus not directly cleared from plasma (see **Figure 3.5b**)

inclusion criteria. In E3/E3 homozygotes, the HFD produced significantly faster apoA-I FCRs in the larger alpha sizes, consistent with what we reported in **Figure 3.6** (~150% faster, p=0.05 for alpha-1; p=0.04 for alpha-2) (**Figure 3.9a)**. In contrast, there were no significant dietary differences in the heterozygotes (**Figure 3.9b**). When we compared the two sets of genotypes, the E3/E3 homozygotes had about 70% faster apoA-I FCRs compared to apoE heterozygotes on the HFD (p=0.07 in alpha-1 and alpha-3, p=0.09 when pooling all sizes together) (**Figure 3.9c**) and 140% faster apoA-I FCRs on the LFD (**Figure 3.9d**). As a negative control, we found no differences in apoA-I FCRs between E3/E3 and heterozygotes in the E- subspecies on either diet, indicating that the participants were not otherwise different (**Figure A3.1**).

We next compared apoA-I FCRs on E+ vs. E- HDL to see if they had evidence of "dysfunctional" apoE. As expected, in E3/E3 homozygotes the clearance rates for apoA-I on E+ HDL were substantially faster than those of E-, regardless of diet (**Figure 3.9e-f**). However, in the heterozygotes the clearance rates for apoA-I on E+ HDL were overall not different than those of E- HDL on either diet (**Figure 3.9g-h**). The participant with the E2/E4 genotype had markedly lower apoA-I fractional catabolic rates of E+ HDL on both diets compared to other study participants (**Figure 3.10a**), consistent with previous reports of defective binding of apoE2 to cell surface receptors (36). The apoA-I FCRs of E- HDL, in which no apoE is present, were not different in the E2/E4 individual compared to other study participants (**Figure 3.10b**).
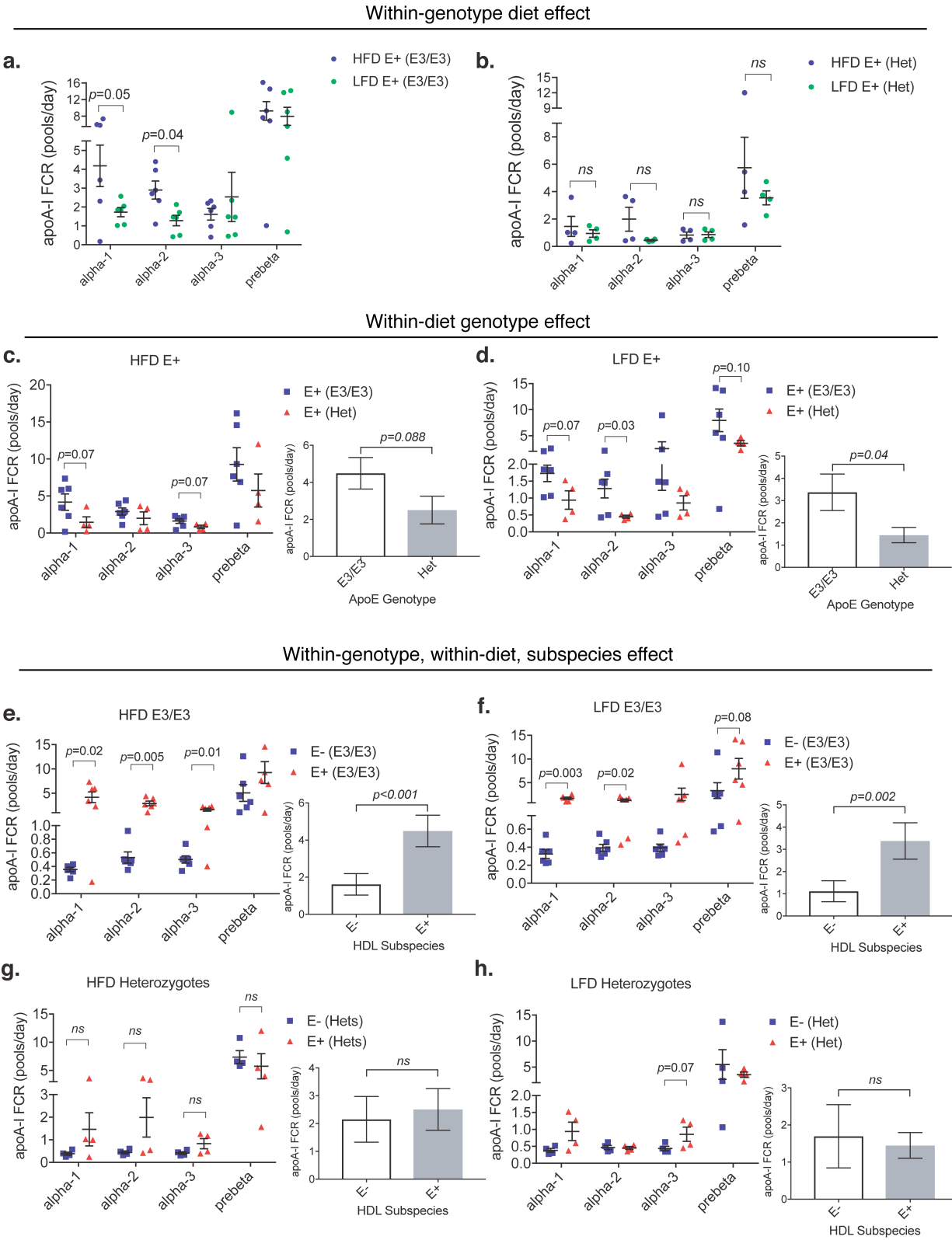
Figure 3.9: High-fat compared to low-fat diet increases clearance rate of HDL containing apoE in apoE3/E3 homozygotes but not in apoE heterozygotes.

Figure 3.9 (continued): High-fat compared to low-fat diet increases clearance rate of HDL containing apoE in apoE3/E3 homozygotes but not in apoE heterozygotes. ApoE3/E3 homozygotes have faster apoA-I clearance rates than apoE heterozygotes on high- or low-fat diets. ApoA-I fractional catabolic rates (FCR, pools/day) are shown in 6 E3/E3 homozygotes compared to 4 apoE heterozygotes (pooled: 1 E2/E3, 2 E4/E3, 1 E2/E4) (Het). Error bars = SEM. P-value shown for two-tailed t-test, unpaired (a, b) or paired (c-h). ns = not significant (p>0.15). **(A)** Dietary effects on HDL containing apoE (E+) in E3/E3. **(B)** Dietary effects on HDL containing apoE (E+) in heterozygotes. **(C)** HDL containing apoE (E+) on the high fat diet. Inset: All HDL sizes pooled together (n=24 for E3/E3, n=16 for Het) **(D)** HDL containing apoE (E+) on the low fat diet. Inset: All HDL sizes pooled together (n=24 for E3/E3, n=16 for Het) **(E)** ApoE3/E3 homozygotes: ApoA-I FCR in HDL either containing or not containing apoE on the high fat diet. Inset: All HDL sizes pooled together (n=24) **(F)** ApoE3/E3 homozygotes: ApoA-I FCR in HDL either containing or not containing apoE on the low fat diet. Inset: All HDL sizes pooled together (n=24) **(G)** ApoE heterozygotes: ApoA-I FCR in HDL either containing or not containing apoE on the high fat diet. Inset: All HDL sizes pooled together (n=16) **(H)** ApoE heterozygotes: ApoA-I FCR in HDL either containing or not containing apoE on the low fat diet. Inset: All HDL sizes pooled together (n=16); error bars = SEM
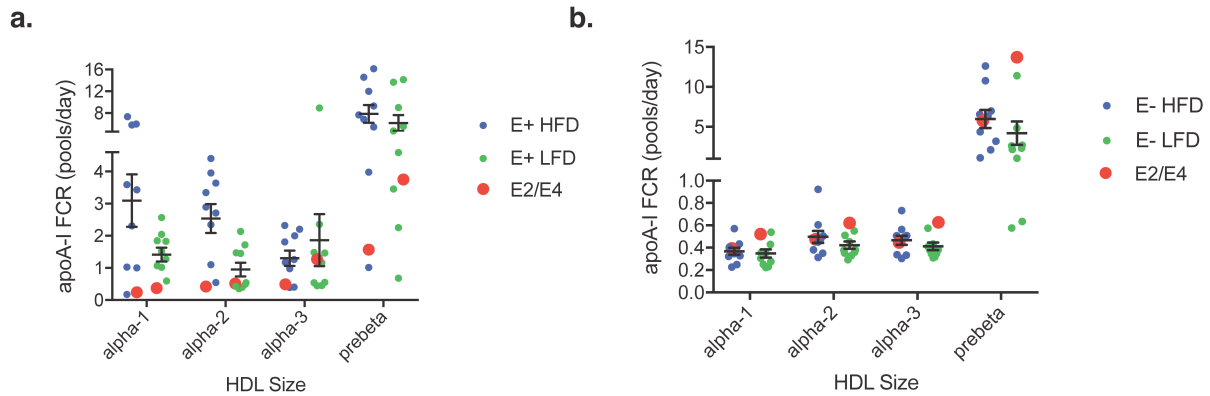
Figure 3.10: HDL clearance rates are low in E2/E4 genotype (n=1). (A) ApoA-I fractional catabolic rates (FCR) in HDL containing apoE (E+) across two diets (HFD = high fat diet; LFD = low fat diet) among 9 study participants: 6 with E3/E3, 2 with E4/E3, and 1 with E2/E3 (individual dots), and one participant with E2/E4 apoE genotype (large red dot). Black bar = mean; error bars = SEM. **(B)** Negative control: apoA-I fractional catabolic rates (FCR) in HDL not containing apoE (E-) across two diets (HFD = high fat diet; LFD = low fat diet) among 9 study participants (individual dots). Additional participant with E2/E4 apoE genotype is shown in large red dot. Black bar = mean; error bars = SEM.

3.4. Discussion

This is the first study to assess the ability of dietary intervention to impact the metabolism of human HDL in ways that are meaningful to reverse cholesterol transport. We chose to focus on subspecies of HDL containing apoE, which has been shown to increase HDL biogenesis, size expansion, and clearance (ref. (10), **Chapter 2**). We show here that, relative to a low fat diet, a high-unsaturated fat diet increases synthesis, size interconversion, and clearance from circulation of this subspecies. These effects potentially render this HDL subspecies more biologically active in metabolic pathways that involve reverse cholesterol transport.

The first dietary intervention trial to measure HDL apoA-I kinetics, published nearly three decades ago by Brinton et al., concluded that high saturated fat diets increased HDL-C mainly by promoting the synthesis of apoA-I (27). The methodology was labeling homologous apoA-I ex vivo with radioactive ^{125}-I, and returning it to the circulation and monitoring tracer disappearance curves for 2 weeks. Here, we report increased apoA-I synthesis rates on a high unsaturated fat diet (**Figure 3.4a**), which was apparently driven by the E+ subspecies (p=0.03) but also borderline significant in E- HDL (p=0.11) (**Figure 3.7b**). This is not surprising because unsaturated fatty acids, like saturated fatty acids, increase plasma total apoA-I when they replace carbohydrates (25). These results are also in line with another metabolic study that reported reduced apoA-I synthesis upon restriction of dietary fat (28).

No study has examined the effect diet on HDL size expansion. The only published information regarding size expansion in human HDL subspecies showed that size expansion occurs in a unique subspecies that contains apoE but not apoCIII (ref. (10), **Chapter 2**). In that study, size expansion pathways were also detectable in E+ HDL – but to a lesser extent, given the interference by concomitantly present apoCIII. In line with that data, we found mixed evidence of size expansion in E+ HDL (**Figure 3.8b**). This is probably due to interference by apoCIII, which is present in about half of E+ HDL and abrogates all detectable size expansion in this subspecies (ref. (10), **Chapter 2**). It is likely that separation of E+ HDL by apoCIII presence or absence would have elucidated further the dietary effect. We did see 67% increased size contraction from alpha-3 to prebeta on the high fat diet (**Figure 3.8b**). This represents liver uptake of the HDL lipid cargo and generation of prebeta, a critical step of reverse cholesterol transport.

Our study describes a unique effect of HFD to increase apoA-I clearance. The high unsaturated fat diet significantly increased the clearance rates of plasma total apoA-I (by 80% overall, p=0.04; by 33% in the alpha sizes only, p=0.003) (**Figure 3.4b**), in contrast to Brinton et al. who reported a modest but significant increase on the LFD (10% higher, p=0.005). The bigger difference in dietary fat (42% HFD vs. 9% LFD in Brinton et al.) and use of primarily saturated fat (56% of total fat in Brinton et al, in contrast to 25% of total fat in ours) may have contributed to their lower FCR. It is also possible that differences in study participant characteristics could contribute to the differences in dietary effects. For example, obesity is associated with a higher apoA-I

FCR (37-39), and correspondingly, our clearance rates were about double those of the mostly healthy-weight subjects in Brinton et al.

The dietary effect on clearance rates was especially evident in HDL containing apoE (**Figure 3.6d**), which suggest a subspecies-specific effect. ApoE is an essential protein for the metabolism of triglyceride-rich lipoproteins, but it is also present on HDL where it operates in a similar manner (ref. (10), **Chapter 2**). Here, we show that, regardless of diet, HDL containing apoE is cleared much more quickly than HDL not containing apoE (**Figure 3.6a-b**), consistent with the ability of apoE to act as a high affinity liver receptor ligand in vitro (18-23). These results add to those we recently published in a subset of the same participants (ref. (10), **Chapter 2**), now adding for the first time the comparison of E+ and E- in the context of a low fat diet.

These points raise the question of whether increased HDL catabolism is beneficial. Historically, increased clearance was not thought to be favorable, as this would result in lower apoA-I and HDL-C. However, these actions together (more synthesis, size interconversion, and clearance) could render HDL more biologically active in reverse cholesterol transport and improve HDL function. Interestingly, the increases in FCR were mainly evident in the largest HDL containing apoE, which undergo size expansion from smaller HDL and contain the most cholesterol. This suggests a functional difference between large and small HDL. Indeed, the large cholesterol-rich HDL would be the most favorable vehicle for delivering excess cholesterol to the liver for excretion.

The effect of diet was qualitatively similar in HDL not containing apoE (**Figure 3.6c**), but our study was underpowered to detect significant differences.

What is the clinical significance of these metabolic findings? There is minimal evidence connecting HDL subspecies metabolism with clinical outcomes. We showed that the subspecies of HDL containing apoE but not apoCIII not only has the metabolic properties described here, but also in a separate large population-based cohort is associated with a reduced risk of coronary heart disease (ref. (10), **Chapter 2**). Thus, the combination of increased synthesis, size expansion, and clearance from plasma is likely beneficial. Future studies should examine dietary effects in HDL subspecies that are also defined by presence or absence of apoCIII, as this protein acts in opposition to apoE in regulating lipoprotein metabolism (refs. (10, 40), **Chapter 2**). One possible manifestation of this protein-protein interaction is in size expansion. In the present study, dietary differences in size expansion were mixed, likely due to interference by masked, concomitantly present apoCIII (**Figure 3.8b**).

Brinton et al and others (25) have reported that dietary fat increases the concentration of apoA-I and HDL-C. In our study, the HFD-driven higher synthesis and clearance rates (**Figures 3.4b-c**) combined led to similar pool sizes (**Figures 3.3e, 3.4d**). Again, differences in macronutrient and specific fatty acid compositions, or differences in the study population, could have led to these divergent findings. Finally, differences in tracer methodology could have influenced the dietary effects in unknown ways.

We also found some evidence of a genotype-specific effect within the E+ HDL subspecies. To our knowledge, there has been no comparison of HDL metabolism by apoE genotype in this manner. The high fat diet significantly increased the clearance of only the apoE3 homozygotes (**Figure 3.9a**); there were no dietary differences among heterozygotes (anyone who was not E3/E3, which is considered "wild-type" (41)) (**Figure 3.9b**). ApoE heterozygotes trended to lower apoA-I clearance rates than their E3/E3 counterparts (**Figure 3.9c-d**). Surprisingly, apoE heterozygotes also did not have the expected increased apoA-I clearance rates over HDL not containing apoE (**Figure 3.9g-h**). This suggests that apoE could be dysfunctional in these participants. ApoE2 has almost no binding capabilities to LDL-R (36), which would be an important clearance mechanism for HDL containing apoE. In contrast, apoE4 has normal LDL-R binding (36), and has been shown to have increased catabolism compared to apoE3 (42). Although the exact mechanisms remain undetermined, it is thought that apoE4 1) associates more with remnant lipoproteins than with HDL and 2) leads to increased degradation of LDL-R (41, 42), which potentially explains the reduced apoA-I clearance in this study. To our knowledge, there is no evidence in the literature of HDL apoA-I metabolism in apoE heterozygotes. Our sample sizes were too small to make any definitive conclusions and are mainly hypothesis generating.

A critical finding of this study is that simply measuring plasma concentrations or pool sizes can obscure strong metabolic effects. We found no effect of diet on apoA-I pool size overall (**Figure 3.4d**) or in HDL subspecies either containing or not containing apoE (**Figure 3.7a**). However, the high unsaturated fat diet significantly increased synthesis

137

and clearance (**Figure 3.4b-c**) of plasma total apoA-I and of HDL containing apoE (**Figures 3.6d, 3.7b, 3.8**). We also report borderline significant increases in synthesis and clearance of apoA-I on HDL not containing apoE (**Figure 3.6c, 3.7b**). In both subspecies, pool sizes were not different across diets (**Figure 3.7a**). Thus, therapeutics aimed at increasing HDL-C or apoA-I could be misguided efforts, and conversely, ones that do not alter levels of HDL-C or apoA-I could have unseen metabolic effects. A potentially more useful approach is designing therapies that, regardless of their consequent effects on HDL-C or apoA-I, target the steps of reverse cholesterol transport: increasing HDL biogenesis, facilitating size expansion by cholesterol efflux, and increasing clearance of cholesterol-rich large HDL. We have seen all aspects of this process in HDL containing apoE (ref. (10), **Chapter 2**), which are further driven by dietary unsaturated fat.

Strengths of our study are in the study population, dietary intervention, and robustness of kinetic models. Our study population is heterogeneous, including both males and females over a large age range, with the clinically relevant low HDL, high BMI phenotype (**Table 3.1**). The diets were completely controlled rather than allowing participants to self-report food intake. Additionally, both diets were isocaloric, removing the confounding effects of weight change on HDL and apoA-I levels. Both diets featured contemporary foods and were not extreme in their macronutrient formulations; our intent was to study the differences between ordinary healthy diets. Finally, our kinetic models (ref. (10), **Chapters 2, 4**) were universally used across all participants on both diets, strengthening the concept that the framework for HDL metabolism is conserved across

heterogeneous humans. A major limitation of our study is the lack of a normal HDL-C, non-obese comparison group. We also suffered from a small overall sample size leading to insufficient power to detect differences in HDL not containing apoE.

In summary, we have shown for the first time that an intervention can facilitate reverse cholesterol transport in humans particularly by driving the metabolism of HDL subspecies (**Figure 3.11**). Compared to a low fat diet, a diet high in unsaturated fat preferentially increases the appearance in plasma of HDL containing apoE, promotes size interconversion, and increases the clearance from plasma of this HDL subspecies. These metabolic properties could render this HDL subspecies more proficient in reverse cholesterol transport, the hallmark of HDL function.

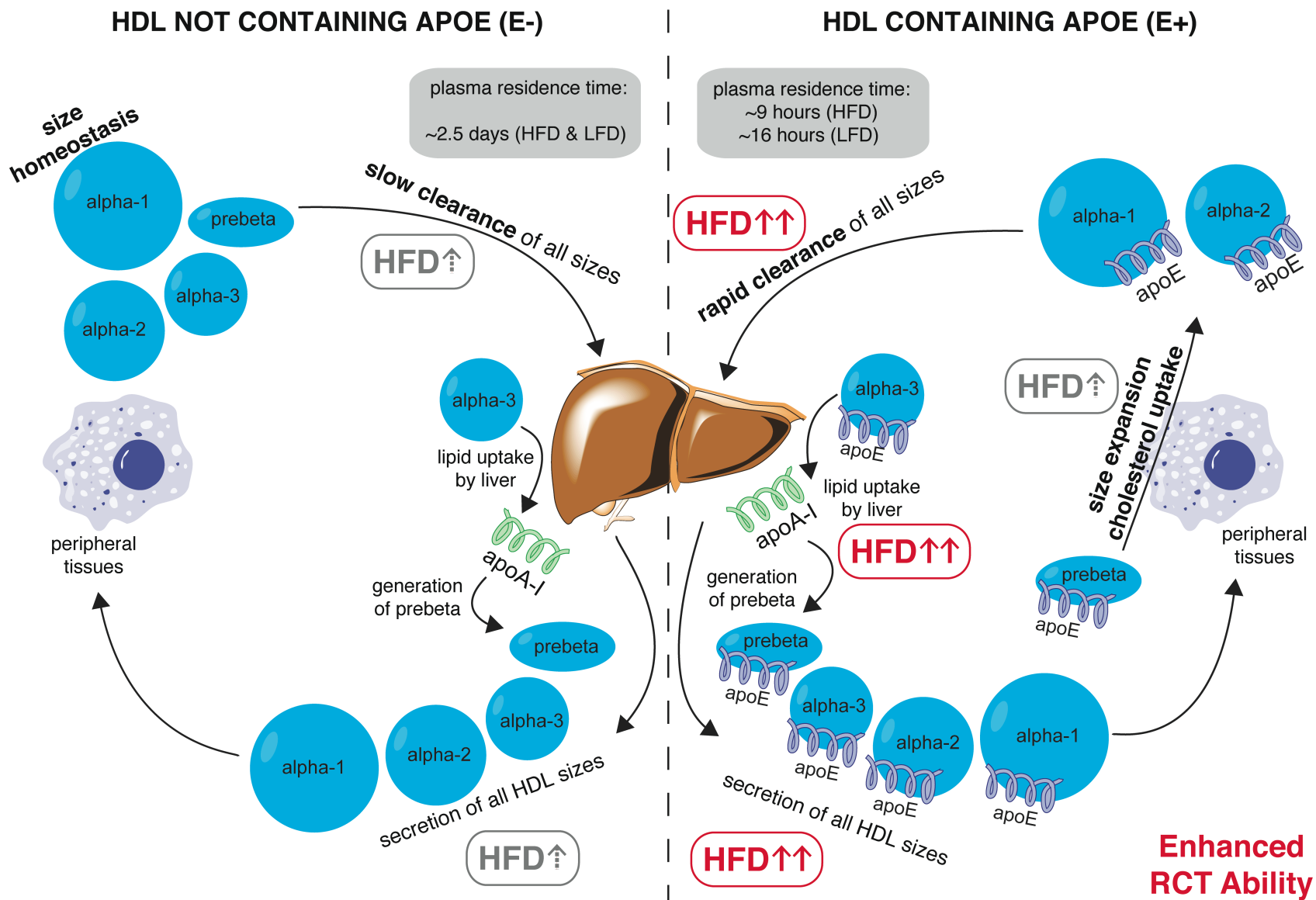### 3.5.   Acknowledgments

Figure 3.11: Model of reverse cholesterol transport stimulated by dietary unsaturated fat (HFD) through HDL containing apoE.

Figure 3.11 (continued): Model of reverse cholesterol transport stimulated by dietary unsaturated fat (HFD) through HDL containing apoE. In the left panel, HDL not containing apoE is secreted in all sizes by the liver, which is weakly stimulated by HFD (gray box with dashed up-arrow). This HDL subspecies visits peripheral tissues (represented by the macrophage), where it may take up cholesterol but insufficient to increase HDL to a larger size category. This HDL subspecies is cleared slowly by the liver with an average residence time of about 2.5 days, regardless of diet. In the right panel, the HFD significantly increases secretion of all sizes of HDL containing apoE (red box with bold red arrows). This HDL visits peripheral tissues, takes up cholesterol, and undergoes size expansion, which is stimulated by HFD. HFD significantly increases clearance of this subspecies as well as size contraction from alpha-3, representing lipid uptake and prebeta generation at the liver, reducing the residence time to about 9 hours (HFD) and 16 hours (low fat diet, LFD). These actions together may represent enhanced reverse cholesterol transport (RCT) driven by high unsaturated fat diets.

## 3.6.	References

1. Nanjee MN et al. Intravenous apoA-I/lecithin discs increase pre-beta-HDL concentration in tissue fluid and stimulate reverse cholesterol transport in humans. *J. Lipid Res.* 2001;42(10):1586–1593.

2. Colvin PL, Moriguchi E, Barrett PH, Parks JS, Rudel LL. Small HDL particles containing two apoA-I molecules are precursors in vivo to medium and large HDL particles containing three and four apoA-I molecules in nonhuman primates. *J. Lipid Res.* 1999;40(10):1782–1792.

3. Sacks FM et al. Selective delipidation of plasma HDL enhances reverse cholesterol transport in vivo. *J. Lipid Res.* 2009;50(5):894–907.

4. Zhang Y et al. Overexpression of apolipoprotein A-I promotes reverse transport of cholesterol from macrophages to feces in vivo. *Circulation* 2003;108(6):661–663.

5. Moore RE et al. Increased atherosclerosis in mice lacking apolipoprotein A-I attributable to both impaired reverse cholesterol transport and increased inflammation. *Circ. Res.* 2005;97(8):763–771.

6. Cuchel M, Rader DJ. Macrophage reverse cholesterol transport: key to the regression of atherosclerosis? *Circulation* 2006;113(21):2548–2555.

7. Cuchel M et al. A novel approach to measuring macrophage-specific reverse cholesterol transport in vivo in humans. *J. Lipid Res.* 2017;58(4):752–762.

8. Mendivil CO, Furtado J, Morton AM, Wang L, Sacks FM. Novel Pathways of Apolipoprotein A-I Metabolism in High-Density Lipoprotein of Different Sizes in Humans. *Arterioscler. Thromb. Vasc. Biol.* 2016;36(1):156–165.

9. Kypreos KE, Zannis VI. Pathway of biogenesis of apolipoprotein E-containing HDL in vivo with the participation of ABCA1 and LCAT. *Biochem. J.* 2007;403(2):359–367.

10. Morton AM et al. Apolipoproteins E and CIII interact to regulate HDL metabolism and coronary heart disease risk. *JCI Insight* 2018;3(4). doi:10.1172/jci.insight.98045

11. Mahley RW, Huang Y, Weisgraber KH. Putting cholesterol in its place: apoE and reverse cholesterol transport. *J. Clin. Invest.* 2006;116(5):1226–1229.

12. Koo C, Innerarity TL, Mahley RW. Obligatory role of cholesterol and apolipoprotein E in the formation of large cholesterol-enriched and receptor-active high density lipoproteins. *J. Biol. Chem.* 1985;260(22):11934–11943.

13. Settasatian N, Barter PJ, Rye K-A. Remodeling of apolipoprotein E-containing spherical reconstituted high density lipoproteins by phospholipid transfer protein. *J. Lipid Res.* 2008;49(1):115–126.

14. Innerarity TL, Pitas RE, Mahley RW. Receptor binding of cholesterol-induced high-density lipoproteins containing predominantly apoprotein E to cultured fibroblasts with mutations at the low-density lipoprotein receptor locus. *Biochemistry* 1980;19(18):4359–4365.

15. Hui DY, Innerarity TL, Mahley RW. Lipoprotein binding to canine hepatic membranes. Metabolically distinct apo-E and apo-B,E receptors. *J. Biol. Chem.* 1981;256(11):5646–5655.

16. Blum CB, Deckelbaum RJ, Witte LD, Tall AR, Cornicelli J. Role of apolipoprotein E-containing lipoproteins in abetalipoproteinemia. *J. Clin. Invest.* 1982;70(6):1157–1169.

17. Funke H et al. Uptake of apolipoprotein E-containing high density lipoproteins by hepatic parenchymal cells. *Arteriosclerosis* 1984;4(5):452–461.

18. Mahley RW, Innerarity TL. Lipoprotein receptors and cholesterol homeostasis. *Biochim. Biophys. Acta* 1983;737(2):197–222.

19. Beisiegel U, Weber W, Ihrke G, Herz J, Stanley KK. The LDL-receptor-related protein, LRP, is an apolipoprotein E-binding protein. *Nature* 1989;341(6238):162–164.

20. Mahley RW, Weisgraber KH, Innerarity TL. Interaction of plasma lipoproteins containing apolipoproteins B and E with heparin and cell surface receptors. *Biochim. Biophys. Acta* 1979;575(1):81–91.

21. Futamura M et al. Two-step mechanism of binding of apolipoprotein E to heparin: implications for the kinetics of apolipoprotein E-heparan sulfate proteoglycan complex formation on cell surfaces. *J. Biol. Chem.* 2005;280(7):5414–5422.

22. Williams KJ, Chen K. Recent insights into factors affecting remnant lipoprotein uptake. *Curr. Opin. Lipidol.* 2010;21(3):218–228.

23. Gonzales JC, Gordts PLSM, Foley EM, Esko JD. Apolipoproteins E and AV mediate lipoprotein clearance by hepatic proteoglycans. *J. Clin. Invest.* 2013;123(6):2742–2751.

24. Ikewaki K, Rader DJ, Zech LA, Brewer HB. In vivo metabolism of apolipoproteins A-I and E in patients with abetalipoproteinemia: implications for the roles of apolipoproteins B and E in HDL metabolism. *J. Lipid Res.* 1994;35(10):1809–1819.

25. Mensink RP, Zock PL, Kester ADM, Katan MB. Effects of dietary fatty acids and carbohydrates on the ratio of serum total to HDL cholesterol and on serum lipids and apolipoproteins: a meta-analysis of 60 controlled trials. *Am. J. Clin. Nutr.* 2003;77(5):1146–1155.

26. Appel LJ et al. Effects of protein, monounsaturated fat, and carbohydrate intake on blood pressure and serum lipids: results of the OmniHeart randomized trial. *JAMA* 2005;294(19):2455–2464.

27. Brinton EA, Eisenberg S, Breslow JL. A low-fat diet decreases high density lipoprotein (HDL) cholesterol levels by decreasing HDL apolipoprotein transport rates. *J. Clin. Invest.* 1990;85(1):144–151.

28. Vélez-Carrasco W et al. Dietary restriction of saturated fat and cholesterol decreases HDL ApoA-I secretion. *Arterioscler. Thromb. Vasc. Biol.* 1999;19(4):918–924.

29. Sacks FM et al. Dietary Fats and Cardiovascular Disease: A Presidential Advisory From the American Heart Association. *Circulation* 2017;136(3):e1–e23.

30. Zheng C, Khoo C, Ikewaki K, Sacks FM. Rapid turnover of apolipoprotein C-III-containing triglyceride-rich lipoproteins contributing to the formation of LDL subfractions. *J. Lipid Res.* 2007;48(5):1190–1203.

31. Mendivil CO, Zheng C, Furtado J, Lel J, Sacks FM. Metabolism of very-low-density lipoprotein and low-density lipoprotein containing apolipoprotein C-III and not other small apolipoproteins. *Arterioscler. Thromb. Vasc. Biol.* 2010;30(2):239–245.

32. Talayero B et al. Obesity Favors Apolipoprotein E and CIII-containing High-density Lipoprotein Subfractions Associated with Risk of Heart Disease. *J. Lipid Res.* 2014;55(10):2167–2177.

33. Nikkilä EA, Kekki M. Plasma triglyceride metabolism in thyroid disease. *J. Clin. Invest.* 1972;51(8):2103–2114.

34. Barrett PH et al. SAAM II: Simulation, Analysis, and Modeling Software for tracer and pharmacokinetic studies. *Metab. Clin. Exp.* 1998;47(4):484–492.

35. Friedewald WT, Levy RI, Fredrickson DS. Estimation of the concentration of low-density lipoprotein cholesterol in plasma, without use of the preparative ultracentrifuge. *Clin. Chem.* 1972;18(6):499–502.

36. Weisgraber KH, Innerarity TL, Mahley RW. Abnormal lipoprotein receptor-binding activity of the human E apoprotein due to cysteine-arginine interchange at a single site. *J. Biol. Chem.* 1982;257(5):2518–2521.

37. Welty FK, Lichtenstein AH, Lamon-Fava S, Schaefer EJ, Marsh JB. Effect of body mass index on apolipoprotein A-I kinetics in middle-aged men and postmenopausal women. *Metab. Clin. Exp.* 2007;56(7):910–914.

38. Ji J et al. High-density lipoprotein (HDL) transport in the metabolic syndrome: application of a new model for HDL particle kinetics. *J. Clin. Endocrinol. Metab.* 2006;91(3):973–979.

39. Ooi EMM et al. High-density lipoprotein apolipoprotein A-I kinetics in obesity. *Obes. Res.* 2005;13(6):1008–1016.

40. Zheng C, Khoo C, Furtado J, Sacks FM. Apolipoprotein C-III and the metabolic basis for hypertriglyceridemia and the dense low-density lipoprotein phenotype. *Circulation* 2010;121(15):1722–1734.

41. Mahley RW, Rall SC. Apolipoprotein E: far more than a lipid transport protein. *Annu Rev Genomics Hum Genet* 2000;1(1):507–537.

42. Gregg RE et al. Abnormal in vivo metabolism of apolipoprotein E4 in humans. *J. Clin. Invest.* 1986;78(3):815–821.

Chapter 4

Kinetic model development

This chapter was adapted with permission from:

Morton AM, Koch M, Mendivil CO, Furtado JD, Tjønneland A, Overvad K, Wang L, Jensen MK, Sacks FM. Apolipoproteins E and CIII interact to regulate HDL metabolism and coronary heart disease risk. JCI Insight. 2018 Feb 22;3(4). pii: 98045. doi: 10.1172/jci.insight.98045. **(Supplemental Methods)**

4.1. Establishing final kinetic models

All compartmental modeling in **Chapters 2-3** was performed using SAAM-II, a commercially available modeling software (The Epsilon Group, Charlottesville, VA) (1). Various models were tested and examined for visual and statistical fits. For all models, the input/forcing function was free plasma leucine D3 enrichment.

Because the canonical stepwise enlargement model is not a good fit for human HDL apoA-I kinetic data (2), and the tracer enrichment curves in the present study were not compatible with a major precursor-product relationship between prebeta HDL and alpha HDL, we began model testing with the published Mendivil et al. model (2). The MENDIVIL MODEL was optimized for plasma apoA-I on HDL without separating into apolipoprotein-based subspecies. It is characterized by direct secretion of all HDL sizes and certain size conversion pathways, as shown below
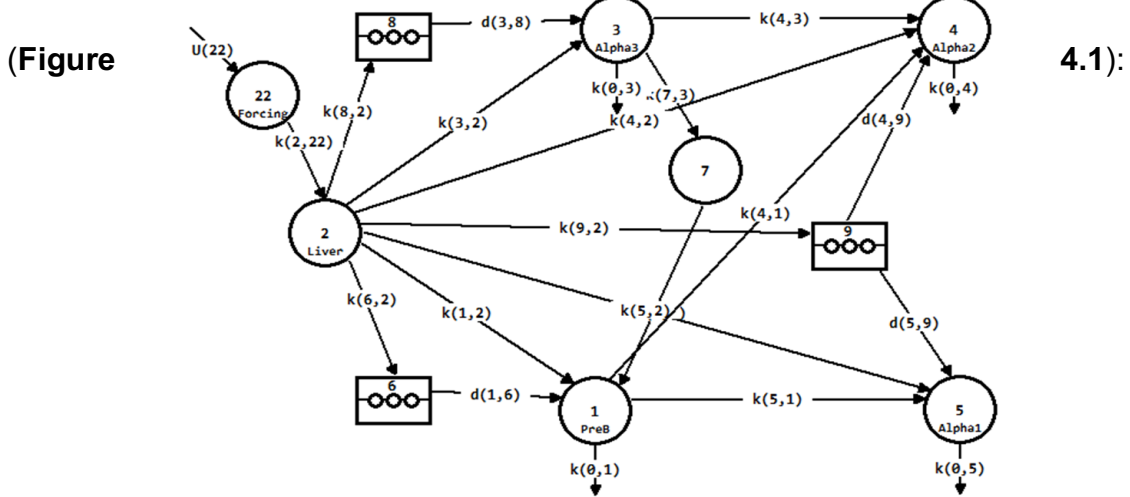
(Figure

4.1):

Figure 4.1 The Mendivil model. Reprinted with permission from Mendivil CO, Furtado J, Morton AM, Wang L, Sacks FM. *ATVB* (2016): 36:156-165.

147

The model fits to the tracer enrichment curves were visually satisfactory for most

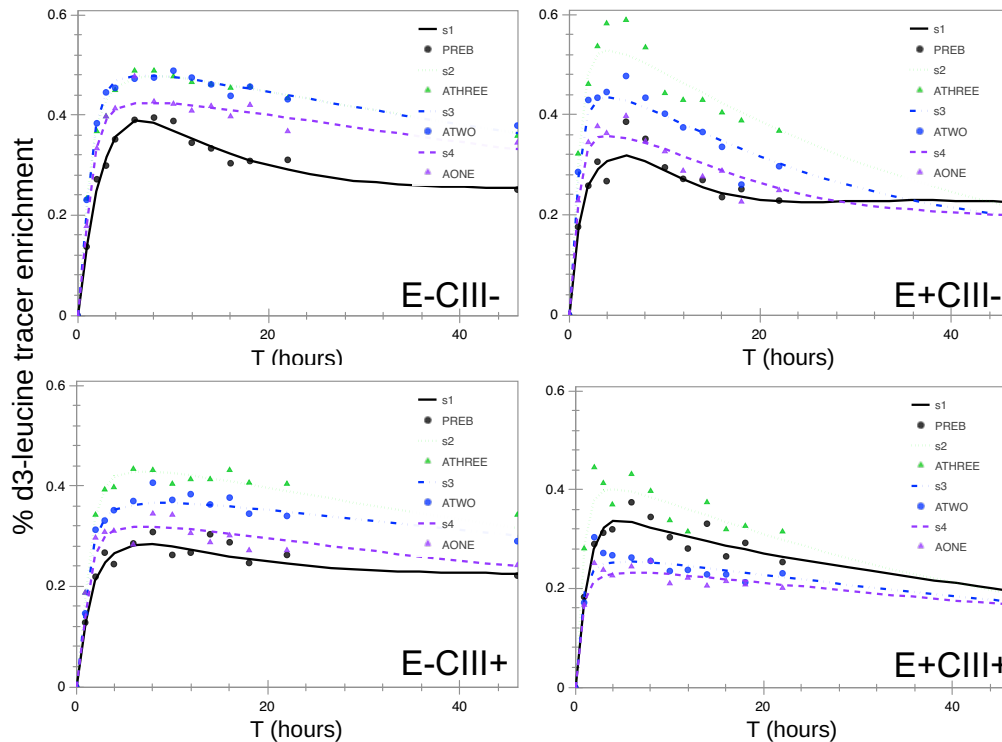subspecies and sizes, as shown on the next page (**Figure 4.2**):

Figure 4.2 Model fits of 4 HDL subspecies to the Mendivil model (Figure 4.1)

However, there were a few aspects of the MENDIVIL MODEL that warranted further

optimization: several parameters hit lower limits (zero) depending on the

subspecies, suggesting redundancy and over-parameterization; the delay times

were often very small, leading us to question if they were necessary; and

coefficients of variance for many parameters were over 50%, meaning that the

modeling software was not precisely estimating them. Given that over-

parameterization was the main concern, we removed the delay compartments to

alpha-1, -2 and -3 since they were all <1 hour. We assessed the need for size

expansion pathways for E-CIII-, the major subspecies, by creating a model that is

primarily defined by direct secretion and clearance of all sizes of HDL (MINIMUM
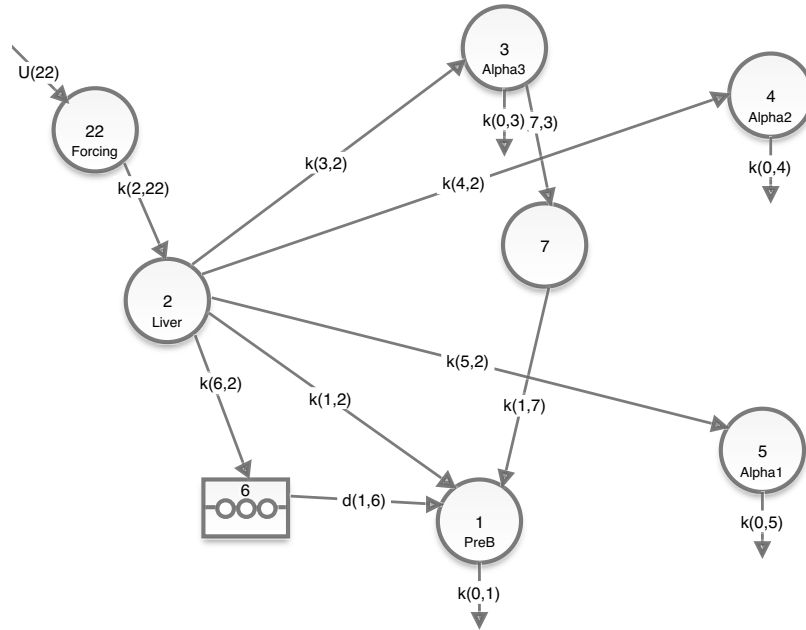
MODEL) (**Figure 4.3**):

Figure 4.3 The "**minimum model**" is characterized by direct secretion of all HDL sizes from the source compartment (here labeled as "liver," but also representing intestinal lipoprotein synthesis), an intravascular remodeling compartment for prebeta (the box labeled "6"), size contraction from alpha-3 to prebeta (the circle labeled "7"), and direct clearance of all HDL sizes. Plasma leucine enrichment is modeled as a forcing function.

The fits for the MINIMUM MODEL are shown on the next page (**Figure 4.4**).
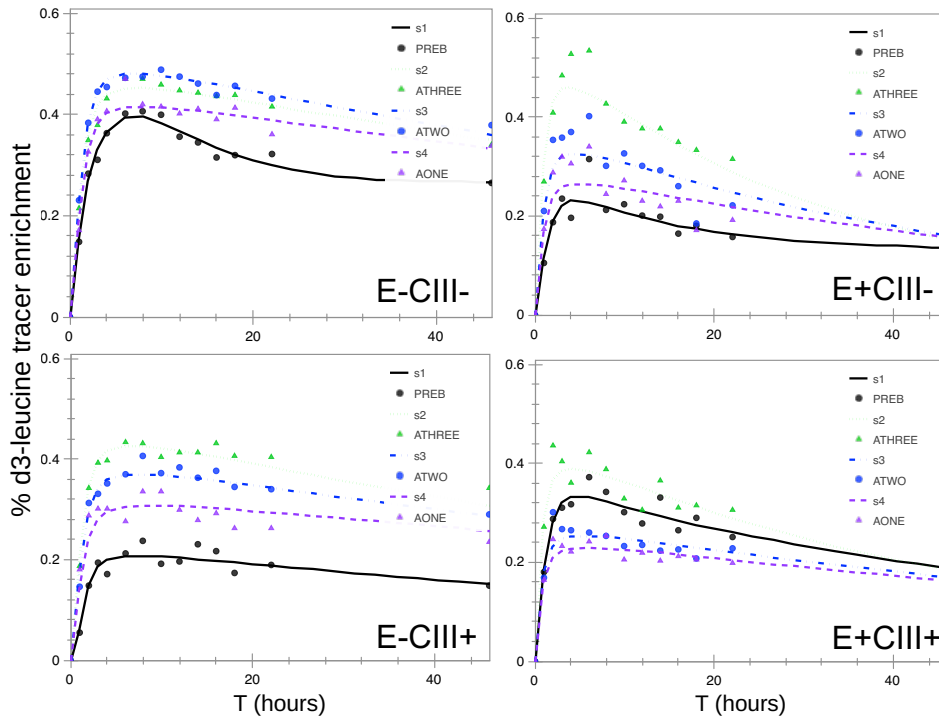
Figure 4.4 Model fits of 4 HDL subspecies to the Minimum Model
(Figure 4.3)

The MINIMUM MODEL visually fit the major HDL fraction E-CIII-, failed to fit the

complex behavior of E+CIII-, and fit but had unused parameters in E-CIII+ and

E+CIII+. We chose to focus first on finalizing the model for E-CIII-, the major HDL

subspecies, to use it as a starting point for the other subspecies.

The next phase of modeling was to check the model for statistical precision.

SAAM-II modeling software provides parameter standard deviations, coefficients

of variation (CV), and 95% confidence intervals after every attempt at solving.

The CV gives a judgment of the error associated with estimating the parameter,

relative to the value of the parameter. For the normal distribution, about 95% of

the values fall within 2 standard deviations of the set, so a CV of 50%

150

corresponds to a 95% confidence interval with a lower limit approximately equal to zero. Thus, if a parameter value has a CV less than 50%, the 95% confidence interval excludes zero, and the pathway can be assumed to be real. In some cases, the CVs are reported to be well above 100%, which can be a clue that a parameter is unnecessary in the model. For example, the E-CIII- model parameters after running the final MINIMUM MODEL were as follows (**Table 4.1**):

Table 4.1: Model parameters for the E-CIII- subspecies using the Minimum Model (Figure 4.3)					
Parameter	Value (pools/hr)	Std. Dev.	Coef. of Var. (%)	95% Confidence Interval	
INPUT	37.14	12.54	33.77	12.22	62.06
delay6	3.30	6.95	210.54	-10.51	17.11
k(0,1)	0.05	0.10	188.73	-0.14	0.25
k(0,3)	0.00	0.03	986.58	-0.05	0.05
k(0,4)	0.01	0.01	38.40	0.00	0.02
k(0,5)	0.01	0.00	38.11	0.00	0.02
k(1,2)	0.10	0.03	33.85	0.03	0.17
k(1,7)	0.04	0.04	100.36	-0.04	0.11
k(2,22)	11.66	1.20	10.25	9.29	14.04
k(3,2)	0.54	0.18	33.35	0.18	0.90
k(4,2)	0.44	0.15	33.35	0.15	0.73
k(5,2)	0.26	0.09	33.77	0.09	0.43
k(6,2)	0.05	0.10	207.68	-0.16	0.26
k(7,3)	0.01	0.03	251.97	-0.04	0.06

The k(0,3) parameter, representing the rate constant for removal of alpha-3 HDL from circulation, had a coefficient of variance (CV) of 987%. Deleting this pathway did not significantly alter the fractional catabolic rates (FCRs), but made all other parameter estimates more accurate, even the ones not associated with alpha-3 or prebeta (**Table 4.2**).

Table 4.2: Model parameters and FCRs for the E-CIII- subspecies using the Minimum Model (Figure 4.3) after deleting parameter k(0,3)					
Parameter	Value (pools/hr)	Std. Dev.	Coef. of Var. (%)	95% Confidence Interval	
INPUT	37.21	12.52	33.64	12.34	62.08
delay6	3.73	4.20	112.71	-4.62	12.08
k(0,1)	0.06	0.02	36.97	0.02	0.11
k(0,4)	0.01	0.01	38.23	0.00	0.02
k(0,5)	0.01	0.00	37.95	0.00	0.02
k(1,2)	0.10	0.03	30.80	0.04	0.16
k(1,7)	0.04	0.03	85.85	-0.03	0.10
k(2,22)	11.74	0.70	5.99	10.34	13.14
k(3,2)	0.54	0.17	32.02	0.20	0.88
k(4,2)	0.44	0.14	32.14	0.16	0.72
k(5,2)	0.26	0.08	32.61	0.09	0.42
k(6,2)	0.06	0.05	75.08	-0.03	0.15
k(7,3)	0.01	0.00	38.04	0.00	0.02
FCR (pools/day)					
	alpha-1	alpha-2	alpha-3		prebeta
With k(0,3)	0.27	0.32	0.30		1.26
Without k(0,3)	0.27	0.32	0.30		1.51

Removing this parameter directs all of the alpha-3 apoA-I into a processing compartment representing HDL that is remodeled at the liver to eventually become prebeta HDL. The only remaining parameters with high CVs are associated with non-sampled compartments (the prebeta delay compartment between source and plasma (Compartment 6) and the "remodeling" compartment connecting alpha-3 to prebeta (Compartment 7). We termed this model the "BARE MINIMUM MODEL" based on its parsimony.

The model fits were virtually superimposable, regardless of the presence of k(0,3) (**Figure 4.5**):
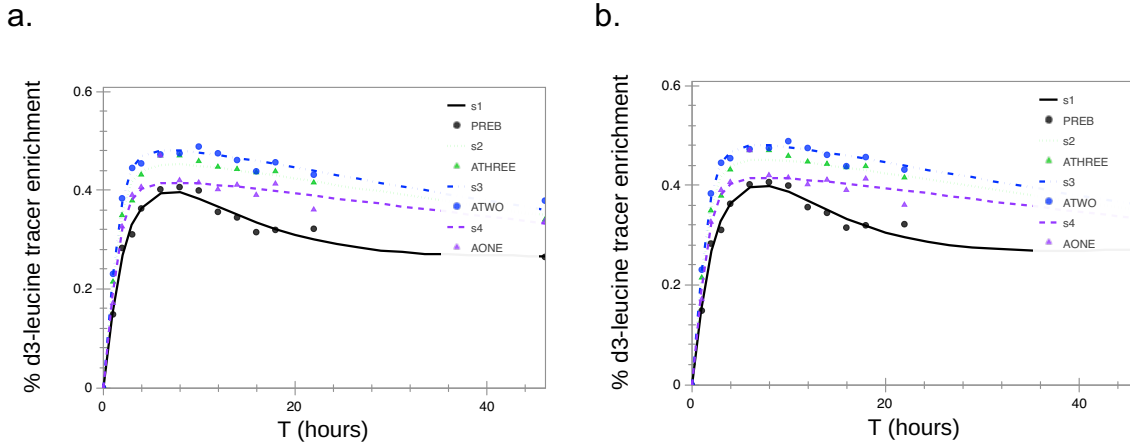
a.

b.

Figure 4.5 Comparison of model fits using Minimum Model (Figure 4.5a, with k(0,3)) vs. Bare Minimum Model (Figure 4.5b, without k(0,3))

We also considered the possibility that prebeta did not need the "remodeling" compartment at all, and deleted it from the model while keeping k(0,3) (required to give alpha-3 HDL a removal mechanism and to maintain steady state). However, the prebeta fit was poor, leading us to conclude that the non-sampled "prebeta remodeling" compartment was absolutely necessary to fit the complex behavior of the prebeta size fraction (**Figure 4.6**):
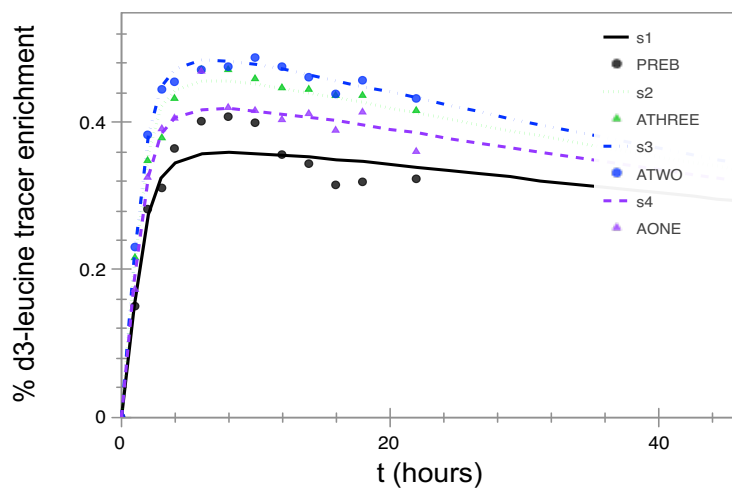

Figure 4.6 Model fit of apoA-I tracer enrichment in E-CIII- HDL without a prebeta regeneration pathway.

We next considered the possibility that, although the "prebeta remodeling" compartment was necessary to fit prebeta, it did not necessarily have to come from alpha-3. We tested this compartment (grey circle) originating from alpha-1 or alpha-2 along with keeping or removing (red "X") the direct clearance arrows, which is shown on the next page (**Figure 4.7**).
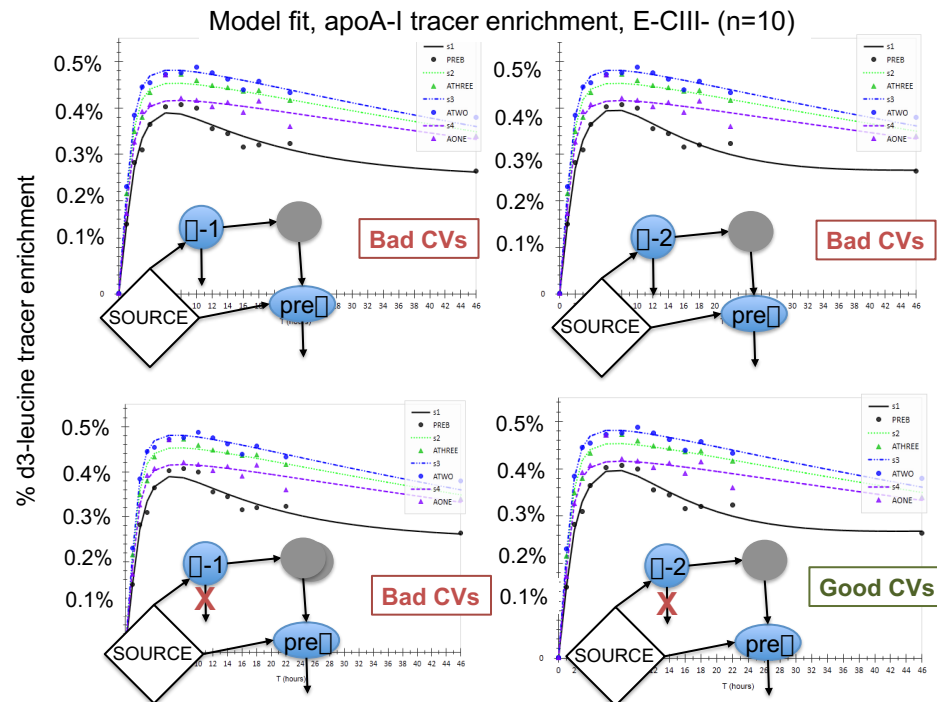
Figure 4.7 Testing permutations of the prebeta remodeling compartment originating from various larger HDL sizes along with direct clearance of larger HDL sizes.

Although the visual fits were all similar, the only combination that had acceptable CVs was the "prebeta precursor" compartment originating from alpha-2 without an extra removal pathway for alpha-2 (bottom right corner). Upon comparing the MINIMUM MODEL to the model in which the "prebeta precursor" compartment came

from alpha-2 or alpha-3, the results show that both models are visually identical

and give nearly identical rate constants (**Table 4.3**).

Table 4.3: Comparison of fractional catabolic rates (FCR, pools/day) in the Minimum Model (Figure 4.3) vs. two models in which the prebeta precursor compartment originated from different larger HDL sizes				
FCR (pools/day)				
	alpha-1	alpha-2	alpha-3	prebeta
Minimum model	0.27	0.32	0.30	1.26
From alpha-2	0.27	0.32	0.30	1.27
From alpha-3	0.27	0.32	0.30	1.51

Thus, we could not resolve the differences between the two origin pathways. We

did not find evidence in the literature to support alpha-2 converting to prebeta,

and kept the remodeling compartment originating from alpha-3 HDL; the model is

shown in **Figure 2.3A**, the BARE MINIMUM MODEL. This model gave a satisfactory fit

except for E+CIII-. For this subspecies, we tested size expansion pathways from

prebeta to alpha-1 and alpha-2 (schematic shown in **Figure 2.3B**). These model

fits (**Figure 2.6A**) are visually superior to the fits from the MENDIVIL MODEL,

especially in regards to hitting the final time points. Additionally, the size

expansion pathways were successful in capturing the complex behavior of the

E+CIII- fraction, though some of the peak time points were not completely

reached by the model. However, fitting these points manually would require

extremely high (and physiologically implausible) FCRs. This model provided the

lowest sum of squared residuals because it captured later timepoints very well.

We confirmed this by exporting the values for the weighted residuals at each time

point for each HDL size, squaring them, and summing them (Weighted Residual

Sum of Squares, WRSS). By F test, which rewards parsimony, the more complex model reduced the WRSS substantially enough to justify the additional parameters (**Figure 2.7**).

The modeling for individual participants begins once a model for a given subspecies has been chosen that has a full cassette of low-CV parameters. This involves loading the "final" model to the PopKinetics program, a component of SAAM-II (3). Study subject files are specified and the program fits the model to the data for each individual subject. Population-wide parameter values and statistics are given at the end of the iterations. Errors generally occur when parameters hit upper and lower limits. A lower limit can indicate that a certain metabolic pathway is not compatible with the data. Upper limits may be physiologically implausible (i.e. 20 pools/hour) and demonstrate that the program cannot fit the data to the given model. In either case, the program skips the subject and moves on to the next one. The entire process takes several iterations of PopKinetics solving with manual review and optimization of each participant's data.

In some cases, we removed outlier points to improve the fit. Outliers in the middle of the time range are not considered "high leverage" (their inclusion, or removal, has no effect on the model prediction) and were generally not removed. However, observations at the earliest and latest time points have a lot of leverage and can skew the fit or cause errors in fitting. Because there were

several early time points in the initial ascending slope of the enrichment curve, an outlier in this zone was removed if it did not follow the general trend of the rest of the data. However, the latest time point was always included unless it led to convergence errors in solving, because it was the only time point at that end.

We also used Bayesian estimation to improve parameter estimation. From the SAAM-II manual: *"The SAAM II Bayesian feature allows the incorporation of prior knowledge of the model parameters into the modeling of the kinetic data. The additional information is entered as a mean and standard deviation for one or more of the parameters in the model. The values can come from previous individual experiments, analysis of a population, or from published results."* In this case, we used parameter means and standard deviations from the model results using the mean enrichment and mass data of the all study participants. Bayesian estimation was only used for estimating rate constants involved in calculating fractional catabolic rates, which show more consistency across individuals than do rate constants involved in secretion pathways.

The individual modeling process concludes when all of the parameter CV's are below 50%. Exceptions are made for parameters associated with non-sampled pools (delays and the "prebeta precursor" compartment), which are more difficult to fit with precision.

4.2.   Individual variation in modeling

For each subspecies, I sought a single model that was able to describe the apoA-I metabolism of all study participants; however, some subspecies had variation in the models that best fit each participant. This was only an issue in the E+CIII+ and E+CIII- subspecies (and their "parent" subspecies, E+).

E+CIII+: The most common variant was removal of the delay compartment for prebeta secretion. Additionally, two participants needed a delay compartment for alpha-3, which had a more complex shape than the bare minimum model could accommodate. I also removed the prebeta remodeling compartment in two participants due to extraordinarily high CVs and convergence errors when solving the model.

E+CIII-: The best model for the mean enrichment and mass data featured size expansion from prebeta to alpha-1 and alpha-2. Individually, there was some variation in the type of size expansion. Out of 10 participants, 9 required size expansion pathways in the model to visually fit the data and improve the model statistics. Of the 9 participants with size expansion, five had both pathways (from prebeta to alpha-1 and to alpha-2), and four only had size expansion to alpha-1. For the participants with size expansion, I modeled them using both the BARE MINIMUM MODEL (**Figure 2.3a**) and complex model (BARE MINIMUM MODEL plus size expansion, **Figure 2.3b**) for comparison with an F test. The formula for calculating F is:

$$F = \frac{(WRSS_1 - WRSS_2)(N - P_2)}{WRSS_2(P_2 - P_1)}$$

Where WRSS is the weighted residual sum of squares, N is the number of data points, and P is the number of model parameters. The subscript "1" indicates the simpler model. The test has a Fisher distribution with (P_2-P_1, N-P_2) degrees of freedom (df). The results are shown below, demonstrating that the complex model was justified in its additional parameters in nine out of ten study participants given its significant reduction in WRSS (**Table 4.4**). This information was illustrated in **Figure 2.7**.

Table 4.4: Results from the F test for the 10 study participants from **Chapter 2**										
ID	WRSS1	P1	WRSS2	P2	N	F	df1	df2	Fcrit	p value
227	6.85	13	6.82	15	54	0.10	2	39	3.24	0.90
233	8.95	13	6.42	16	54	4.99	3	38	2.85	0.005
243	28.85	13	13.70	17	54	10.22	4	37	2.63	0.00001
244	20.05	13	12.17	16	52	7.77	3	36	2.87	0.0004
248	8.37	13	4.70	17	51	6.63	4	34	2.65	0.0005
250	10.36	13	6.55	16	50	6.60	3	34	2.88	0.0012
268	19.60	13	13.41	16	53	5.69	3	37	2.86	0.003
282	10.76	13	7.85	16	52	4.45	3	36	2.87	0.009
286	8.17	13	6.51	15	53	4.83	2	38	3.24	0.014
296	27.42	13	16.98	16	50	6.97	3	34	2.88	0.0009

F tests are more useful for comparing models than the Aikake Information Criterion (AIC) or Bayes Information Criterion (BIC), which do not have distributions and thus cannot be statistically compared (4).

HDL containing apoE (**Figure 2.2**): There was variation in the extent of size expansion among study participants. Additional size expansion pathways, which improved visual fit and model statistics, were used in only half (9/18) of the participants' models. This likely reflects antagonism by apoCIII also present in this subspecies. Of the nine that did have size expansion pathways from prebeta, four had expansion only to alpha-1, two had expansion only to alpha-2, and three had both pathways (from prebeta to alpha-1 and to alpha-2).

4.3.   Testing other hypotheses

A guiding principle of modeling is parsimony – to find the simplest model that can explain the data (5). However, there were certain aspects of biology that we wanted to test additional to the final models we chose (**Figure 2.3a-b**): size expansion in HDL not containing apoE and conversion of HDL subspecies.

Size expansion in HDL not containing apoE: Though the focus of our study was to test the effects of apoE and apoCIII on apoA-I metabolism, there are many other proteins present on HDL that could also be participating in classical reverse cholesterol transport. These proteins are generally present at minor amounts on HDL particles, but their influence could be quantifiable. Thus, though we described the metabolism of apoA-I on HDL not containing apoE using the BARE MINIMUM MODEL (**Figure 3.3A**), we also tested size expansion in HDL not containing apoE. In this subspecies, we found evidence of size expansion in 4/18 participants, accounting for an average of 6% of total flux in those participants.

Other proteins present in E- are presumably acting to cause this size expansion. However, given that they probably comprise only 1-5% of the mass of HDL, their effects are likely being masked. We also tested the E-CIII+ subspecies to see if apoCIII was promoting size expansion in the absence of apoE. In E-CIII+, 5/10 people showed size expansion of some kind. However, size expansion pathways did not improve any of the visual fits or parameter CVs, so we used the BARE MINIMUM MODEL for all kinetic analyses in these subspecies.

Transfer of apoA-I between subspecies: In vitro, it has been shown that apoA-I, apoE and apoCIII are exchangeable apolipoproteins (6). Therefore, we wanted to determine if apoA-I could move between subspecies (or, equivalently, that HDL could gain or lose apoE or apoCIII). For example, as this occurs, an E+CIII- HDL could become an E-CIII- if all apoE molecules are lost; or E+CIII- could become an E+CIII+ if apoCIII is acquired. To see if we had any evidence of conversion of one subspecies to another, we examined all possible combinations of the tracer enrichment curves of each HDL size to assess evidence of precursor-product relationship between any two subspecies. Precursor-product evidence could suggest, but not confirm, that apoA-I is moving between subspecies (or, equivalently, that HDL is gaining or losing apoE or apoCIII). A subspecies change requires acquisition of at least one molecule of or complete loss of apoCIII or apoE. An example for the alpha-3 size is shown in **Figure 4.8**.
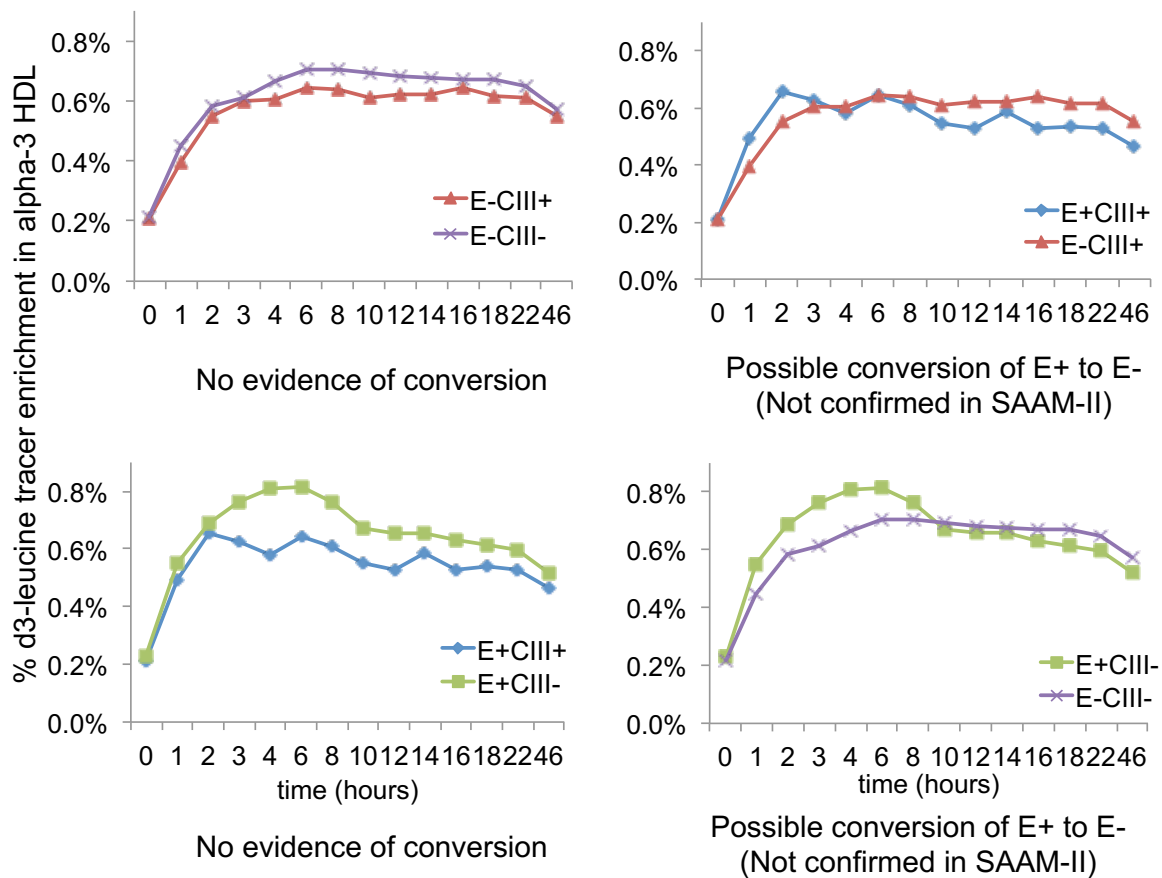
Figure 4.8 Tracer enrichment curves for apoA-I across four subspecies. Combinations of 2 subspecies at a time are shown to assess evidence of subspecies interconversion.

The enrichment curves for CIII+ and CIII- holding apoE constant (left panels) were parallel over the entire study period, providing no evidence of conversion of apoA-I HDL from CIII+ to CIII- HDL or vice versa. On the other hand, the enrichment curves for E+ and E- holding apoCIII constant (right panels) were compatible with some conversion of an E+ HDL subspecies to an E- subspecies, se tested models that included a transfer pathway from an E+ to an E- subspecies. The rate constants for this pathway hit zero, thus not confirming the

existence of this pathway. Conversion of an E+ to an E- subspecies could occur

only if all apoE molecules left an HDL E+ particle. However, a small amount of

loss of apoCIII or apoE from E+ or CIII+ that does not produce a subspecies

change would not be recognized in this system. Finally, because the enrichment

curves are compatible with conversion of E+ to E-, but not with acquisition of

apoE by E- HDL, any apoE leaving the HDL could not be moving to E- HDL.

4.4.   References

1. Barrett PH et al. SAAM II: Simulation, Analysis, and Modeling Software for tracer and pharmacokinetic studies. *Metab. Clin. Exp.* 1998;47(4):484–492.

2. Mendivil CO, Furtado J, Morton AM, Wang L, Sacks FM. Novel Pathways of Apolipoprotein A-I Metabolism in High-Density Lipoprotein of Different Sizes in Humans. *Arterioscler. Thromb. Vasc. Biol.* 2016;36(1):156–165.

3. The Epsilon Group. *PopKinetics User Guide [Internet]*

4. Burnham KP, Anderson DR. *Model Selection and Multimodel Inference*. Springer-Verlag; 2003:

5. Thorburn WM. Occam's razor. *Mind* 1915;24(2):287–288.

6. Sundaram M, Yao Z. Intrahepatic role of exchangeable apolipoproteins in lipoprotein assembly and secretion. *Arterioscler. Thromb. Vasc. Biol.* 2012;32(5):1073–1078.

CHAPTER 5

Discussion

5.1. Results summary and perspectives

This dissertation pursued unanswered questions in the field of HDL biology. I was primarily interested in whether HDL subspecies defined by protein content could direct HDL metabolism. I also wanted to discern whether these subspecies-dependent differences could be leveraged using dietary intervention. In this dissertation, I showed first that HDL subspecies have distinct metabolic features in relation to reverse cholesterol transport, and secondly that dietary intervention can be an effective tool to make HDL more proficient in that process. These findings raise several points of discussion. In this chapter, I will focus on the importance of HDL subspecies and remark on the concept of masking effects. I will conclude the chapter by discussing some yet unanswered questions and provide some possible follow-up studies to address these points.

Chapter 2 is the first demonstration of the effects of a subspecies on HDL apoA-I metabolism. HDL containing apoE but not apoCIII (E+CIII-) uniquely exhibits increased synthesis into plasma, size expansion from small to large HDL, and increased clearance from circulation. These actions comprise the critical steps of reverse cholesterol transport. In a separate case-cohort study, this subspecies is associated with reduced risk of coronary heart disease, thus providing a clinical connection to the metabolic findings. Importantly, apoCIII abrogates the effects of apoE both metabolically and with respect to coronary heart disease risk, such that HDL that contains both proteins (E+CIII+) no longer exhibits the unique metabolic functions or has a protective association. ApoCIII does not have effects on HDL metabolism in the absence of apoE,

as detailed in **Chapter 4**. These results were not unprecedented, given that apoE and apoCIII have opposing effects in lipoprotein metabolism in vitro and in vivo (reviewed in (1)). However, the complete nullification of apoE-mediated effects by apoCIII was admittedly astonishing. These findings constitute both the first demonstration of subspecies interacting in humans, and the first connection between HDL subspecies metabolism and clinical outcome.

Chapter 3 is the first demonstration of dietary intervention on the metabolism of HDL subspecies. Dietary unsaturated fat increases the synthesis and clearance of HDL apoA-I in humans, primarily working through HDL containing apoE to facilitate the steps of reverse cholesterol transport. HDL containing apoE has increased synthesis, more size interconversion, and increased clearance from circulation. This is also the first crossover study on the effects of dietary unsaturated fat versus carbohydrate on HDL metabolism. Previous studies examined saturated fat versus carbohydrate (2) or differences between dietary fat sources (3).

As a complement to the metabolic findings, I also present a study on the impact of a pharmaceutical therapeutic on lipoprotein subspecies concentrations in plasma **(Appendix 1)**. Epanova (omega-3 carboxylic acids), comprised mostly of ecosapentaenoic acid (EPA, 20:5n-3) but also docosahexaenoic acid (DHA, 22:6n-3), effectively reduces triglycerides in a high-risk population but also increases LDL-C (4). Using samples from the original clinical trial, I found that this increase in LDL-C was limited to the subspecies of LDL not containing apoCIII, which has a null association

with coronary heart disease risk (5). Epanova does not increase LDL containing apoCIII, which is associated with increased risk.

These studies underscore the importance of studying the metabolism of HDL subspecies rather than considering HDL as a homogenous particle. HDL is heterogeneous, existing across a size gradient and containing many proteins that could govern its metabolism and function (6). Because HDL subspecies comprise a minority of HDL in plasma, their effects are masked when considering HDL as a whole. The overall failure of HDL therapeutics, which solely focused on increasing HDL-C, ultimately underscored the need to appraise HDL more acutely. Even in my research on HDL subspecies, effect-masking manifested in several aspects. During the kinetic modeling process, I originally saw mixed evidence of size expansion in HDL containing apoE, which I later discovered was caused by the apoCIII that was concomitantly present. Had we only examined HDL subspecies defined by apoE, we would be left with unanswered questions on size expansion and also an incomplete appreciation of the ability of apoE to enhance clearance of HDL. Secondly, the dietary intervention used in our studies did not change the concentration of HDL-C or the plasma concentrations of apoA-I, apoE, or apoCIII. Only through kinetic modeling did we discover the rich metabolic effects of dietary unsaturated fat. Ultimately, my work provides additional evidence for the argument that HDL is not as simple as its cholesterol content.

These studies also underscore the importance of examining how pharmacological interventions affect HDL subspecies. Epanova **(Appendix 1)** had no effects on HDL

subspecies defined by presence or absence of apoCIII, which is not surprising given that HDL has very little apoCIII compared to LDL and VLDL (1). Other than the work presented in this dissertation, there is minimal literature on the effect of treatments on HDL subspecies. Recently, it was discovered that the failed CETP inhibitor torcetrapib raises the concentration of apoCIII in HDL (7), a clearly negative consequence. It is unclear to what degree the increase in apoCIII is responsible for the failure of the drug to protect against cardiovascular disease, as torcetrapib was also plagued with off-target effects (8). Would anacetrapib, the only CETP inhibitor to successfully (albeit modestly) reduce cardiovascular disease mortality, have similar effects on HDL subspecies?

The studies presented in this dissertation have uncovered only the first layer of information regarding the effect of HDL subspecies on HDL metabolism. In the next section, I will present some yet unanswered questions from these studies and outline some future work to address these concerns.

5.2. Unanswered questions and future directions

One original aim of these studies that remains unanswered is an extension of the dietary intervention analysis to subspecies of HDL defined by presence or absence of both apoE and apoCIII. The ability of apoCIII to abolish the metabolic effects of apoE on HDL is likely robust to dietary intervention. Nevertheless, it would be informative to know if the mechanism by which dietary unsaturated fat drives HDL metabolism is due to its ability to concomitantly reduce HDL containing apoCIII. In **Appendix 1**, I showed

that a therapeutic derived from polyunsaturated fats robustly decreased plasma apoCIII, but it did not affect HDL containing apoCIII (9). It is possible that redistribution of apoCIII could have occurred, such that less apoCIII was present on HDL containing apoE.

The mechanistic limitations of kinetic modeling are worth noting. Compartmental modeling does not prove that reverse cholesterol transport is taking place, but rather provides a framework to explain changes in tracer enrichment over time. Demonstrating reverse cholesterol transport definitively would require visually tracking cholesterol movement from peripheral macrophages onto an HDL particle and then eventually to the feces. This is currently not possible to measure in humans. A complementary approach to our kinetic studies was recently developed by Daniel Rader and colleagues, who tested the feasibility of using injected nanoparticles made of albumin-bound ^{3}H-cholesterol to track reverse cholesterol transport in humans (10). They were able to show in humans that the cholesterol tracer initially disappeared from plasma and later reappeared in HDL (precipitated from plasma using a phosphotungstic acid solution), that it moved from free cholesterol to cholesterol ester (representing conversion by LCAT), and that it eventually appeared in the feces. As this was a feasibility study, Rader and colleagues did not separate HDL into different sizes or partition by HDL protein content. A complementary study to our kinetic findings would be to assess rate of appearance of cholesterol nanoparticles into different HDL subspecies, and whether subspecies-containing cholesterol appears in the feces at different rates. An alternate and more feasible approach is to first assess the ability of HDL subspecies to efflux cholesterol from labeled macrophages *in vitro*. Cholesterol

efflux capacity, while comprising only one step of reverse cholesterol transport, has a strong inverse association with both carotid intima-media thickness and risk of coronary artery disease independent of HDL-C (11). Mechanistic studies in animal models could also determine to what extent labeled cholesterol appears in the feces of mice injected with reconstituted HDL subspecies. Taken together, these different approaches could lend credence to our argument that reverse cholesterol transport is taking place.

As mentioned in the previous section, the results here highlight the importance of studying the effects of therapeutics on HDL subspecies. An obvious first step is to retrospectively examine how existing HDL drugs affected HDL subspecies. As a starting point, our lab has recently acquired participant samples from two clinical trials of CETP inhibitors. We are testing how each drug affected plasma concentrations of a cassette of HDL subspecies, including those defined by apoCIII or apoE presence. These post hoc analyses will hopefully suggest mechanisms responsible for the unforeseen consequences of these failed HDL therapeutics.

It is also important to assess prospectively if therapeutics increase the concentration or functionality of subspecies that have demonstrated beneficial effects, such as HDL containing apoE but not apoCIII (E+CIII-). A promising example is antisense inhibition of apoCIII, which robustly increases HDL-C and lowers triglycerides in healthy volunteers and in patients with hypertriglyceridemia (12, 13). Further analyses on lipoprotein subspecies remain to be tested. A long-term objective is to develop a therapeutic that increases the concentration of HDL containing apoE but not apoCIII – which we have

shown enhances reverse cholesterol transport and has cardioprotective effects. All future HDL therapeutics should be assessed in their ability to impact HDL metabolism in ways that are meaningful for reverse cholesterol transport, as we have shown with dietary intervention.

Finally, these studies are only the first glimpses into the effects that resident proteins have on HDL metabolism. Given the vast array of proteins on HDL, it is almost certain that other proteins have impacts on the HDL metabolism and should be topics of future studies.

5.3.   Concluding remarks

Fifty years prior to the publishing of this dissertation, John Glomset, without knowing, predicted the existence of reverse cholesterol transport (14). Petar Alaupovic, a few years later, contributed invaluably to the field of HDL biology by arguing that we should focus on the protein content of HDL rather than on its inert lipid components (15). Since then, HDL biology has taken a circuitous route to arrive at the place it is today. This dissertation has shown that HDL subspecies have metabolic and clinical significance and should be considered and leveraged in future HDL therapeutics.

5.4.   References

1. Sacks FM. The crucial roles of apolipoproteins E and C-III in apoB lipoprotein metabolism in normolipidemia and hypertriglyceridemia. *Curr. Opin. Lipidol.* 2015;26(1):56–63.

2. Brinton EA, Eisenberg S, Breslow JL. A low-fat diet decreases high density lipoprotein (HDL) cholesterol levels by decreasing HDL apolipoprotein transport rates. *J. Clin. Invest.* 1990;85(1):144–151.

3. Matthan NR et al. Dietary hydrogenated fat increases high-density lipoprotein apoA-I catabolism and decreases low-density lipoprotein apoB-100 catabolism in hypercholesterolemic women. *Arterioscler. Thromb. Vasc. Biol.* 2004;24(6):1092–1097.

4. Kastelein JJP et al. Omega-3 free fatty acids for the treatment of severe hypertriglyceridemia: the EpanoVa fOr Lowering Very high triglyceridEs (EVOLVE) trial. *J Clin Lipidol* 2014;8(1):94–106.

5. Mendivil CO, Rimm EB, Furtado J, Chiuve SE, Sacks FM. Low-density lipoproteins containing apolipoprotein C-III and the risk of coronary heart disease. *Circulation* 2011;124(19):2065–2072.

6. Davidson WS, Shah AS. HDL Proteome Watch [Internet]. *httphomepages.uc.edudavidswmHDLproteome.html* http://homepages.uc.edu/~davidswm/HDLproteome.html. cited January 14, 2018

7. Bagdade J, Barter P, Quiroga C, Alaupovic P. Effects of Torcetrapib and Statin Treatment on ApoC-III and Apoprotein-Defined Lipoprotein Subclasses (from the ILLUMINATE Trial). *Am. J. Cardiol.* 2017;119(11):1753–1756.

8. Barter PJ et al. Effects of torcetrapib in patients at high risk for coronary events. *N. Engl. J. Med.* 2007;357(21):2109–2122.

9. Morton AM et al. The effect of omega-3 carboxylic acids on apolipoprotein CIII−containing lipoproteins in severe hypertriglyceridemia. *J Clin Lipidol* 2016;10(6):1442–1451.e4.

10. Cuchel M et al. A novel approach to measuring macrophage-specific reverse cholesterol transport in vivo in humans. *J. Lipid Res.* 2017;58(4):752–762.

11. Khera AV et al. Cholesterol efflux capacity, high-density lipoprotein function, and atherosclerosis. *N. Engl. J. Med.* 2011;364(2):127–135.

12. Graham MJ et al. Antisense oligonucleotide inhibition of apolipoprotein C-III reduces plasma triglycerides in rodents, nonhuman primates, and humans. *Circ. Res.* 2013;112(11):1479–1490.

13. Gaudet D et al. Antisense Inhibition of Apolipoprotein C-III in Patients with Hypertriglyceridemia. *N. Engl. J. Med.* 2015;373(5):438–447.

14. Glomset JA. The plasma lecithins:cholesterol acyltransferase reaction. *J. Lipid Res.* 1968;9(2):155–167.

15. Alaupovic P. Apoliproproteins and lipoproteins. *Atherosclerosis* 1971;13(2):141–146.

APPENDIX 1

The effect of omega-3 carboxylic acids on apolipoprotein CIII–containing lipoproteins in severe hypertriglyceridemia

This chapter was adapted with permission from:

Abstract

Background: Lipoprotein subspecies containing apoCIII adversely affect cardiovascular disease (CVD) risk; for example, low density lipoprotein (LDL) with apoCIII is a stronger CVD predictor than LDL without apoCIII. The Epanova for Lowering Very High Triglycerides (EVOLVE) trial showed that Epanova (omega-3 carboxylic acids [OM3-CA]) significantly lowered TG and apoCIII but raised LDL-C. However, it is unknown what subspecies of LDL were affected by treatment.

Objective: To determine how lipoprotein subspecies are affected by omega-3 fatty acid treatment, we studied the effect of OM3-CA on apoCIII concentrations in high density lipoprotein (HDL), LDL, and very low density lipoprotein (VLDL) and on the concentrations of subspecies of HDL, LDL, and VLDL that contain or do not contain apoCIII.

Methods: We analyzed plasma from a subset of subjects from the EVOLVE trial, a 12-week double-blind study of 399 subjects with fasting TG of 500 to 2000 mg/dL who were randomized to OM3-CA 2, 3, or 4 g/d or olive oil (placebo).

Results: OM3-CA significantly reduced plasma apoCIII relative to placebo, as well as apoCIII in HDL, and apoCIII in LDL. Treatment did not significantly affect the concentration of LDL with apoCIII, a subspecies highly associated with CVD risk. OM3-CA increased selectively the concentration of LDL that does not contain apoCIII, a

subspecies with a weak relation to coronary heart disease. The reduction in apoCIII was associated with plasma increases in eicosapentaenoic acid, docosahexaenoic acid, and arachidonic acid and decreases in linoleic, palmitic, and oleic acids.

Conclusion: Reduction in apoCIII may be a mechanism for the TG-lowering effects of OM3-CA. The increase in LDL-C seen in the EVOLVE trial may not be associated with increased risk of CVD.

A1.1 Introduction

ApoCIII, a small protein present on some HDL, LDL, and VLDL, promotes dyslipidemia by inhibiting the hepatic clearance of triglyceride-rich lipoproteins (1-6) and activates atherogenic processes (7-9). The concentration of apoCIII on apoB lipoproteins strongly predicts coronary heart disease (CHD) (10), and lipoprotein subspecies containing apoCIII adversely affect CVD risk. For example, the concentration of LDL with apoCIII, measured by apoB, is a stronger predictor of CVD than LDL without apoCIII (11, 12), and HDL with apoCIII, measured by its cholesterol concentration, is associated with increased incident CHD, whereas HDL without apoCIII has a stronger inverse association than total HDL cholesterol (HDL-C) (13). Heterozygous carriers of a null mutation of apoCIII have lower postprandial serum triglycerides (TG), higher levels of HDL-C, and lower levels of LDL cholesterol (LDL-C) and are less likely to have subclinical atherosclerosis (14), and two large analyses recently showed that loss of function mutations in the *APOC3* gene were associated with lower TG and reduced risk of CHD (15) and ischemic CVD (16).

Severe hypertriglyceridemia, defined as TG >500mg/dL (17), affects approximately 3.8 million Americans and is a risk factor for pancreatitis as well as CVD (18, 19). Omega-3 fatty acids have been shown to be effective for the treatment of severe hypertriglyceridemia (20-22). Other clinical trials also have shown that omega-3 fatty acids reduce plasma total apoCIII in addition to their TG-lowering effects (23-25), although which omega-3 fatty acids mediate this effect is less understood. Furthermore, there is a lack of information on the effect of omega-3 fatty acids on lipoprotein

subspecies containing apoCIII. Because certain subpopulations or "subspecies" of HDL and LDL have metabolically diverse phenotypes as well as relations to CVD risk when partitioned by presence or absence of apoCIII, it is important to consider each lipoprotein subspecies independently.

Omega-3 free fatty acids (or omega-3 carboxylic acids [OM3-CA] [Epanova]) contain 50-60% EPA and 15-25% DHA along with other potentially active omega-3 fatty acids in free fatty acid form. They are a more bioavailable form of omega-3 than commercially available fish oil supplements and prescription strength omega-3 ethyl esters because they do not rely on the action of pancreatic lipase to release fatty acids from dietary triglycerides, a necessary step before absorption can occur (26). OM3-CA are FDA approved and indicated in the USA as an adjunct to diet to reduce TG levels in adult patients with severe ($\geq$ 500 mg/dL) hypertriglyceridemia (27). The EpanoVa fOr Lowering Very high triglyceridEs (EVOLVE, NCT01242527) trial showed that OM3-CA significantly lowered TG and apoCIII but raised LDL-C (25). Because some lipoprotein subspecies are more harmful than others (11, 12), we studied the effect of OM3-CA on apoCIII concentrations in HDL, LDL, and VLDL, and on the concentrations of subspecies of HDL, LDL, and VLDL that contain or do not contain apoCIII.

A1.2 Materials and methods

Sample preparation: The samples used in this study were plasma from the EVOLVE trial (25), a 12-week, double-blind, multi-center study of 399 subjects which included 74 clinical sites in the United States (30 sites) Europe (34 sites), and India (10 sites).

Subjects had severe hypertriglyceridemia (fasting TG between 500-2000 mg/dL) and were excluded if they had a recent history (within past 6 months) of a cardiovascular event. Subjects in the EVOLVE trial were randomized to OM3-CA 2, 3, or 4 g/d or olive oil (placebo, 4g/d). The current analysis included a subset of subjects (n=273) who were randomized to olive oil, OM3-CA 2 g/d, or OM3-CA 4 g/d and who had a baseline and end-of-treatment sample. Plasma was shipped in packages containing solid CO_2 and was kept at $-80°C$ until laboratory use.

Sequential immunoaffinity column chromatography: Goat anti-human apoCIII Sepharose-4B^{TM} 5.22 mg/mL resin (Academy Biomedical, Houston, TX, USA; Cat: 33A-G1 Resin) was applied to Bio-Rad Poly-Prep chromatography columns (Hercules, California, USA; Cat: 7311550). Frozen plasma was thawed and gently mixed before applying to column to centrifuge for 16 h at 4°C. Unbound (apoCIII−) fraction was collected by washing the column 3 times with PBS. Bound (apoCIII+) fraction was eluted with 3M sodium thiocyanate (Sigma-Aldrich Co., St. Louis, MO, USA; Cat: 71938-250G) in PBS three times and washed once with PBS. Eluents were concentrated using Spin-X columns 10,000 MWCO (Corning Inc., Corning, NY, USA; Cat: 431488) and adjusted with PBS to weigh 1.0 g before transferring to ultracentrifuge tubes (Beckman Coulter, Jersey City, NJ, USA; Cat: 355657). This method is described in more detail by Zheng et al (28). Column efficiency was examined and found to be 98% or better.

Ultracentrifugation: The bound and unbound fractions were further separated by density

ultracentrifugation. Samples were spun for 16 hours at 15°C and 25,000 rpm in the

outermost row of a Beckman 25-Ti rotor with a Beckman L8-70M ultracentrifuge

(Beckman Coulter, Inc., Jersey City, NJ, USA). VLDL was collected by aspiration of the

top 200 μL using a Pasteur pipette. The lipoprotein subspecies of the combined

immunoaffinity chromatography and ultracentrifugation were as follows: VLDL without

apoCIII, VLDL with apoCIII, LDL+HDL without apoCIII, and LDL+HDL with apoCIII.

Sandwich ELISA: Sandwich ELISA procedures, using affinity-purified polyclonal

antibodies, were performed to determine concentrations of apoB, apoCIII, and apoA-I in

whole plasma and the lipoprotein fractions. 96-well plates were coated with rabbit anti-

human apoCIII polyclonal antibody (Academy Biomedical, Houston, TX, USA; Cat: 33A-

R1b), goat anti-human apoA-I polyclonal antibody (Academy Biomedical, Houston, TX,

USA; Cat: 11A-G2b), or goat anti-human apoB-100/48 polyclonal antibody (Academy

Biomedical, Houston, TX, USA; Cat: 20A-G1b) and blocked in casein (Thermo

Scientific, Tewksbury, MA, USA; Cat: 37582) for at least 1 hour. For HDL experiments,

apoB was first precipitated using dextran sulfate (20 g/L, pH 7.0) and magnesium

chloride (1.0 mol/L, pH 7.0), as previously described(29), leaving behind HDL with or

without apoCIII. Samples were applied to the plates and incubated for at least 1 h at

37°C before washing with either a 0.5% bovine serum albumin (BSA) (apoCIII-coated

plates) or 2% BSA buffer with 0.1% Tween (apoB- and apoA-I–coated plates). The

plates were then incubated with appropriate secondary antibodies (Academy

Biomedical, Houston, TX, USA) for 1 h at 37°C and detected using *o*-phenylenediamine

(Sigma-Aldrich Co., St. Louis, MO, USA; Cat: P9187-50SET). All assays were completed in triplicate, and any sample with an intra-assay coefficient of variation over 15% was repeated. Final data were exported to Microsoft Excel for analysis and database management.

Statistical analysis: This is a post-hoc and hypothesis-generating study. The primary end points were the concentrations of apoCIII in whole plasma, in HDL, in LDL, and in VLDL, and the concentrations of apoA-I and apoB in lipoproteins that contained or did not contain apoCIII. Effect of treatment on these lipoproteins was calculated by subtracting the baseline concentration from the concentration at end of treatment. Generalized linear models (GLM) were used with treatment as a factor and baseline value as a covariate to compare changes from baseline in the placebo group with changes from baseline in each of the treatment groups and to test whether these changes were significantly different from zero ($p<0.05$). For fatty acid correlations (Table 3 and Supplemental Figure 2), apolipoprotein data were scatterplotted against fatty acid percent change after removing placebo values. Spearman *rho* and p-values are shown (for n=178, after removing placebo). We did not adjust p-values for multiple comparisons. All statistical tests were performed using Stata 14 (StataCorp LP, College Station, TX, USA).

A3.3 Results

Table A1.1 summarizes the characteristics of the participants at baseline. The

participants were predominantly white (93%), men (77%), and non-Hispanic (93%). The

average age of the subjects was 52 years, and 34% of subjects were being treated with

statins or cholesterol absorption inhibitors. The subjects were randomized to each

treatment group (placebo, OM3-CA 2g/d or OM3-CA 4 g/d). Table 2 shows the average

baseline lipid measurements for each group. The mean baseline TG level was 740

mg/dL. The mean baseline apoCIII concentration in whole plasma was 26 mg/dL, in

HDL was 8 mg/dL, in LDL was 10 mg/dL, and in VLDL was 8 mg/dL.

Treatment with OM3-CA for 12 weeks significantly reduced plasma apoCIII from

baseline relative to the change from baseline in the placebo group (2g: −4.2 mg/dL,

p=0.002; 4g: −5.0 mg/dL, p<0.0001) (**Table A1.2**, **Figure A1.1**). Treatment with OM3-

CA also reduced apoCIII in HDL (2g: −0.6, mg/dL, p=0.12; 4g: −1.0 mg/dL, p=0.01), and

apoCIII in LDL (2g: −2.9 mg/dL, p<0.0001; 4g: −3.3 mg/dL, p<0.0001) relative to

placebo. Epanova did not significantly affect the apoCIII concentration in VLDL (2g: −0.6

mg/dL, p=0.3; 4g: −0.7 mg/dL, p=0.3). Therefore most of the reduction in plasma total

apoCIII was in LDL.

Statin use did not affect the response to treatment. There were 33 statin users in the 2g

and 31 in the 4g group. OM3-CA significantly lowered apoCIII and LDL apoCIII in both

Table A1.1: Baseline characteristics of study participants (n=273).

Characteristic	Placebo (Olive Oil) (n=93)	OM3-CA, 2 g/d (n=92)	OM3-CA, 4 g/d (n=88)	Total (n=273)
Women, n (%)	22 (24)	18 (20)	24 (27)	64 (23)
Ethnicity, n (%)				
Non-Hispanic	88 (95)	86 (94)	81 (92)	255 (93)
Hispanic/Latino	5 (5)	6 (7)	7 (8)	18 (7)
Race, n (%)				
White	89 (96)	85 (92)	80 (91)	254 (93)
Black/African American	0 (0)	0 (0)	2 (2)	2 (1)
Asian	4 (4)	5 (5)	6 (7)	15 (5)
Other or mixture	0 (0)	2 (2)	0 (0)	2 (1)
Age, years, mean +/- SD	51 +/- 11	51 +/- 10	53 +/- 11	52 +/- 11
Statin or ezetimibe users, n (%)	30 (32)	33 (36)	31 (35)	94 (34)

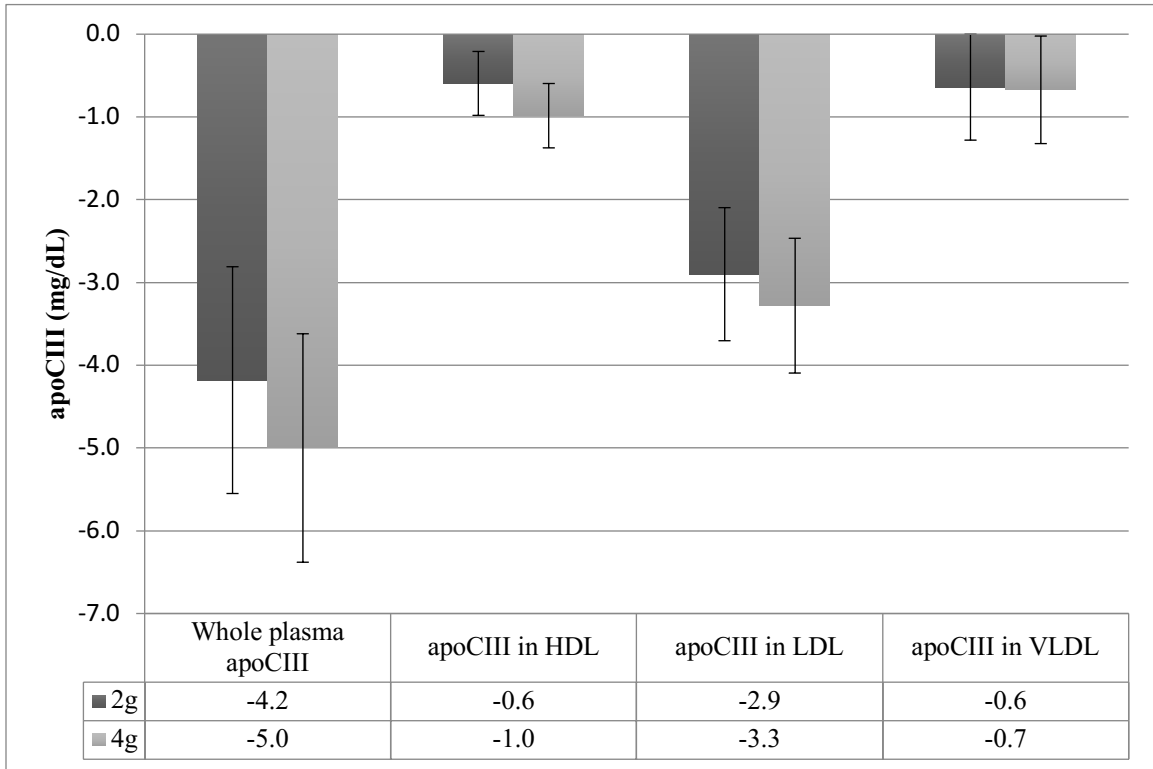OM3-CA = omega-3 carboxylic acids; SD = standard deviation

	Whole plasma apoCIII	apoCIII in HDL	apoCIII in LDL	apoCIII in VLDL
■2g	-4.2	-0.6	-2.9	-0.6
■4g	-5.0	-1.0	-3.3	-0.7

Figure A1.1: ApoCIII concentrations: placebo-adjusted mean change assessed by generalized linear model (GLM). Significance is denoted by p<0.05 and is denoted by an asterisk (*). Error bars reflect standard error.

dosage groups. Additionally, we performed interaction testing for all outcome variables to determine if there was effect modification according to statin use. All the interaction tests were not significant indicating that the effects of OM3-CA are similar regardless of concomitant statin use.

Figure A1.2 shows the effect of treatment on the apoB concentration in LDL. Treatment did not significantly increase the apoB concentration of LDL with apoCIII (2g: 0.3 mg/dL, p=0.7; 4g: 0.4 mg/dL, p=0.6) (**Figure A1.2a**, **Table A1.2**). OM3-CA increased selectively and significantly the concentration of apoB in LDL that does not contain apoCIII, a subspecies that has a weak relation to CHD (11, 12), by 10.9 mg/dL (2g, p=0.047) and 15.2 mg/dL (4g, p=0.006) from baseline relative to the change in the placebo group (**Figure A1.2b**, **Table A1.2**).

We also investigated the effect of treatment on the apoA-I concentration of HDL with or without apoCIII. Relative to placebo, OM3-CA did not significantly alter from baseline the concentration of apoA-I in HDL that contains apoCIII (2g: 0.4 mg/dL, p=0.6; 4g: −0.3 mg/dL, p=0.6) or does not contain apoCIII (2g: 0.9 mg/dL, p=0.9; 4g: −1.2 mg/dL, p=0.9) (**Table A1.2**).

Relative to placebo, OM3-CA did not alter the apoB concentration of VLDL that contains or does not contain apoCIII (2g: 0.02 mg/dL, p=0.9; 4g: 0.06 mg/dL, p=0.7) (**Table A1.2**). Treatment also did not change from baseline the apoB concentration of VLDL without apoCIII (2g: 0.3 mg/dL, p=0.7; 4g: 0.8 mg/dL, p=0.2).

a.

	apoB in LDL with apoCIII
■ 2g	0.3
■ 4g	0.4

b.

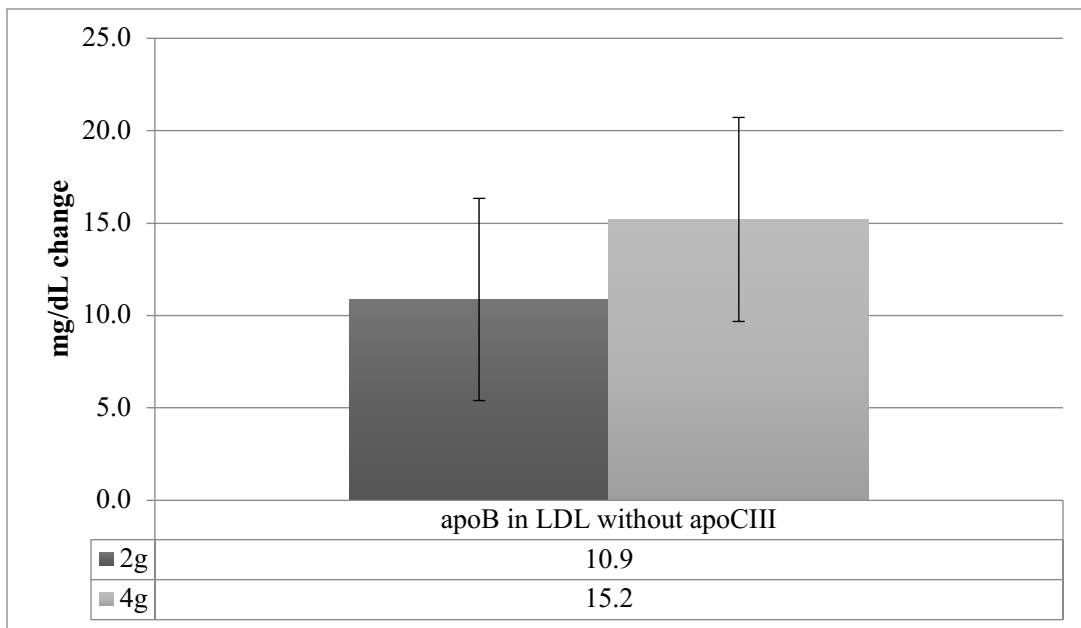|	apoB in LDL without apoCIII
■ 2g	10.9
■ 4g	15.2
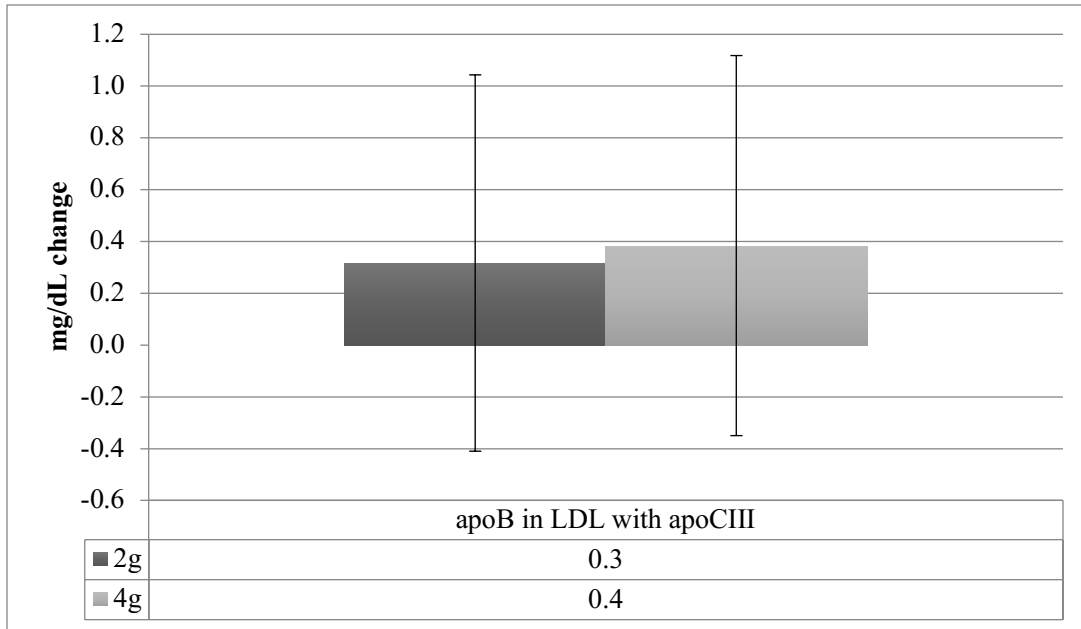
Figure A1.2: a.) ApoB concentration in LDL with apoCIII: placebo-adjusted mean change. b.) ApoB concentration in LDL without apoCIII: placebo-adjusted mean change determined by generalized linear model (GLM). Significance is denoted by $p < 0.05$ and is denoted by an asterisk (*). Error bars reflect standard error.

Table A1.2: Baseline and end-of-treatment (EOT) concentrations in mg/dL in lipoprotein measurements across the 3 randomized treatment groups. P values are from placebo-adjusted mean change determined by generalized linear model (GLM) with baseline value as a covariate.

| | Placebo | | | | OM3-CA 2g | | | | | OM3-CA 4g | | | | |
| | Baseline | | EOT | | Baseline | | EOT | | | Baseline | | EOT | | |
Variable	Mean	SD	Mean	SD	Mean	SD	Mean	SD	p-value	Mean	SD	Mean	SD	p-value
Whole plasma apoCIII	25	9	27	14	27	9	24	10	.002	26	9	22	8	<0.001
apoA-I with apoCIII	28	8	26	7	24	6	25	6	0.61	26	6	25	6	0.64
apoA-I without apoCIII	135	75	128	58	123	57	124	53	0.90	127	58	124	55	0.87
apoCIII in HDL	8	3	8	4	9	4	8	4	0.12	8	4	7	3	0.01
VLDL apoB with apoCIII	2	1	2	1	2	1	2	1	0.90	2	1	2	1	0.71
VLDL apoB without apoCIII	9	6	9	7	9	6	9	5	0.66	8	5	8	5	0.17
apoCIII in VLDL	8	3	8	4	8	5	8	5	0.32	7	4	7	5	0.30
LDL apoB with apoCIII	8	7	8	7	8	6	8	6	0.66	8	6	8	6	0.60
LDL apoB without apoCIII	102	60	102	63	107	55	117	65	0.047	104	56	119	67	0.01
apoCIII in LDL	10	6	11	6	8	5	9	5	<0.001	10	6	9	4	<0.001
TG	740	440	880	870	760	320	640	440	<0.001	725	400	560	330	<0.001

OM3-CA increased the plasma concentrations of several fatty acids, including EPA, docosapentaenoic acid (DPA), and docosahexaenoic acid (DHA), while reducing concentrations of others, including oleic and palmitic acids (**Figure A1.3**).

To consider the metabolic effects of fatty acids on apolipoprotein concentration independent of treatment, we examined the Spearman correlation coefficients between the changes in fatty acids and the changes in lipid/lipoprotein concentrations (**Table A1.3**). Decreases in levels of whole plasma apoCIII correlated significantly (R>|0.15|) with increases in levels EPA (20:5n-3), DHA (22:6n-3), linoleic (18:2n-6), and with decreases in arachidonic (20:4n-6), palmitic (16:0), and oleic (18:1n-9) acids. These effects were similar for the changes in apoCIII concentration of HDL, LDL, and VLDL. In general, changes in HDL apoA-I levels did not correlate with changes in fatty acid levels, with the exception of changes in HDL apoA-I without apoCIII and total HDL apoA-I correlating positively with increases in EPA. Changes in the concentration of LDL apoB with apoCIII, while not significant, correlated positively with decreases in palmitic acid.. Increases in LDL apoB without apoCIII correlated positively with increases in linoleic acid and inversely with decreases in palmitic acid. Though omega-3 fatty acids did not significantly lower the concentration of total VLDL apoB, decreases in VLDL apoB in individuals correlated significantly with increases in omega-3 and omega-6 fatty acids. Decreases in TG correlated inversely with increases in EPA, DHA, and linoleic acid, and positively with decreases in arachidonic, palmitic, and oleic acids, similar to whole plasma apoCIII.
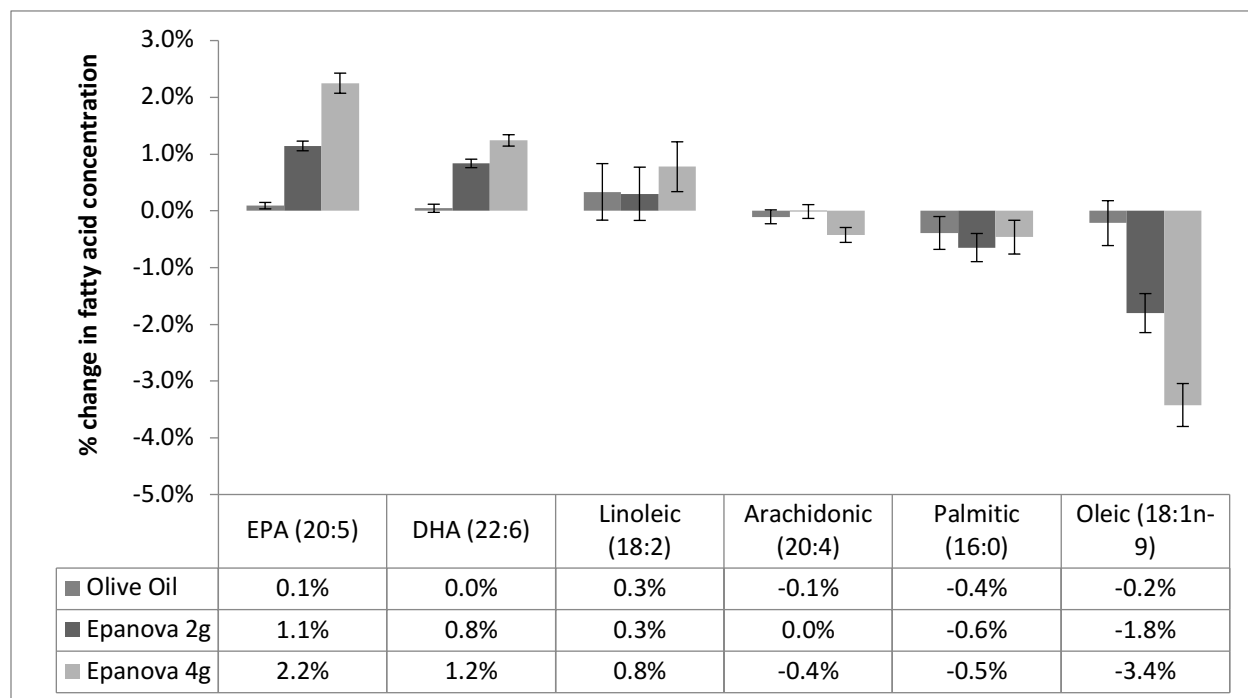
	EPA (20:5)	DHA (22:6)	Linoleic (18:2)	Arachidonic (20:4)	Palmitic (16:0)	Oleic (18:1n-9)
Olive Oil	0.1%	0.0%	0.3%	-0.1%	-0.4%	-0.2%
Epanova 2g	1.1%	0.8%	0.3%	0.0%	-0.6%	-1.8%
Epanova 4g	2.2%	1.2%	0.8%	-0.4%	-0.5%	-3.4%

Figure A1.3: Percent changes in plasma concentrations of fatty acids relative to total

fatty acid levels as assessed by gas chromatography. Error bars reflect standard error.

DHA = docosahexaenoic acid

Table A1.3: Spearman correlation coefficients of changes in relative fatty acid concentrations (%) compared with changes in lipid/lipoprotein concentrations (mg/dL). n=178, after removal of placebo group. Significant (p<0.05) values are boxed. DHA = docosahexaenoic acid

Fatty acid	Whole plasma apoCIII	HDL apoCIII	HDL apoA-I with apoCIII	HDL apoA-I without apoCIII	Total HDL apoAI	LDL apoCIII	LDL apoB with apoCIII	LDL apoB without apoCIII	Total LDL apoB	VLDL apoCIII	VLDL apoB with apoCIII	VLDL apoB without apoCIII	Total VLDL apoB	TG
OMEGA 3														
EPA (20:5)	-0.25	-0.13	0.01	0.15	0.16	-0.12	-0.03	0.1	0.14	-0.2	-0.12	-0.2	0.07	-0.29
DHA (22:6)	-0.41	-0.28	-0.04	0.12	0.11	-0.22	-0.07	0.1	0.08	-0.29	-0.14	-0.31	-0.28	-0.49
OMEGA 6														
Linoleic (18:2)	-0.31	-0.21	-0.1	-0.1	-0.1	-0.21	-0.09	0.15	0.14	-0.19	-0.2	-0.13	-0.16	-0.38
Arachidonic (20:4)	-0.48	-0.36	-0.04	-0.01	-0.01	-0.2	-0.07	0.12	0.11	-0.46	-0.25	-0.33	-0.34	-0.72
SATURATED														
Palmitic (16:0)	0.4	0.3	0.07	0.05	0.05	0.22	0.25	-0.16	-0.12	0.27	0.33	0.26	0.31	0.38
OMEGA 9														
Oleic (18:1 n-9)	0.4	0.27	0.1	-0.02	-0.02	0.22	-0.06	-0.13	-0.13	0.31	0.09	0.25	0.23	0.58

A3.4 Discussion

This study showed that treatment with OM3-CA significantly reduced the concentrations

of apoCIII in whole plasma, HDL, and LDL. Importantly, OM3-CA did not raise the apoB

concentration of LDL with apoCIII, a subspecies of LDL that is associated with an

increased risk of CHD (11, 12). The effect of OM3-CA to raise the apoB concentration of

LDL was limited to the LDL subspecies without apoCIII, a subspecies weakly associated

with CHD (11, 12). Therefore, the results suggest that the increase in LDL-C reported in

the EVOLVE trial (25) is comprised of LDL without apoCIII and not LDL with apoCIII.

Epanova contains 50-60% EPA and 15-25% DHA along with other potentially active

omega-3 fatty acids in free fatty acid form. We found that the reduction in apoCIII

correlated highly with the increases in concentration of these omega-3 polyunsaturated

fatty acids (**Table A1.3**), suggesting a causal role for omega-3 fatty acids in the

reduction of apoCIII. However, the evidence supporting the ability of omega-3 fatty

acids to lower apoCIII is not universally consistent, and most studies recruit

normotriglyceridemic individuals, which may not be generalizable to patients with severe

hypertriglyceridemia. A 4-week double-blind, placebo-controlled, parallel study in

healthy adult volunteers with mean TG of 103 mg/dL reported that EPA or DHA did not

affect plasma total apoCIII relative to oleic acid (30). A 12-week study, which is more

comparable to the design of our study, in individuals with TG levels between 75-285

mg/dL found that supplementation with EPA reduced the concentration of apoCIII in

VLDL without altering levels of plasma total apoCIII (31); the authors postulated that

apoCIII distribution may have shifted to HDL (which was not measured). However, the participants in our study, having high TG, could be more responsive to treatment that affects apoCIII, which is strongly correlated with TG. Icosapent ethyl, a high-purity prescription form of EPA ethyl ester approved to reduce TG levels in patients with severe hypertriglyceridemia, reduced levels of apoCIII in the MARINE trial relative to paraffin oil (21, 32). Taken together, these studies demonstrate that omega-3's may be most effective in lowering apoCIII in hypertriglyceridemic populations.

The mechanism by which OM3-CA lowers apoCIII is not fully elucidated and further knowledge will require human kinetic studies. Transcriptional regulation of apoCIII is complex and is directed by an ensemble of transcription factor binding sites (33-35). DHA supplementation has been shown to inhibit *APOC3* gene transcription in porcine liver isolates relative to beef tallow (high-saturated fat) control, but not relative to soybean oil (combination of omega-3 and omega-6 unsaturated fatty acids) (36). The same study showed that in human hepatoma SK-HEP-1 cells, DHA significantly reduced the *APOC3* promoter activity relative to oleic acid (C18:1n-9), palmitic acid (C16:0), or no fatty acids. This result is supported by our findings, as increases in DHA and decreases in oleic and palmitic acids during OM3-CA treatment were correlated with decreases in apoCIII. Another study showed in SV129 mice that fish oil supplementation compared to fenofibrate reduced plasma protein levels of apoCIII by ~80% without altering hepatic mRNA apoCIII expression, leading the authors to conclude that apoCIII is not under transcriptional control by fish oils (37). Fibrates, as well as omega-3 and omega-6 polyunsaturated fatty acids, are ligands for PPARα in the

liver, which then form heterodimers with retinoid-X receptors (RXR) and bind to promoter regions of target genes (38-41). Fibrates have been shown to decrease human and rat liver apoCIII mRNA accompanied with reduced secretion of apoCIII protein in primary human hepatocytes (42, 43). In contrast, when PPARα mRNA is knocked down in human HepG2 cells using short hairpin RNA, apoCIII mRNA and protein levels increase as compared to cells that did not have PPARα knockdown upon treatment with a fibrate or synthetic activator of PPARα (44). Therefore, evidence from several *in vitro* studies as well as animal models suggests that PPARα is involved in the response of apoCIII to omega-3 fatty acids, although perhaps not directly.

The mechanism by which PPARα regulates apoCIII gene expression probably involves a displacement of HNF-4α from the C3P location of the *APOC3* promoter region (45) rather than a direct effect on transcription, as the *APOC3* gene does not have a direct binding pocket for PPARα-RXR (35). Conditionally knocking out the HNF-4α in the hepatocyte using the Cre-loxP system results in dramatic reductions in apoCIII mRNA levels (46), and individuals who are heterozygous for the HNF-4α gene have significantly reduced serum apoCIII (47). Saturated fatty acids have been shown to increase HNF-4α binding activity, resulting in more apoCIII expression (48); this is corroborated by strong positive correlations seen between plasma palmitic acid and apoCIII concentrations in our study. Palmitic acid is the most common saturated fat in the diet, suggesting an important link between diet and apoCIII. PPARα can also stimulate Rev-Erba, which represses expression of *APOC3* (49, 50).

Polyunsaturated fats have other positive effects on lipid metabolism, such as suppressing SREBP-1c promoter activity by inhibiting LXR binding to LXR response elements, leading to reduced lipoprotein synthesis (51). PUFAs also repress SREBP-1c activation by directly inhibiting UBXD8, an endoplasmic reticulum membrane protein that facilitates the degradation of INSIG, which normally sequesters the SCAP-SREBP complex and prevents its activation (52, 53). This causes SCAP-SREBP to remain in the endoplasmic reticulum, preventing SREBP-1c-mediated cholesterol and fatty acid synthesis. Finally, DHA, but not other PUFAs, can stimulate removal of mature nuclear SREBP-1c in rat hepatocytes via a mechanism dependent on the 26S-proteasome and Erk pathways (54).

Although omega-6 fatty acids were differentially affected by treatment (e.g. linoleic acid increased, but arachidonic acid decreased), we found that the reduction in apoCIII was highly inversely correlated with the changes in these two omega-6 fatty acids (**Table A1.3**). While at first this may seem contradictory, the negative correlation is likely due to the fact that almost all polyunsaturated fatty acids activate PPARα and thus stimulate its downstream effects, including the reduction of apoCIII (41). It has been shown that arachidonic acid inhibits SREBP-1c more robustly than EPA and DHA, thus reducing lipogenesis to a greater extent, via a mechanism independent of PPARα (51). Though arachidonic acid, a downstream omega-6 fatty acid, decreased in this study, likely due to competitive inhibition for enzymes (55, 56), linoleic acid and omega-3 fatty acids increased much more than arachidonic acid decreased. This overall increase in

PPARα-activating polyunsaturated fatty acid ligands is likely responsible for reducing apoCIII.

The reduction in apoCIII may be a mechanism for the TG-lowering effects of OM3-CA (**Figure A1.4**). Although the apoCIII concentration in VLDL did not change, the reduction in apoCIII was manifest in LDL, which in hypertriglyceridemia is mostly a product of VLDL metabolism (57). Another possibility is that apoCIII may not have changed in VLDL because apoCIII could have been transferred from HDL, which showed a decrease in apoCIII concentration. ApoCIII promotes hypertriglyceridemia by impairing hepatic clearance of TG-rich lipoproteins (1-6) and, in high amounts, may also interfere with lipolysis via lipoprotein lipase and hepatic lipase (3, 58-61). In humans, antisense inhibition of apoCIII robustly lowers plasma apoCIII and triglycerides (62). Thus, treatment with OM3-CA confers a favorable lipid profile by reducing plasma TG as reported in the EVOLVE trial and, as we have shown here, by lowering apoCIII. The reduction in TG is likely due to direct effects of omega-3 fatty acids on lipoprotein metabolism through SREBP-1c (51, 52), and indirect effects through apoCIII reduction, which further lower TG levels.

Although increases in LDL-C are generally regarded as unfavorable, it is important to remember that certain subpopulations of LDL have metabolically diverse phenotypes as well as relations to CVD risk. When partitioning LDL by presence or absence of apoCIII, the risk of CVD is mainly apparent in LDL with apoCIII (11, 12), a subspecies of LDL that was not increased by OM3-CA in this study.
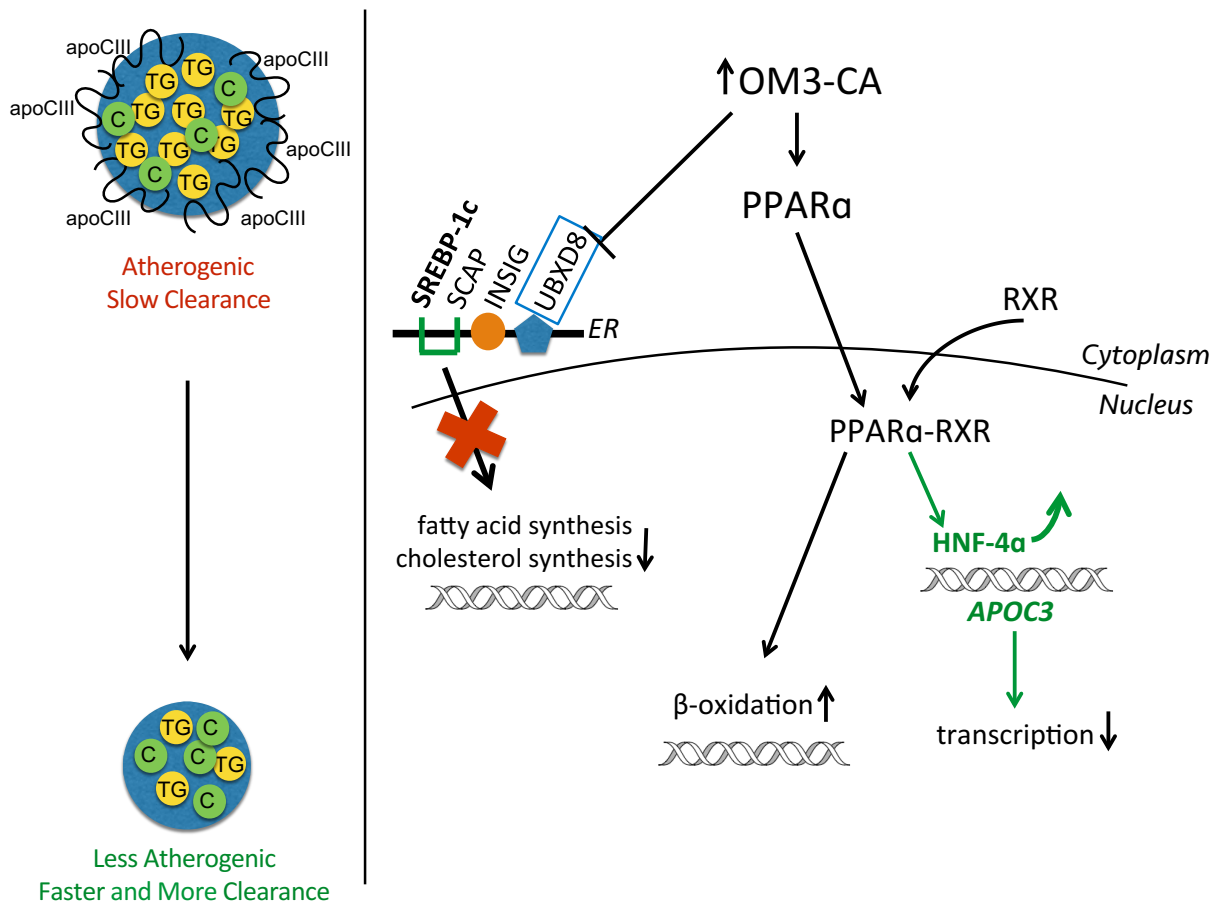
Figure A1.4: Potential mechanism of the TG- and apoCIII-lowering effects of omega-3 carboxylic acids and their effect on lipoprotein metabolism.

Figure A1.4 (continued): Potential mechanism of the TG- and apoCIII-lowering effects of omega-3 carboxylic acids and their effect on lipoprotein metabolism. Omega-3 carboxylic acids (OM3-CA) bind and activate UBXD8, an ER membrane protein that facilitates the degradation of INSIG. INSIG normally sequesters the SCAP-SREBP complex and prevents its activation. Taken together, this leads to inhibition of proteolytic processing of mature SREBP-1c and downregulation of SREBP-1c target genes including fatty acid synthesis and cholesterol synthesis. OM3-CA also activates PPARα, which translocates to the nucleus and dimerizes with RXR, carrying out it a variety of downstream effects. These include increased β-oxidation and, importantly, the displacement of HNF-4α from the *APOC3* gene promoter, resulting in reduced *APOC3* transcription, mRNA and protein levels. The end result is that atherogenic TG-rich lipoproteins lose their TG and apoCIII, leading to faster clearance and better prognosis.

OM3-CA did not affect the concentrations of VLDL apoB subspecies with or without apoCIII (**Table A1.2**). Several studies have shown that omega-3 supplementation reduces VLDL apoB levels by reducing production and/or increasing clearance (63-66). However, some of these studies used much higher amounts of omega-3's than the present study. In our study, when both VLDL subspecies are combined in a single variable, we see a non-significant reduction of total VLDL apoB across the treatment (OM3-CA 2g: -0.4 mg/dL, p=0.7; OM3-CA 4g: -0.5 mg/dL, p=0.26). However, individual decreases in total VLDL apoB levels correlated significantly with increases in DHA and linoleic acid, and with decreases in palmitic and oleic acids (**Table A1.3**).

In this post-hoc, hypothesis generating study, we have shown that OM3-CA selectively increases the predominant subspecies of LDL that does not contain apoCIII, a subspecies of LDL that has a weaker relation to risk of CVD (11, 12). This raises the possibility that the increase in LDL-C caused by OM3-CA in the EVOLVE trial (25) may not increase risk of CVD in severe hypertriglyceridemia. Beyond the context of severe hypertriglyceridemia, these findings are potentially most relevant to high risk subjects with related risk factors such as hypertension, diabetes, or current cardiovascular disease.

A1.5 Funding disclosures

W.A. is a former employee of AstraZeneca. M.D. is a former employee of Omthera

Pharmaceuticals, Inc. and AstraZeneca. F.S. has served as a consultant to Omthera

Pharmaceuticals, Inc. F.S. and J.F. are inventors on US Patent 8,846,321 B2 entitled

"Association of levels of HDL-cholesterol apolipoprotein CIII with the risk of coronary

heart disease and cardiovascular events."

A1.6 References

1. Clavey V, Lestavel-Delattre S, Copin C, Bard JM, Fruchart JC. Modulation of lipoprotein B binding to the LDL receptor by exogenous lipids and apolipoproteins CI, CII, CIII, and E. *Arterioscler. Thromb. Vasc. Biol.* 1995;15(7):963–971.

2. Mendivil CO, Zheng C, Furtado J, Lel J, Sacks FM. Metabolism of very-low-density lipoprotein and low-density lipoprotein containing apolipoprotein C-III and not other small apolipoproteins. *Arterioscler. Thromb. Vasc. Biol.* 2010;30(2):239–245.

3. Ginsberg HN et al. Apolipoprotein B metabolism in subjects with deficiency of apolipoproteins CIII and AI. Evidence that apolipoprotein CIII inhibits catabolism of triglyceride-rich lipoproteins by lipoprotein lipase in vivo. *J. Clin. Invest.* 1986;78(5):1287–1295.

4. Sehayek E, Eisenberg S. Mechanisms of inhibition by apolipoprotein C of apolipoprotein E-dependent cellular metabolism of human triglyceride-rich lipoproteins through the low density lipoprotein receptor pathway. *J. Biol. Chem.* 1991;266(27):18259–18267.

5. de Silva HV et al. Overexpression of human apolipoprotein C-III in transgenic mice results in an accumulation of apolipoprotein B48 remnants that is corrected by excess apolipoprotein E. *J. Biol. Chem.* 1994;269(3):2324–2335.

6. Aalto-Setälä K et al. Mechanism of hypertriglyceridemia in human apolipoprotein (apo) CIII transgenic mice. Diminished very low density lipoprotein fractional catabolic rate associated with increased apo CIII and reduced apo E on the particles. *J. Clin. Invest.* 1992;90(5):1889–1900.

7. Kawakami A et al. Apolipoprotein CIII in apolipoprotein B lipoproteins enhances the adhesion of human monocytic cells to endothelial cells. *Circulation* 2006;113(5):691–700.

8. Kawakami A et al. Apolipoprotein CIII induces expression of vascular cell adhesion molecule-1 in vascular endothelial cells and increases adhesion of monocytic cells.

Circulation 2006;114(7):681–687.

9. Hiukka A et al. ApoCIII-enriched LDL in type 2 diabetes displays altered lipid composition, increased susceptibility for sphingomyelinase, and increased binding to biglycan. *Diabetes* 2009;58(9):2018–2026.

10. Sacks FM et al. VLDL, apolipoproteins B, CIII, and E, and risk of recurrent coronary events in the Cholesterol and Recurrent Events (CARE) trial. *Circulation* 2000;102(16):1886–1892.

11. Mendivil CO, Rimm EB, Furtado J, Chiuve SE, Sacks FM. Low-density lipoproteins containing apolipoprotein C-III and the risk of coronary heart disease. *Circulation* 2011;124(19):2065–2072.

12. Lee S-J, Campos H, Moye LA, Sacks FM. LDL containing apolipoprotein CIII is an independent risk factor for coronary events in diabetic patients. *Arterioscler. Thromb. Vasc. Biol.* 2003;23(5):853–858.

13. Jensen MK, Rimm EB, Furtado JD, Sacks FM. Apolipoprotein C-III as a Potential Modulator of the Association Between HDL-Cholesterol and Incident Coronary Heart Disease. *J Am Heart Assoc* 2012;1(2):jah3–e000232–jah3–e000232.

14. Pollin TI et al. A null mutation in human APOC3 confers a favorable plasma lipid profile and apparent cardioprotection. *Science* 2008;322(5908):1702–1705.

15. TG and HDL Working Group of the Exome Sequencing Project, National Heart, Lung, and Blood Institute et al. Loss-of-function mutations in APOC3, triglycerides, and coronary disease. *N. Engl. J. Med.* 2014;371(1):22–31.

16. Jørgensen AB, Frikke-Schmidt R, Nordestgaard BG, Tybjaerg-Hansen A. Loss-of-function mutations in APOC3 and risk of ischemic vascular disease. *N. Engl. J. Med.* 2014;371(1):32–41.

17. Berglund L et al. Evaluation and treatment of hypertriglyceridemia: an Endocrine Society clinical practice guideline. *J. Clin. Endocrinol. Metab.* 2012;97(9):2969–2989.

18. Maki KC, Bays HE, Dicklin MR. Treatment options for the management of hypertriglyceridemia: strategies based on the best-available evidence. *J Clin Lipidol* 2012;6(5):413–426.

19. Christian JB, Bourgeois N, Snipes R, Lowe KA. Prevalence of Severe (500 to 2,000 mg/dl) Hypertriglyceridemia in United States Adults. *Am. J. Cardiol.* 2011;107(6):891–897.

20. Hauenschild A et al. Successful treatment of severe hypertriglyceridemia with a formula diet rich in omega-3 fatty acids and medium-chain triglycerides. *Ann. Nutr. Metab.* 2010;56(3):170–175.

21. Fares H, Lavie CJ, DiNicolantonio JJ, O'Keefe JH, Milani RV. Icosapent ethyl for the treatment of severe hypertriglyceridemia. *Ther Clin Risk Manag* 2014;10:485–492.

22. Blair HA, Dhillon S. Omega-3 carboxylic acids (Epanova): a review of its use in patients with severe hypertriglyceridemia. *Am J Cardiovasc Drugs* 2014;14(5):393–400.

23. Davidson MH, Maki KC, Bays H, Carter R, Ballantyne CM. Effects of prescription omega-3-acid ethyl esters on lipoprotein particle concentrations, apolipoproteins AI and CIII, and lipoprotein-associated phospholipase A(2) mass in statin-treated subjects with hypertriglyceridemia. *J Clin Lipidol* 2009;3(5):332–340.

24. Maki KC, Bays HE, Dicklin MR, Johnson SL, Shabbout M. Effects of prescription omega-3-acid ethyl esters, coadministered with atorvastatin, on circulating levels of lipoprotein particles, apolipoprotein CIII, and lipoprotein-associated phospholipase A2 mass in men and women with mixed dyslipidemia. *J Clin Lipidol* 2011;5(6):483–492.

25. Kastelein JJP et al. Omega-3 free fatty acids for the treatment of severe hypertriglyceridemia: the EpanoVa fOr Lowering Very high triglyceridEs (EVOLVE) trial. *J Clin Lipidol* 2014;8(1):94–106.

26. Davidson MH, Johnson J, Rooney MW, Kyle ML, Kling DF. A novel omega-3 free fatty acid formulation has dramatically improved bioavailability during a low-fat diet compared with omega-3-acid ethyl esters: the ECLIPSE (Epanova(®) compared to Lovaza(®) in a pharmacokinetic single-dose evaluation) study. *J Clin Lipidol* 2012;6(6):573–584.

27. AstraZeneca Pharmaceuticals LP. Omega-3 carboxylic acids (Epanova): US prescribing information 2013 [Internet]http://www1.astrazeneca-us.com/pi/epanova.pdf. cited

28. Zheng C, Khoo C, Ikewaki K, Sacks FM. Rapid turnover of apolipoprotein C-III-containing triglyceride-rich lipoproteins contributing to the formation of LDL subfractions. *J. Lipid Res.* 2007;48(5):1190–1203.

29. Warnick GR, Benderson J, Albers JJ. Dextran sulfate-Mg2+ precipitation procedure for quantitation of high-density-lipoprotein cholesterol. *Clin. Chem.* 1982;28(6):1379–1388.

30. Buckley R, Shewring B, Turner R, Yaqoob P, Minihane AM. Circulating triacylglycerol and apoE levels in response to EPA and docosahexaenoic acid supplementation in adult human subjects. *Br. J. Nutr.* 2004;92(3):477–483.

31. Homma Y et al. Effects of eicosapentaenoic acid on plasma lipoprotein subfractions and activities of lecithin:cholesterol acyltransferase and lipid transfer protein. *Atherosclerosis* 1991;91(1-2):145–153.

32. Bays HE et al. Eicosapentaenoic acid ethyl ester (AMR101) therapy in patients with very high triglyceride levels (from the Multi-center, plAcebo-controlled, Randomized,

double-blINd, 12-week study with an open-label Extension [MARINE] trial). *Am. J. Cardiol.* 2011;108(5):682–690.

33. Ogami K, Hadzopoulou-Cladaras M, Cladaras C, Zannis VI. Promoter elements and factors required for hepatic and intestinal transcription of the human ApoCIII gene. *J. Biol. Chem.* 1990;265(17):9808–9815.

34. Reue K, Leff T, Breslow JL. Human apolipoprotein CIII gene expression is regulated by positive and negative cis-acting elements and tissue-specific protein factors. *J. Biol. Chem.* 1988;263(14):6857–6864.

35. Zannis VI, Kan HY, Kritis A, Zanni EE, Kardassis D. Transcriptional regulatory mechanisms of the human apolipoprotein genes in vitro and in vivo. *Curr. Opin. Lipidol.* 2001;12(2):181–207.

36. Chen Y-J et al. Docosahexaenoic acid suppresses the expression of FoxO and its target genes. *J. Nutr. Biochem.* 2012;23(12):1609–1616.

37. Dallongeville J et al. Peroxisome proliferator-activated receptor alpha is not rate-limiting for the lipoprotein-lowering action of fish oil. *J. Biol. Chem.* 2001;276(7):4634–4639.

38. Calder PC. Mechanisms of action of (n-3) fatty acids. *J. Nutr.* 2012;142(3):592S–599S.

39. Bishop-Bailey D. Peroxisome proliferator-activated receptors in the cardiovascular system. *Br. J. Pharmacol.* 2000;129(5):823–834.

40. Kersten S, Desvergne B, Wahli W. Roles of PPARs in health and disease. *Nature* 2000;405(6785):421–424.

41. Forman BM, Chen J, Evans RM. Hypolipidemic drugs, polyunsaturated fatty acids, and eicosanoids are ligands for peroxisome proliferator-activated receptors alpha and delta. *Proc. Natl. Acad. Sci. U.S.A.* 1997;94(9):4312–4317.

42. Staels B et al. Fibrates downregulate apolipoprotein C-III expression independent of induction of peroxisomal acyl coenzyme A oxidase. A potential mechanism for the hypolipidemic action of fibrates. *J. Clin. Invest.* 1995;95(2):705–712.

43. Srivastava RAK, Jahagirdar R, Azhar S, Sharma S, Bisgaier CL. Peroxisome proliferator-activated receptor-alpha selective ligand reduces adiposity, improves insulin sensitivity and inhibits atherosclerosis in LDL receptor-deficient mice. *Mol. Cell. Biochem.* 2006;285(1-2):35–50.

44. Liu C, Guo Q, Lu M, Li Y. An experimental study on amelioration of dyslipidemia-induced atherosclesis by Clematichinenoside through regulating Peroxisome proliferator-activated receptor-α mediated apolipoprotein A-I, A-II and C-III. *Eur. J. Pharmacol.* [published online ahead of print: May 12, 2015];

doi:10.1016/j.ejphar.2015.04.015

45. Hertz R, Bishara-Shieban J, Bar-Tana J. Mode of action of peroxisome proliferators as hypolipidemic drugs. Suppression of apolipoprotein C-III. *J. Biol. Chem.* 1995;270(22):13470–13475.

46. Hayhurst GP, Lee YH, Lambert G, Ward JM, Gonzalez FJ. Hepatocyte nuclear factor 4alpha (nuclear receptor 2A1) is essential for maintenance of hepatic gene expression and lipid homeostasis. *Mol. Cell. Biol.* 2001;21(4):1393–1403.

47. Shih DQ et al. Genotype/phenotype relationships in HNF-4alpha/MODY1: haploinsufficiency is associated with reduced apolipoprotein (AII), apolipoprotein (CIII), lipoprotein(a), and triglyceride levels. *Diabetes* 2000;49(5):832–837.

48. Ceccarelli V et al. Effect of dietary saturated fatty acids on HNF-4α DNA binding activity and ApoCIII mRNA in sedentary rat liver. *Mol. Cell. Biochem.* 2011;347(1-2):29–39.

49. Vu-Dac N et al. The nuclear receptors peroxisome proliferator-activated receptor alpha and Rev-erbalpha mediate the species-specific regulation of apolipoprotein A-I expression by fibrates. *J. Biol. Chem.* 1998;273(40):25713–25720.

50. Coste H, Rodríguez JC. Orphan nuclear hormone receptor Rev-erbalpha regulates the human apolipoprotein CIII promoter. *J. Biol. Chem.* 2002;277(30):27120–27129.

51. Yoshikawa T et al. Polyunsaturated fatty acids suppress sterol regulatory element-binding protein 1c promoter activity by inhibition of liver X receptor (LXR) binding to LXR response elements. *J. Biol. Chem.* 2002;277(3):1705–1711.

52. Georgiadi A, Kersten S. Mechanisms of gene regulation by fatty acids. *Adv Nutr* 2012;3(2):127–134.

53. Lee JN et al. Identification of Ubxd8 protein as a sensor for unsaturated fatty acids and regulator of triglyceride synthesis. *Proc. Natl. Acad. Sci. U.S.A.* 2010;107(50):21424–21429.

54. Botolin D, Wang Y, Christian B, Jump DB. Docosahexaneoic acid (22:6,n-3) regulates rat hepatocyte SREBP-1 nuclear abundance by Erk- and 26S proteasome-dependent pathways. *J. Lipid Res.* 2006;47(1):181–192.

55. Kaur G, Cameron-Smith D, Garg M, Sinclair AJ. Docosapentaenoic acid (22:5n-3): a review of its biological effects. *Prog. Lipid Res.* 2011;50(1):28–34.

56. Nakamura MT, Nara TY. Structure, function, and dietary regulation of delta6, delta5, and delta9 desaturases. *Annu. Rev. Nutr.* 2004;24(1):345–376.

57. Zheng C, Khoo C, Furtado J, Sacks FM. Apolipoprotein C-III and the metabolic basis for hypertriglyceridemia and the dense low-density lipoprotein phenotype.

Circulation 2010;121(15):1722–1734.

58. Kinnunen PK, Ehnolm C. Effect of serum and C-apoproteins from very low density lipoproteins on human postheparin plasma hepatic lipase. *FEBS Lett.* 1976;65(3):354–357.

59. Krauss RM, Herbert PN, Levy RI, Fredrickson DS. Further observations on the activation and inhibition of lipoprotein lipase by apolipoproteins. *Circ. Res.* 1973;33(4):403–411.

60. Larsson M, Vorrsjö E, Talmud P, Lookene A, Olivecrona G. Apolipoproteins C-I and C-III inhibit lipoprotein lipase activity by displacement of the enzyme from lipid droplets. *J. Biol. Chem.* 2013;288(47):33997–34008.

61. Sacks FM. The crucial roles of apolipoproteins E and C-III in apoB lipoprotein metabolism in normolipidemia and hypertriglyceridemia. *Curr. Opin. Lipidol.* 2015;26(1):56–63.

62. Graham MJ et al. Antisense oligonucleotide inhibition of apolipoprotein C-III reduces plasma triglycerides in rodents, nonhuman primates, and humans. *Circ. Res.* 2013;112(11):1479–1490.

63. Wong ATY et al. Omega-3 fatty acid ethyl ester supplementation decreases very-low-density lipoprotein triacylglycerol secretion in obese men. *Clin. Sci.* 2013;125(1):45–51.

64. Chan DC et al. ω-3 Fatty Acid Ethyl Esters Diminish Postprandial Lipemia in Familial Hypercholesterolemia. *J. Clin. Endocrinol. Metab.* 2016;:jc20162217.

65. Ouguerram K, Maugeais C, Gardette J, Magot T, Krempf M. Effect of n-3 fatty acids on metabolism of apoB100-containing lipoprotein in type 2 diabetic subjects. *Br. J. Nutr.* 2006;96(1):100–106.

66. Shearer GC, Savinova OV, Harris WS. Fish oil -- how does it reduce plasma triglycerides? *Biochim. Biophys. Acta* 2012;1821(5):843–851.

APPENDIX 2

Supplemental Material for CHAPTER 2:

Apolipoproteins E and CIII interact to regulate HDL metabolism and coronary heart disease risk
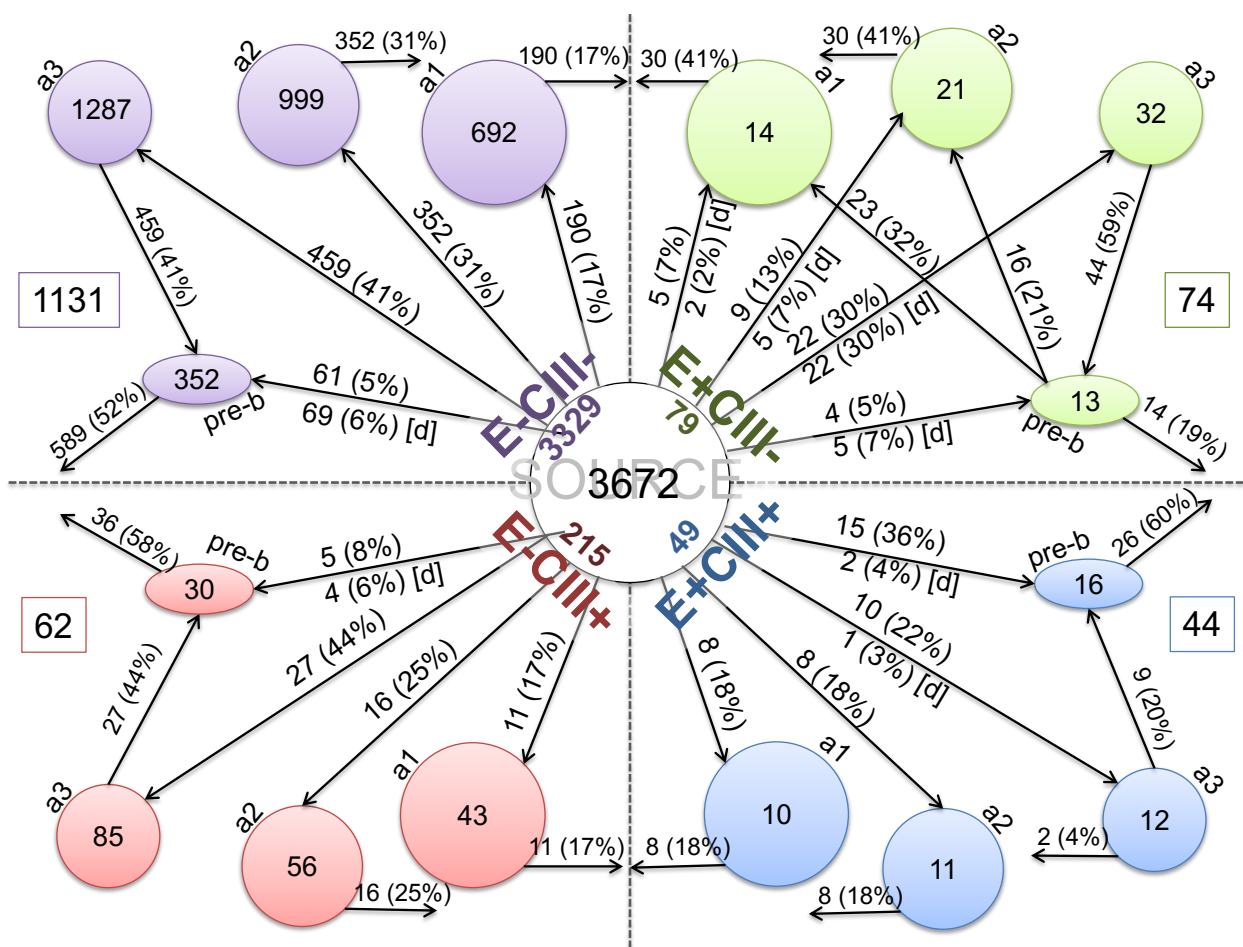
This information appears in the Supplemental Data in:

Figure A2.1: Model-derived apoA-I flux rates and pool sizes across four HDL subspecies and sizes. Numbers inside the center circle (source compartment, representing liver or intestinal synthesis) represent apoA-I pool size for each subspecies and for total plasma. Numbers inside circles (HDL size compartments) represent mean pool size (mg). Numbers above lines represent mean flux in mg/day (% total flux for that subspecies). Numbers below lines with [d] = flux in mg/day (% of total flux for that subspecies) through intravascular delay compartments (not illustrated). Numbers in the colored boxes are total flux for that subspecies in mg/day. a1 = alpha-1; a2 = alpha-2; a3 = alpha-3, pre-b = prebeta
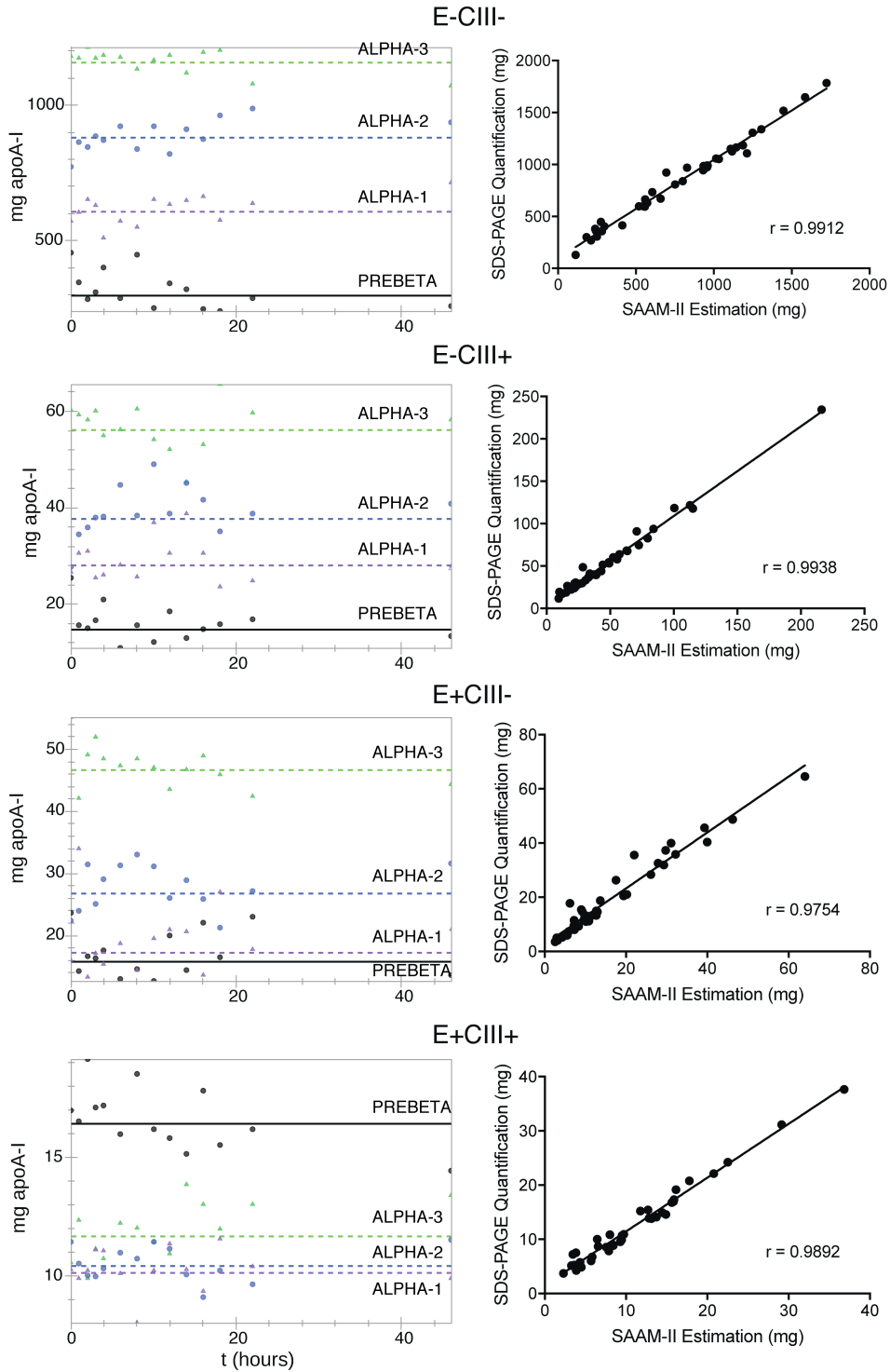
Figure A2.2: Ability of SAAM-II to accurately estimate apoA-I pool sizes calculated from SDS-PAGE densitometry.

Figure A2.2 (continued): Ability of SAAM-II to accurately estimate apoA-I pool sizes calculated from SDS-PAGE densitometry. Left: Mean apoA-I mass (pool size) model fits in SAAM-II for each HDL subspecies (by size). Right: Comparison of SAAM-II model estimation vs. SDS-PAGE quantification (right) for each subspecies (points = each HDL size of each study participant, 40 total per subspecies). Pearson correlation (r) shown. All SAAM-II estimations are within 1 standard deviation of mean SDS-PAGE quantification.

APPENDIX 3

Supplemental Material for CHAPTER 3:

Dietary unsaturated fat increases metabolic pathways in reverse cholesterol transport via HDL containing apoE

Allyson M. Morton, Carlos O. Mendivil, Jeremy D. Furtado, Frank M. Sacks

Table A3.1: Mean (n=9) apoA-I pool sizes (mg), fractional catabolic rates (FCR, pools/day) and synthesis rates (mg/day) in plasma and in subspaces of HDL containing apoE (E+) or not containing apoE (E-). HFD = high unsaturated fat diet, LFD = low fat diet, Δ (HFD - LFD) = change in diet.

Plasma apoA-I

	Pool Size (mg)							FCR (pools/day)							Synthesis (mg/day)						
HDL	HFD		LFD		Δ (HFD - LFD)			HFD		LFD		Δ (HFD - LFD)			HFD		LFD		Δ (HFD - LFD)		
Size	Mean	SEM	Mean	SEM	Mean	SD	p[A]	Mean	SEM	Mean	SEM	Mean	SD	p	Mean	SEM	Mean	SEM	Mean	SD	p
alpha-1	601	89	593	105	8	449	0.96	0.39	0.05	0.32	0.02	3.47	0.15	0.18	180	36	142	37	38	153	0.47
alpha-2	1186	83	1317	143	-131	565	0.51	0.53	0.08	0.39	0.03	11.16	0.25	0.13	579	130	382	72	197	471	0.24
alpha-3	1263	200	1233	164	30	729	0.90	0.51	0.06	0.37	0.02	11.24	0.18	0.05	547	104	297	60	250	359	0.07
prebeta	260	57	246	38	14	237	0.86	5.21	0.85	2.63	0.65	2.32	3.63	0.07	146	35	149	76	-3	174	0.96
total	3310	159	3389	256	-78	522	0.66	0.44[B]	n/a	0.29	n/a	0.15	n/a	**0.04**[C]	1453	162	970	157	483	568	**0.03**

E+ HDL

	Pool Size (mg)							FCR (pools/day)							Synthesis (mg/day)						
HDL	HFD		LFD		Δ (HFD - LFD)			HFD		LFD		Δ (HFD - LFD)			HFD		LFD		Δ (HFD - LFD)		
Size	Mean	SEM	Mean	SEM	Mean	SD	p	Mean	SEM	Mean	SEM	Mean	SD	p	Mean	SEM	Mean	SEM	Mean	SD	p
alpha-1	30	4	24	5	5	23	0.52	3.4	0.8	1.5	0.2	1.9	2.2	**0.03**	34	17	9	4	25	45	0.09
alpha-2	49	11	37	8	12	42	0.41	2.8	0.4	1.0	0.2	1.8	1.4	**0.005**	86	32	26	11	60	112	**0.04**
alpha-3	69	16	53	13	17	17	**0.02**	1.4	0.2	1.9	0.9	-0.5	2.5	0.54	65	15	39	11	26	24	**0.01**
prebeta	21	4	23	6	-2	19	0.75	8.6	1.6	6.5	1.5	2.1	7.1	0.40	27	11	9	2	18	24	0.06
total	169	27	137	23	32	57	0.13	1.3	n/a	0.6	n/a	0.6	n/a	0.057	213	49	84	17	129	149	**0.03**

E- HDL

	Pool Size (mg)			FCR (pools/day)			Synthesis (mg/day)		
HDL	HFD	LFD	Δ (HFD - LFD)	HFD	LFD	Δ (HFD - LFD)	HFD	LFD	Δ (HFD - LFD)

Table A3.1 (continued)

HDL	HFD		LFD		Δ (HFD - LFD)			HFD		LFD		Δ (HFD - LFD)			HFD		LFD		Δ (HFD - LFD)		
Size	Mean	SEM	Mean	SEM	Mean	SD	p	Mean	SEM	Mean	SEM	Mean	SD	p	Mean	SEM	Mean	SEM	Mean	SD	p
alpha-1	571	89	569	102	2	432	0.99	0.36	0.03	0.33	0.03	0.04	0.13	0.43	144	33	125	37	20	138	0.68
alpha-2	1137	76	1280	141	-143	539	0.45	0.50	0.06	0.40	0.03	0.10	0.15	0.09	450	94	361	65	89	359	0.48
alpha-3	1194	193	1180	163	13	724	0.96	0.47	0.04	0.39	0.03	0.08	0.11	0.05	404	88	259	58	145	293	0.18
prebeta	239	57	223	36	16	233	0.84	6.01	1.21	3.15	1.06	2.86	5.49	0.16	98	32	97	45	2	81	0.19
total	3142	156	3252	253	-110	517	0.54	0.35	n/a	0.26	n/a	0.09	n/a	0.12	1096	141	841	100	255	431	0.11

[A] All p-values are for paired two-tailed t-test (n=9 per group). Significant values (p<0.05) are bolded.

[B] All sizes were modeled independently, thus total apoA-I FCR was approximated by dividing plasma apoA-I flux by apoA-I pool size

[C] p-value for paired two-tailed t-test, all sizes pooled together (n=36 per group)
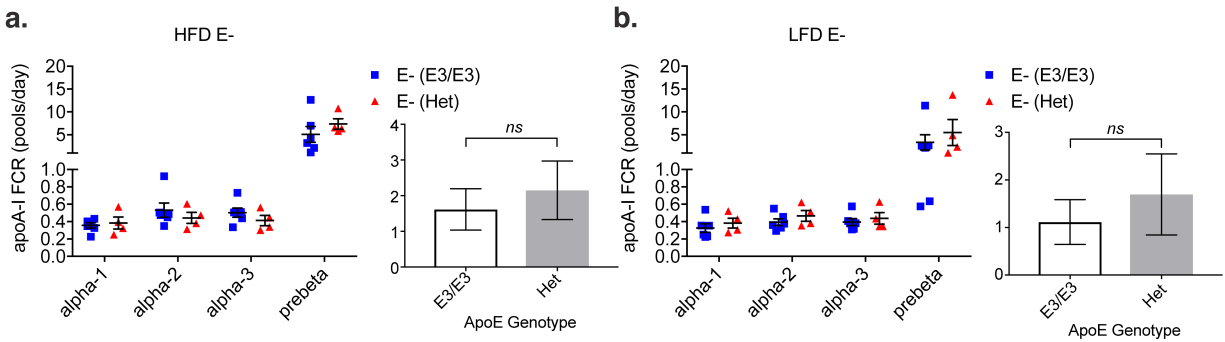
Figure A3.1: ApoE heterozygotes have normal apoA-I clearance rates in HDL not containing apoE. ApoA-I fractional catabolic rates (FCR, pools/day) across four sizes of HDL are shown in 6 E3/E3 homozygotes compared to 4 apoE heterozygotes (pooled: 1 E2/E3, 2 E4/E3, 1 E2/E4) (Het). Inset: All HDL sizes pooled together (n=24 for E3/E3, n=16 for Het). Error bars = SEM. P-value shown for unpaired two-tailed t-test. The clearance rates for HDL containing apoE are abnormally low (see **Figure 3.9**).